LBL-21832 c.2

Lawrence Berkeley Laboratory

UNIVERSITY OF CALIFORNIA

RECEIVED
LAWRENCE
BERKELEY LABORATORY
AUG 13 1986
LIBRARY AND
DOCUMENTS SECTION

CHEMICAL BIODYNAMICS DIVISION

PICOSECOND DYNAMICS OF SOLVATION: TIME-RESOLVED FLUORESCENCE OF 4-AMINOPHTHALIMIDE IN SOLUTION

L.F. Buhse
(Ph.D. Thesis)

TWO-WEEK LOAN COPY
This is a Library Circulating Copy
which may be borrowed for two weeks.

June 1985

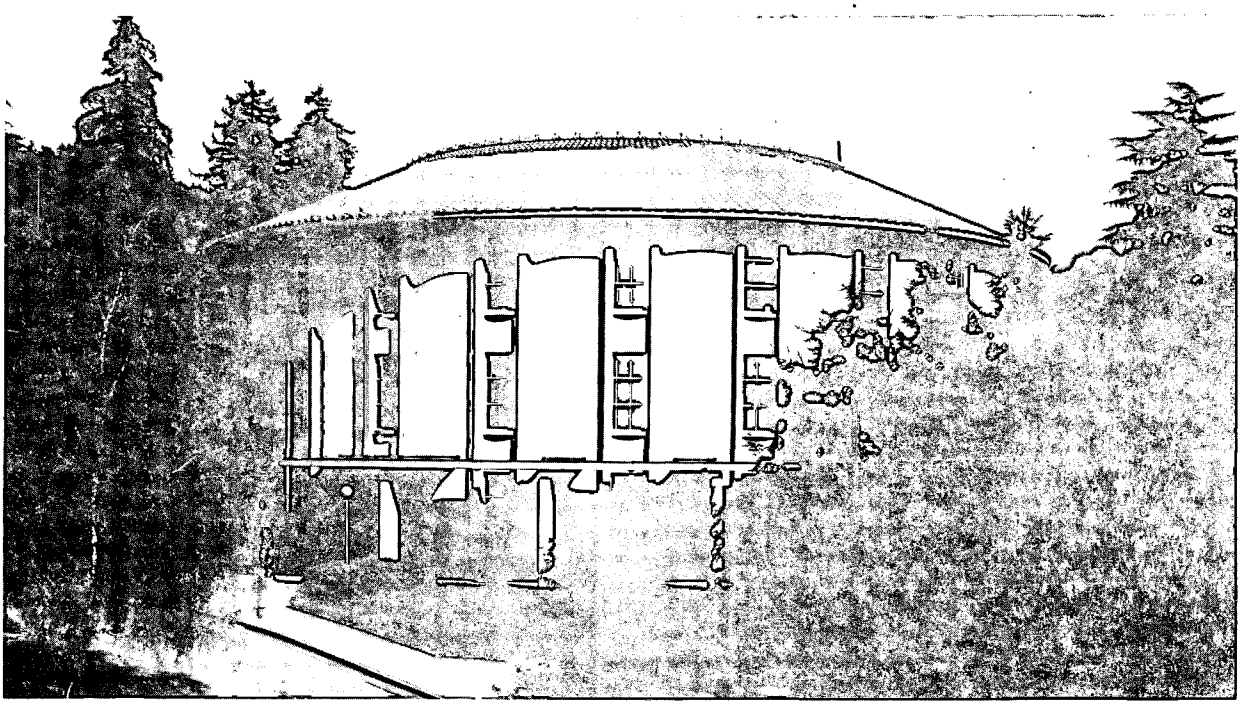

LBL-21832 c.2

Prepared for the U.S. Department of Energy under Contract DE-AC03-76SF00098

DISCLAIMER

This document was prepared as an account of work sponsored by the United States Government. While this document is believed to contain correct information, neither the United States Government nor any agency thereof, nor the Regents of the University of California, nor any of their employees, makes any warranty, express or implied, or assumes any legal responsibility for the accuracy, completeness, or usefulness of any information, apparatus, product, or process disclosed, or represents that its use would not infringe privately owned rights. Reference herein to any specific commercial product, process, or service by its trade name, trademark, manufacturer, or otherwise, does not necessarily constitute or imply its endorsement, recommendation, or favoring by the United States Government or any agency thereof, or the Regents of the University of California. The views and opinions of authors expressed herein do not necessarily state or reflect those of the United States Government or any agency thereof or the Regents of the University of California.

Picosecond Dynamics of Solvation: Time-Resolved Fluorescence of 4-Aminophthalimide in Solution

Lucinda Fisher Buhse
Ph.D. Thesis

Lawrence Berkeley Laboratory
Uiniversity of California
Berkeley, California 94720

June 1985

The United States Department of Energy has the right to use this thesis for any purpose whatsoever including the right to reproduce all or any part thereof.

Picosecond Dynamics of Solvation:

Time-Resolved Fluorescence of 4-Aminophthalimide in Solution

Copyright ©1986

Lucinda Fisher Buhse

Picosecond Dynamics of Solvation: Time-Resolved Fluorescence of 4-Aminophthalimide in Solution

Lucinda Fisher Buhse

Abstract

The following chapters describe the application of picosecond fluorescence techniques to the study of the dynamics of solvation. The excited state of the molecule 4-aminophthalimide (4AP) has a larger dipole moment than the ground state. Following electronic excitation of the 4AP solute, a polar solvent rearranges around the newly created solute dipole moment. As the solvent rearranges, the fluorescence of the 4AP molecules red shifts. By temporally resolving this red shift in fluorescence, the dynamics of solvation of the 4AP molecule are directly probed. The fluorescence red shift of 4AP is examined in pure solvents as well as a mixed solvent of 1-propanol:toluene. The only pure solvents that cause an observable, time-dependent red shift in the fluorescence of 4AP are the alcohols. For each alcohol, the solvation times measured from the time of the red shifts of fluorescence are found to be well correlated with the dielectric relaxation times of the solvent. This result explains the absence of a time-dependent red shift in the other solvents; the dielectric relaxation times of all other solvents are faster than the time resolution of the instrumentation. The experiments involving the mixed solvent 1-propanol:toluene add another element to the solvation of 4AP. Steady-state spectra, fluorescence lifetime measurements, and rotational reorientation times of the 4AP molecule all imply a larger 1-propanol concentration around the excited-state 4AP molecule than the ground-state. The solvation times of the 4AP solute must now be explained by two separate mechanisms: the dielectric relaxation of the solvent immediately around the 4AP molecule along with the diffusion of additional 1-propanol molecules to the solvent cage immediately surrounding the excited solute molecule. The direct probe of the solvation dynamics of 4AP is valuable in determining the important processes of solvent-solute interactions.

Acknowledgements

I would like to thank Dr. John H. Clark, Sheila W. Yeh and Ward T. Brown for their contributions to the work described here. L.A. Philips, D. Anthon, S. Yeh and W. Brown were helpful in teaching me how to use the instrumentation. I thank T. Maxson and T. Ferrett for helping me with my thesis. I especially thank Moira and Howard Buhse for giving me the inspiration to obtain a Ph.D.

The pure solvent research was supported by the Gas Research Institute Basic Coal Sciences Program under Contract 5081-260-568. The mixed solvent work was supported by the Office of Energy Research, Office of Basic Energy Sciences, Chemical Sciences Division of the Department of Energy under Contract DE-AC03-76SF00098. I appreciate the receipt of a Graduate Opportunity Fellowship in partial payment of my stipend and tuition for the year 1982-1983. I would like to thank AT&T Bell Laboratories for funding my stipend and tuition, 1983-1986.

Table of Contents

Abstract 1

Acknowledgements i

Table of Contents ii

List of Figures iv

List of Tables vi

Chapter 1

Introduction 1

Chapter 2

Experimental 13

A. Materials 13

B. Steady-State Spectra 13

C. Laser System 14

D. Ultrafast Streak Camera 17

E. Analyses of Data 22

Chapter 3

4-Aminophthalimide Fluorescence in Pure Solvents 24

A. Introduction 24

B. Steady-State Spectra 25

C. Fluorescence Lifetimes 34

D. Fast Time Dynamics 53

1. 4AP in 1-Propanol 53

2. 4AP in Other Solvents 62

E. Dielectric Relaxation Times 71

F. Rotations 99

G. Conclusion 105

Chapter 4

4-Aminophthalimide Fluorescence in a Mixed Solvent System 112

A. Introduction 112

B. Steady-State Spectra 113

C. Fluorescence Lifetimes 113

D. Rotations 118

E. Solvation Dynamics 122

F. Dielectric Relaxation Times 126

G. Diffusion 140

H. Combined Mechanism of Relaxation 142

I. Conclusion 149

Chapter 5

Conclusion 150

References 152

List of Figures

1.1 Schematic Picture of Excited-State Solvation 3

1.2 Potential Energy Diagram for Excited-State Solvation 5

1.3 Structure of 4-(N,N'-Dimethylamino)benzonitrile (DMABN) 9

1.4 Structure of 4-Aminophthalimide 11

2.1 Diagram of Actively and Passively Mode-Locked Nd:YAG Laser Cavity . . . 15

2.2 "Picosecond Fluorimeter Apparatus" 18

2.3 Sample Data from the Picosecond Laser/ Streak Camera Apparatus 20

3.1 Steady-State Emission Spectra for 4AP in 1-Propanol and Toluene 26

3.2 Steady-State Excitation Spectra of 4AP in 1-Propanol and Toluene 28

3.3 Structure of Pentaphenyl Pyridinium Phenolate Dye 32

3.4 Structure of TNSDMA 35

3.5 The Two State Emission from TNSDMA 37

3.6 Quantum Yield of TNSDMA Emission as a Function of $E_T(30)$ for Dioxane:H_2O Mixtures 39

3.7 Emission Maxima of 4AP versus $E_T(30)$ Values for Dioxane:H_2O Mixtures 42

3.8 Emission Maxima of 3AP versus $E_T(30)$ Values for Dioxane:H_2O Mixtures 44

3.9 Relative Quantum Yield of Emission of 4AP versus $E_T(30)$ Values for Dioxane:H_2O Mixtures 46

3.10 Fluorescence Lifetime Data for 4AP in 1-Propanol 49

3.11 Log of the Fluorescence Lifetime Data for 4AP in 1-Propanol 51

3.12 Fast Time Dynamics of 4AP in 1-Propanol at the Red and Blue Edges of the Steady-State Spectrum 54

3.13 Fast Time Dynamics of 4AP in 1-Propanol for the Entire Spectrum 56

3.14 Time-Resolved Emission Spectra for 4AP in 1-Propanol 60

3.15 Time-Resolved Emission Spectra for DMABN in Acetonitrile 63

3.16 Gaussian Fits to Time-Resolved Emission Spectra of 4AP in 1-Propanol . . . 65

3.17 Emission Maximum as a Function of Time for 4AP in 1-Propanol 67

3.18 Spectral Width as a Function of Time for 4AP in 1-Propanol 69

3.19 Fast Time Dynamics of 4AP in Acetonitrile 72

3.20 Time-Resolved Emission Spectra for 4AP in Ethanol 74

3.21 Time-Resolved Emission Spectra for 4AP in 1-Butanol 76

3.22 Fast Time Dynamics of 4AP in Formamide 79

3.23 Corrected Dielectric Relaxation Time versus Solvation Time for 4AP in a Series of Alcohols 86

3.24 Structures of 3AP and 4AMP 92

3.25 Steady-State Emission and Excitation Spectra for 4AP, 3AP and 4AMP in 1-Propanol 94

3.26 Rotational Data for 4AP in 1-Propanol at 500 nm 101

3.27 Rotational Anisotropy of 4AP in 1-Propanol at 500 nm 103

3.28 Rotation Time of 4AP in Alcohols as a Function of Viscosity 107

4.1 Steady-State Fluorescence Spectra of 4AP in 1-Propanol:Toluene Mixtures 115

4.2 Fluorescence Lifetime Data for 4AP in 1-Propanol:Toluene Mixtures . . . 120

4.3 Rotation Times of 4AP in 1-Propanol:Toluene Mixtures 124

4.4 Fast Time Dynamics of 4AP in 1-Propanol:Toluene Mixtures at 450 nm . . 127

4.5 Fast Time Dynamics of 4AP in 1-Propanol:Toluene Mixtures at 600 nm . . 129

4.6 Fluorescence Peak Position versus Time for 4AP in 1-Propanol:Toluene Mixtures 131

4.7 Fast Time Dynamics of 4AP in Toluene and a Dilute 1-Propanol in Toluene Solution at 410 nm 134

4.8 Spectral Width as a Function of Time for 4AP in 1-Propanol:Toluene Mixtures 136

4.9 Debye Model for a Diffusional Process 143

List of Tables

3.1 Fluorescence Emission and Excitation Maxima for 4AP in Various Solvents 30

3.2 Fluorescence Maxima and Quantum Yield versus $E_T(30)$ for Dioxane:Water Mixtures 41

3.3 Fluorescence Lifetime of 4AP in Various Solvents 48

3.4 Fit Parameters for 4AP in 1-Propanol 59

3.5 Solvation Times of 4AP in a Series of Alcohols at 20 °C 78

3.6 Dielectric Relaxation Times for Linear Alcohols 84

3.7 Dielectric Data for a Series of Alcohols at 20 °C 85

3.8 Dielectric Relaxation Times for Other Solvents at 20 °C 89

3.9 Solvation Times and Corrected Dielectric Relaxation Times for 4AP in 1-Propanol at a Series of Temperatures 91

3.10 Fit Parameters for a Series of Solutes in 1-Propanol 96

3.11 Solvation Times of Various Solutes in 1-Propanol 98

3.12 Rotation Times of 4AP in Various Alcohols at 20 °C 106

4.1 Concentrations of 1-Propanol used in 1-Propanol:Toluene Mixtures 114

4.2 Steady-State Absorption and Fluorescence Data for 4AP in 1-Propanol:Toluene Mixtures 117

4.3 Fluorescence Lifetimes of 4AP in 1-Propanol:Toluene Mixtures at 20 °C . . 119

4.4 Rotation Times of 4AP in 1-Propanol:Toluene Mixtures at 20 °C 123

4.5 Solvation Times of 4AP in 1-Propanol:Toluene Mixtures at 20 °C 133

4.6 Time of Maximum Spectral Width versus Solvation Time for 4AP in 1-Propanol:Toluene Mixtures 138

4.7 Dielectric Relaxation Times of 1-Propanol:Toluene Mixtures at 20 °C . . . 139

4.8 Solvation Times of 4AP versus Dielectric Relaxation Time of 1-Propanol:Toluene Mixtures 141

4.9 Three Exponential Fits of Peak Position versus Time Data for 4AP in 1-Propanol:Toluene Mixtures 146

4.10 Contributions of Exponentials to Spectral Shifts 148

Chapter 1

Introduction

Solvation describes the interactions between solute and solvent molecules. Solvation processes are fundamental to almost every liquid phase chemical reaction. A solvent can determine the pathway of a reaction by preferentially solvating a certain intermediate over another. Similarly, a change in solvent can change the equilibrium between reactants and products. A more polar solvent will favor the species that is itself more polarizable. Despite this importance, solvation is poorly understood on the microscopic level. The purpose of the following chapters is to better understand the solvation process by studying the dynamics of solvent-solute interactions.

In order to study these dynamics, another important result of the interaction between solvent and solute will be exploited: the effect of solvent on the spectroscopy of a solute molecule. Solvents can drastically affect electronic emission and absorption spectra by decreasing or increasing the energies of the ground- or excited-state species. Figure 1.1 is an example of the kind of solvent-solute interaction that would enable the solvation dynamics to be followed. Shown is a solute molecule that has little or no dipole moment in the ground state, but a large dipole in the excited state. In the ground state, polar solvent molecules will be randomly arranged around the solute. Immediately after electronic excitation of the solute molecule, the solvent will still be frozen in its ground-state configuration, but the solute will have a new dipole moment. The solvent molecules will rearrange to align their dipoles with the newly created dipole of the solute molecule. If the solute molecule fluoresces, a time dependent shift in the fluorescence may be seen as the solvent solvates the excited state. Figure 1.2 represents this same process. The vertical scale is energy and the horizontal axis can be thought of as the degree of organization of the solvent. The solvation of the excited state occurs between points b and c, and the rearrangement of the solvent back to its ground-state configuration occurs between points d and a. Any red shift in fluorescence is caused by changes in both potential energy

curves, a lower-energy excited state fluorescing to a higher-energy ground state. The dynamics between points b and c can be followed if the time of solvent rearrangement is faster than the fluorescence lifetime of the solute molecule. The time of the shift in fluorescence can then be directly related to the dynamics of solvent rearrangement. Since solvent motion may occur on a picosecond timescale, fluorescence of the solute molecule will need to be studied with picosecond time resolution.

Red shifts in fluorescence and absorption spectra have long been used to determine excited-state dipoles and polarization of solutes. Many authors have developed theories which relate the excited-state and ground-state dipole moments of the solute, and the refractive index and dielectric constant of the solvents to the magnitude of a solute's spectral shift[1]. Many different assumptions are necessary to derive these equations which limits their uses. *McRae's*[1,2] theory of solvent effects on spectral shifts is limited to solvents which do not hydrogen bond or interact with each other. A similar theory by *Abe*[3] only allows van der Waals interactions between solvent and solute and solvent and solvent. *Abe's* theory also assumes that the solvent dipoles react instantaneously to the change in solute charge after excitation.[1] Although these theories relate properties of the solvent to observed changes in the spectroscopy of the solute, they do not reveal any information on the kinds of dynamical interactions that are occurring between the solvent and solute.

With the advent of ultrafast techniques, the theory behind the dynamics of the spectral shifts of solutes has become of interest. Most of these theories begin with the results of the steady-state derivations mentioned above. Using the Debye model of an exponential relaxation, *Mazurenko*[4] found the following expression for the relaxation time, τ_R, of the field around an excited solute:

$$\tau_R \approx \tau_d \frac{n^2 + 2}{\epsilon_0 + 2}$$

where τ_d is the dielectric relaxation time of the solvent, n is the refractive index and ϵ_0 is the static dielectric constant of the solvent. *Bagchi et al.*[5] developed a similar theory for

Figure 1.1 Schematic Picture of Excited-State Solvation

A solute molecule which has little or no dipole moment in the ground state will have a polar solvent randomly arranged around it. If a large dipole is created in the solute molecule after electronic excitation, the solvent will have to rearrange to align itself with the new electronic configuration of the solute. This solvation of the excited state will cause a large red shift in the fluorescence spectrum of the solute upon going from a nonpolar to a polar solvent.

Figure 1.1

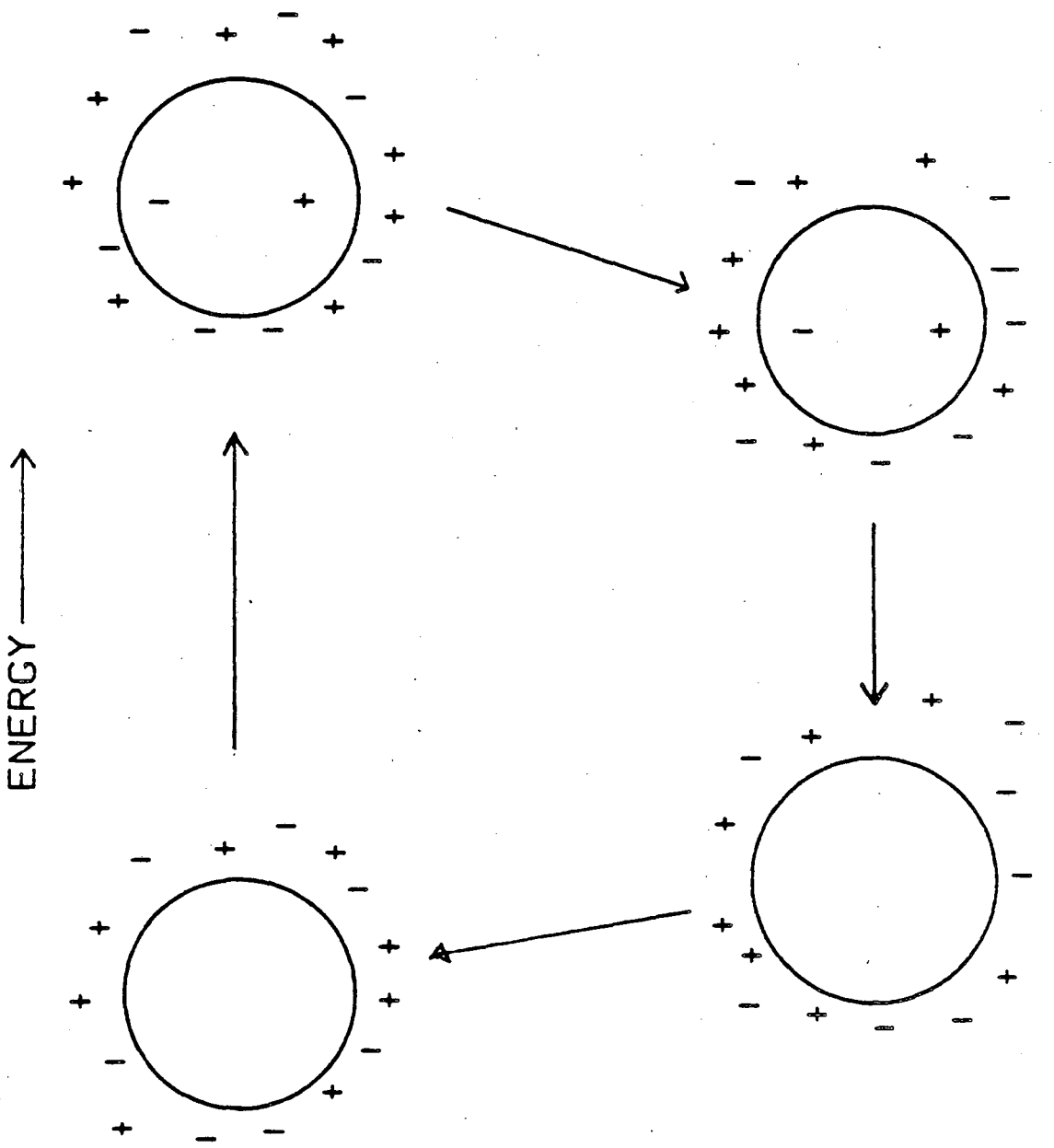

Figure 1.2 Potential Energy Diagram for Excited-State Solvation

This figure is a potential energy diagram for the type of solvation shown in Figure 1.1. The vertical axis represents energy and the horizontal axis is the degree of organization of the solvent. S_0 represents the ground state and S_1 the excited state. Point **a** is the solute with its ground-state electronic configuration with the solvent in its equilibrium ground-state arrangement. After electronic excitation with a photon of energy $h\nu_A$, the solute vibrationally relaxes to point **b**. This point has the excited-state electronic configuration of the solute with the solvent still trapped in the ground-state arrangement. The path from **b** to **c** represents the rearrangement of the solvent to its excited-state equilibrium configuration. Point **d** is then the ground-state electronic configuration of the solute with the solvent in its excited-state equilibrium arrangement. A red shift in fluorescence over time is seen because the solute is fluorescing from a lower-energy excited state to a higher-energy ground state as the solvent rearranges around the solute.

Figure 1.2

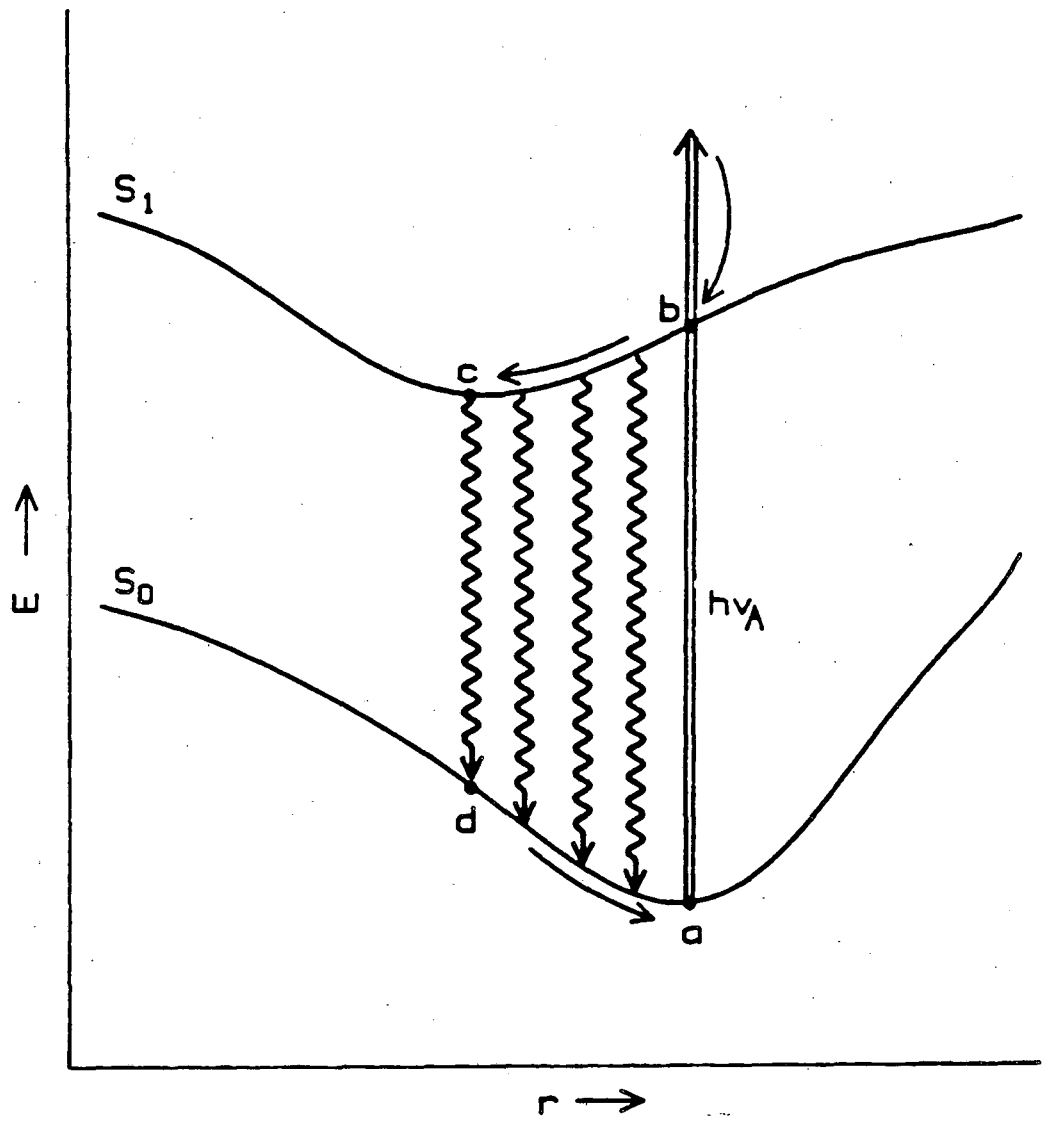

a sphere cavity filled with a dielectric medium with a dielectric constant, ϵ_c, surrounded by a frequency dependent dielectric continuum with high and low frequency dielectric constants of ϵ_∞ and ϵ_0 respectively:

$$\tau_R = \tau_d \frac{\epsilon_c + 2\epsilon_\infty}{\epsilon_c + 2\epsilon_0}.$$

If the assumption that $\epsilon_\infty = n^2$ is used, the above equation is equivalent to *Mazurenko's* equation for an appropriate value of ϵ_c. For these two cases, the relaxation time of the field around the solute, τ_R, is the time of the spectral shift of the fluorescence of the solvent. Both of these equations break down if the change in the dipole moment of the solute is too large or if there is any specific interaction of the solute with the solvent.[5] *Zwan* and *Hynes*[6] approached the problem from a different perspective to obtain expressions for the time dependent shifts for polar interacting solvents. They showed that these spectral shifts were direct measures of the dielectric friction, $\xi(t)$, on the solute molecule. These shifts are thus a valuable way to obtain the dielectric friction of solvents. To test the theories in the literature, the exact dynamics of solvent shifts will be closely examined.

Large red shifts in fluorescence spectra can be due to many different phenomena. Picosecond fluorescence measurements are appropriate for studying many types of excited-state relaxation processes. Two molecules which have large red shifts in their steady-state fluorescence spectra but which would not be good candidates for following solvation dynamics are 1-naphthol and 4-(N,N'-dimethylamino)benzonitrile (DMABN). 1-Naphthol[7] has an emission maximum of 350 nm in most solvents; however, in water the emission maximum is 475 nm. Picosecond fluorescence spectroscopy has shown that this red shift is due to two emitting excited states. In water, the naphthol has a lower pK_a in the excited state than the ground state, so after excitation, the naphthol gives up a proton from the -OH group to the surrounding water, and emission is observed from the anion. Since most solvents do not have the right properties to accept a proton from the 1-naphthol[7], the red-shifted anion fluorescence is only seen in water. DMABN[8,9] also has two emitting excited states. In nonpolar solvents, the emission maximum is 350 nm, while in polar

solvents emission is shifted to 470 nm. The red-shifted emission is from a twisted internal charge transfer (TICT) state, see Figure 1.3. In the ground state, the dimethylamino group is in the same plane as the benzene ring. In the excited state in a polar solvent, a charge transfer from the nitrogen on the amino group to the nitrile group occurs, and the dimethylamino group rotates. A nonpolar solvent can not solvate this TICT state, so emission is from the planar excited state. Both these solutes undergo large changes in electronic character, but any dynamics of the solvent will be obscured by the structural rearrangements of the solute molecule.

The key to following the type of solvation process depicted in Figure 1.2 is finding a molecule with a large change in electronic character after excitation and which does not undergo any physical rearrangement, exciplex formation, or chemical reaction. The molecule chosen for study here is 4-aminophthalimide (4AP), shown in Figure 1.4. A transfer of charge from the N of the amino group to the carbonyls on the five-membered ring causes a change in dipole of this molecule upon electronic excitation. As shown by *Shapiro* and *Winn*[10] with coumarin dyes, strong interactions can occur between carbonyls and polar solvent molecules. Some initial low temperature nanosecond work by *Ware et al.*[11,12] on 4AP suggests that solvation of a quickly forming exciplex can be observed.

The following chapters describe the picosecond dynamics of 4AP fluorescence and relate these dynamics to solvent properties. Chapter 2 describes the experimental approach to this solvation problem. The fluorescence of 4AP in pure solvents is included in Chapter 3 along with some solvation dynamics of similar molecules. Chapter 4 describes the dynamics of 4AP fluorescence in a series of 1-propanol:toluene mixtures.

Figure 1.3 Structure of 4-(N,N′-Dimethylamino)benzonitrile (DMABN)

The ground-state geometry is shown in A. The excited state of DMABN in a nonpolar solvent would also have this geometry. In a polar solvent, the DMABN molecule undergoes a twisted internal charge transfer (TICT), where after an electron transfers from the amino group to the nitrile group, the dimethylamino group rotates to the geometry shown in B.

Figure 1.3

A

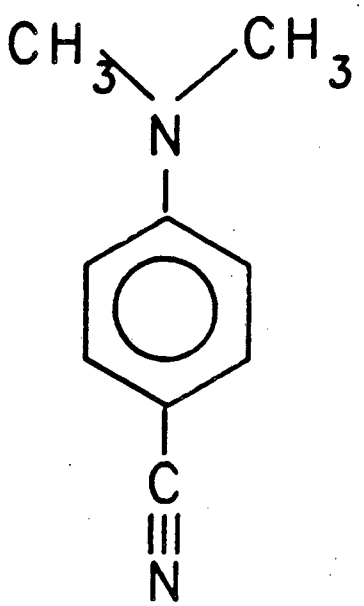

B

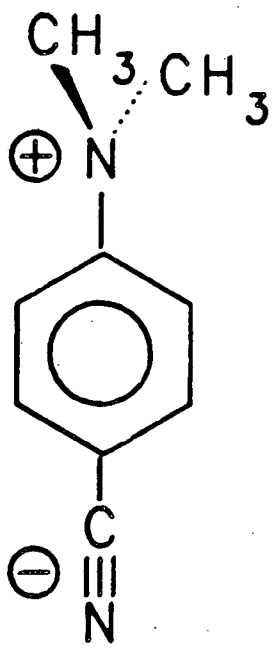

Figure 1.4 Structure of 4-Aminophthalimide (4AP)

The official nomenclature is 5-amino-1H-isoindole-1,3(2H)-dione.

Figure 1.4

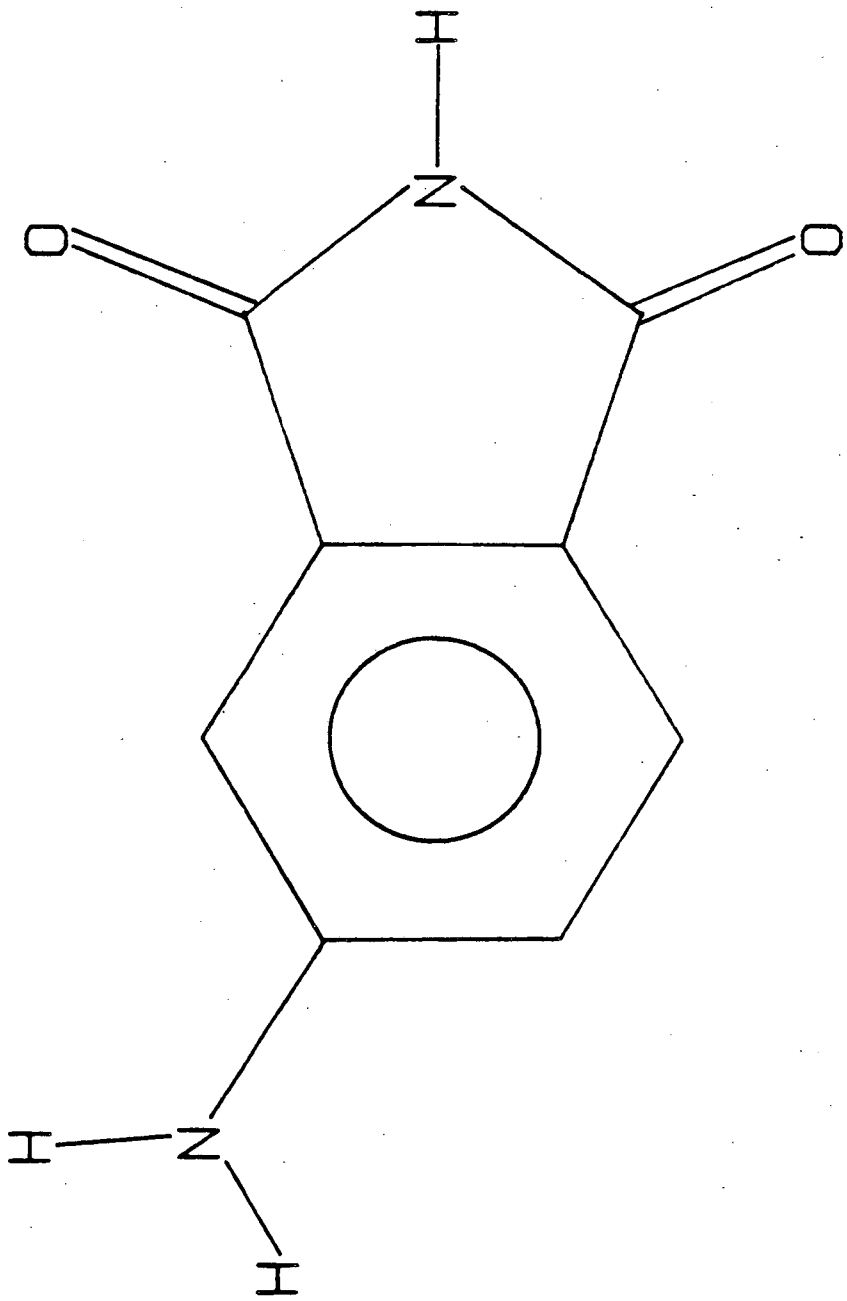

Chapter 2

Experimental

In order to follow the solvation processes, a fluorimeter with picosecond time resolution is necessary. This chapter describes the materials, steady-state spectra, and the instrumentation involved in the "picosecond fluorimeter".

A. Materials

Most solvents were purchased as spectrophotometric grade and used without further purification. The exceptions were formamide and N-methyl-formamide. These solvents were distilled under vacuum from CaO. The aminophthalimides were recrystalized twice from methanol. The pure solvent work described in Chapter 3 was done with an aminophthalimide concentration of 10^{-3}M. The mixed solvent work in Chapter 4 was done with a 4-aminophthalimide concentration of 1.2 x 10^{-4}M except where otherwise indicated. The solutions were not purged of oxygen unless noted. No change in the fast time dynamics was noted after deoxygenation of the solvent, although there was a change in fluorescence lifetime for some solvents (see Chapter 4).

B. Steady-State Spectra

Emission and excitation spectra were taken on a SPEX Fluorolog II. Absorption spectra were taken on a Beckman model 25 spectrophotometer. For all of the aminophthalimides, the absorption and fluorescence excitation spectra were found to match exactly, so the fluorescence excitation spectra are shown in ensuing chapters. Absorption spectra and fluorescence excitation spectra were always taken and compared in order to confirm this finding and to check for impurities. Most solutions would last up to 4 weeks, but before using an older solution, its spectra would be compared to the original ones.

C. Laser System

The light source for the "picosecond fluorimeter" experiments was a modified passively and actively modelocked Quantel YG400 Nd:YAG laser which emits 1064-nm light at a pulse repetition rate of 10Hz. The cavity of the laser is shown in Figure 2.1. The laser was used in its commercially available form, with a few changes. These changes will be briefly described here. The entire laser system has been described in detail elsewhere[13,14]. First, the original stirring dye cell mechanism was replaced by a flowing dye cell. The dye used in the flowing dye cell was Eastman Kodak 9740, dissolved in Q-switch grade 1,2-dichloroethane. The dye concentration was adjusted to maintain a pulse train of 10-12 pulses (counted from 10% of maximum intensity). Second, higher quality optics as well as more stable mounts were used throughout the cavity to improve stability and ease of alignment. Third, a larger and more temperature stable circulating water supply than the one available from Quantel was substituted to prevent cycling of the cavity output power.

The path of the laser is shown in Figure 2.2. One of the pulses toward the middle of the modelocked pulse train from the cavity was extracted by the Quantel PF302 pulse selector. Each selected pulse was 25±5 ps (FWHM) wide. This pulse was amplified in a Quantel 410-07 amplifier with a 1.4% doped Nd:YAG rod. A small fraction of the amplified pulse was used to trigger the streak camera. The rest of the 1064-nm light was delayed to allow the electronics of the streak camera and computer to turn on. The beam was then doubled with a KDP second harmonic generating crystal to 532 nm. The remaining 1064 nm was then summed with the 532 nm to produce 355-nm light. The 355-nm exciting beam was separated from the remaining 532-nm and 1064-nm beams with a prism. A small fraction of the 355 nm pulse was split off with a beam splitter and sent directly into the streak camera to act as a time marker as well as to provide pulse diagnostics. This pulse is called the prepulse. The majority of the beam was sent through a polarizing prism to insure a vertically-polarized exciting beam, and was then focused

Figure 2.1 Diagram of Actively and Passively Mode-Locked Nd:YAG Laser Cavity

The abbreviations and distances between optical elements are included in the diagram.

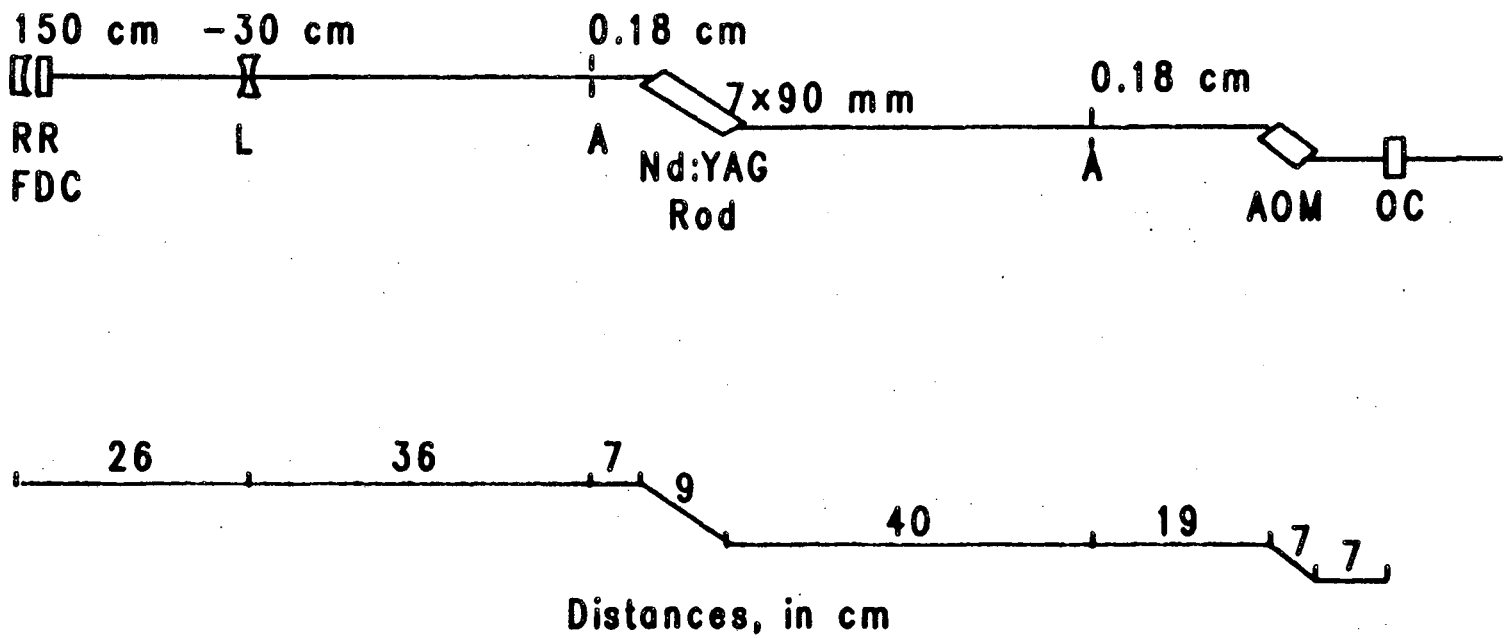

Figure 2.1

RR: Rear Reflector

FDC: Flowing Dye Cell

L: Lens

A: Aperture

AOM: Acousto-optic Modulator

OC: Output Coupler

down into the sample. The variable delay line was used to coordinate the timing of the fluorescence signal with the prepulse when changing streak speeds on the streak camera.

The fluorescence from the sample was collected at a right angle to the excitation pulse through another polarizing prism and was imaged along with the prepulse onto the streak camera entrance slit. A 10 nm bandpass filter could be placed in the path of the fluorescence to select a particular wavelength of emission for detection. For most data acquisitions, the polarizing prism on the detection side of the sample was set at the magic angle (54.7°) with respect to the incident excitation beam. The prism could easily be put at 90° (horizontal) or 0°(vertical) to do rotational reorientation studies (see Chapter 3).

D. Ultrafast Streak Camera

The streak camera detection device was a Hadland Photonics Ltd, Imacon 500 coupled with a Tracor Northern IDARSS diode array detector. The calibrations and details of the streak camera are given elsewhere[15,16]. Basically, the streak camera changes incident photons into electrons. As a first step, a voltage ramp streaks the electrons across a phosphor screen; the rest of the stages in the camera amplify this signal. The images out of the streak camera thus provide a record of intensity versus time. The steak rate of the camera can be changed to allow a large range of times to be examined. The resolution of this streak camera system is 4 ps.

Data collection was controlled by an LSI 11/73 computer capable of taking data at a rate of three streak records per second. The computer determined whether or not a data point was good by looking at the intensity and width of the prepulse. Each data set was the average of 750 successful laser shots. An example of data taken by this system is shown in Figure 2.3. The initial pulse is the prepulse which was separated from the fluorescence signal by the variable delay. The computer aligned each of the 750 streak camera traces by lining up the peak of the prepulse; this process eliminated the time jitter of the streak camera. The prepulse was also used to deconvolute data that had time constants comparable to the width of the laser pulse.

Figure 2.2 "Picosecond Fluorimeter" Apparatus

Diagram of the path of the Nd:YAG picosecond laser and the detection optics with streak camera are shown here. Abbreviations used are: SHG-Second Harmonic Generator, THG-Third Harmonic Generator, BS-Beam Splitter, F-Filter, GT-Prism Polarizer, L-Lens.

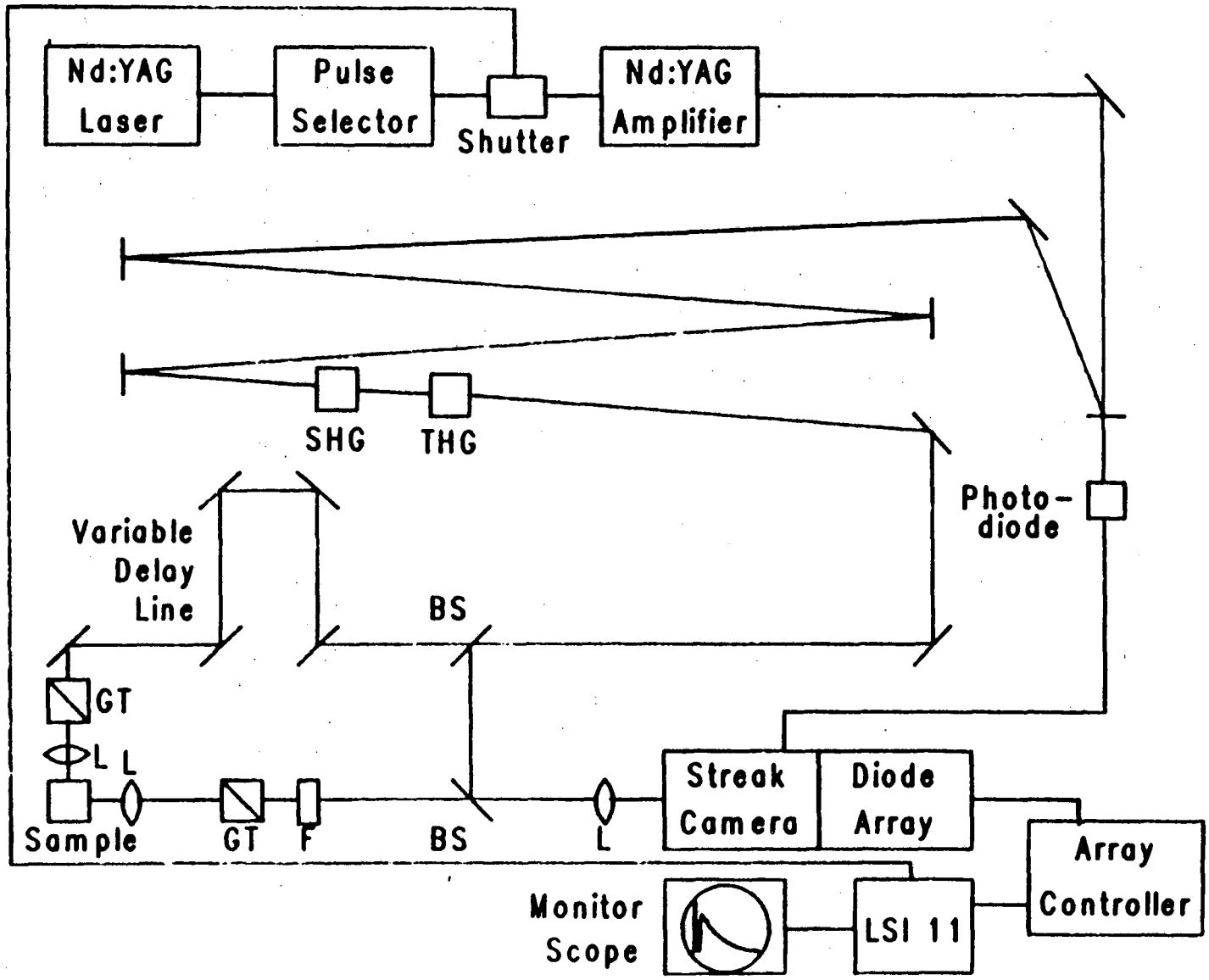
Nd:YAG Laser
Pulse Selector
Shutter
Nd:YAG Amplifier
SHG
THG
Photo-diode
Variable Delay Line
BS
GT
L
L
Sample
GT
F
BS
L
Streak Camera
Diode Array
Array Controller
Monitor Scope
LSI 11

Figure 2.2

Figure 2.3 Sample Data from the Picosecond Laser/ Streak Camera Apparatus: 4AP in 1-Propanol at 500 nm

The initial pulse centered at 100 ps is the prepulse described in the text. The fluorescence signal starts at about 300 ps with a rise of 16 ps and two falls of 142 and 11000 ps. The variables used in the fits are the rise and fall times with amplitudes along with time zero, the time between the prepulse and the signal. Here, time zero was found to be 193 ps.

Figure 2.3

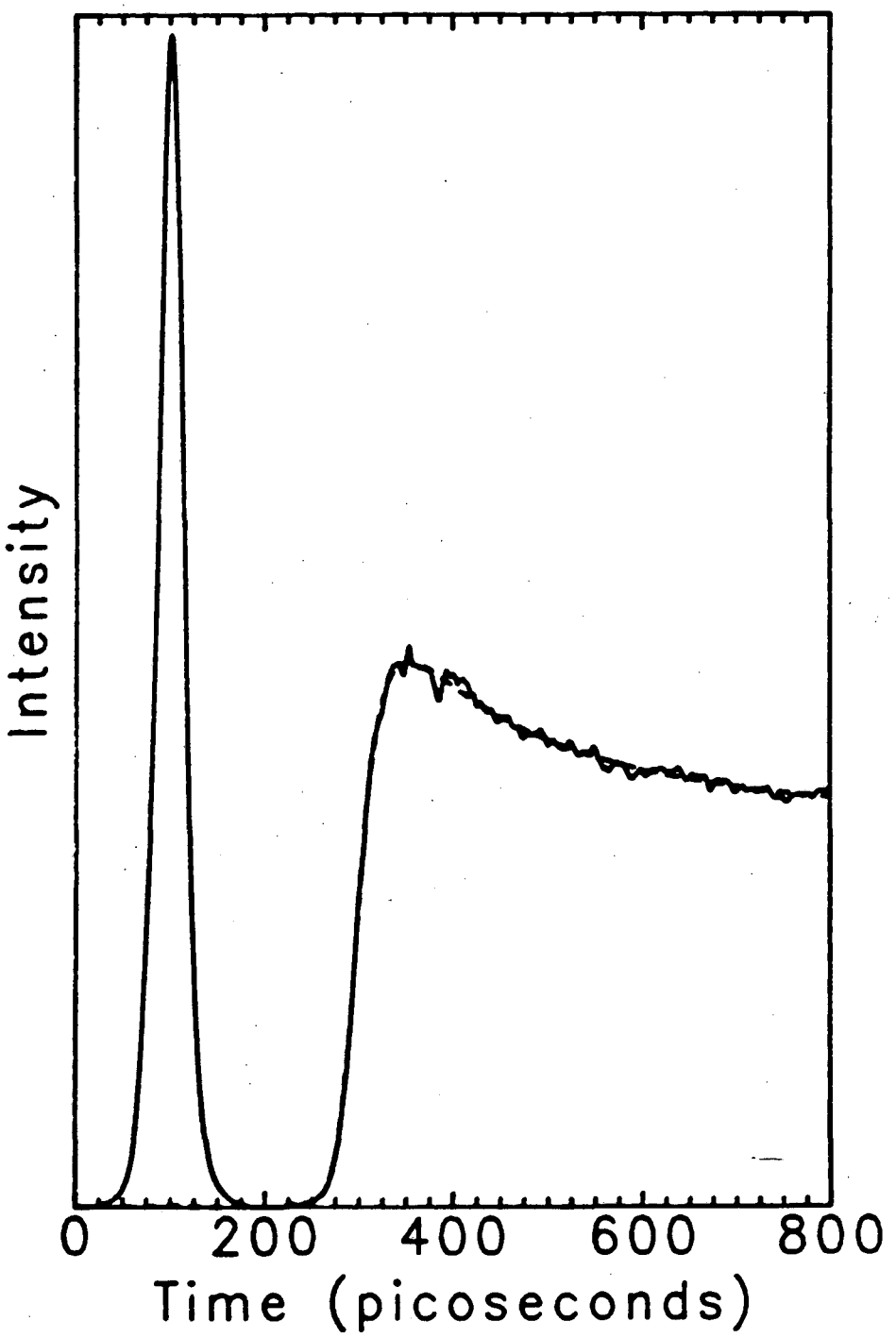

E. Analyses of the Data

For single exponential long lifetime data, analysis was simple. A plot of the natural logarithm of the intensity versus time gives a slope of the fluorescence lifetime. For multi-exponential data with one or more lifetimes comparable to the width of the exciting pulse, a convolute and compare technique called Simplex[17] was used with the prepulse as the model for the exciting pulse. This technique minimized the sum of the squares of the residuals. The fitting routine could fit up to three exponentials for each data set, although one of these was always the fluorescence lifetime of the molecule, which was independently determined. Another variable was time zero, the time between the prepulse and the fluorescence of the sample. Time zero could change for a set delay length depending on wavelength of detection and number of filters in each beam.

If data were taken at every 10 nm for a given sample, a series of intensity versus time spectra at various wavelengths would be seen. In order to see the evolution of the fluorescence spectrum of a molecule, one needs to cut across the other direction to get intensity versus wavelength at various times. The fit parameters for a particular wavelength were analytically integrated over time and normalized to the region of the steady-state spectrum which corresponded to the interference filter profile for the wavelength. These normalization factors insured that the steady-state spectrum was reproduced. The factors took into account the wavelength dependent response of the streak camera and filter, and intensity changes of the exciting beam. The spectrum at a certain time was obtained by taking the intensity at that time at all wavelengths and multiplying each wavelength by its normalization factor.

Quantitative solvation times were obtained by fitting each intensity versus wavelength spectrum to a Gaussian in energy using as variables the position maximum, height and width of the Gaussian. From these fits, fluorescence maxima versus time and width versus time plots could be obtained. The fluorescence maxima versus time plots were fit to two or three exponentials using the Marquardt Method[18], a least squares fitting routine. The

fits took the form

$$E(t) - E_{\infty} = \alpha_1 \, exp(-t/\tau_1) + \alpha_2 \, exp(-t/\tau_2) + \alpha_3 \, exp(-t/\tau_3). \qquad 2.1$$

The E_{∞} value was obtained by taking the maximum of the Gaussian fit at a long time compared with the solvation dynamics.

Examples of all the data fits and calculated plots will be given in the following chapters. As will be seen, the instrumentation and fitting routines are powerful tools for investigating the solvation process.

Chapter 3

4-Aminophthalimide Fluorescence in Pure Solvents

A. Introduction

Ware et al.[11,12] were the first to measure the time dependence of the fluorescence of 4-aminophthalimide, but the extreme dependence of the position of the fluorescence maximum of the molecule on the solvent was well characterized by other workers. Shifts in steady-state spectra were seen by changing temperatures and by adding polar liquids to 4AP solutions of nonpolar solvents.[19,20,21] *Piterskaya*[22] used the temperature dependence of the fluorescence maximum to determine the ground state and excited state dipole moments of aminophthalimides. For 4AP the dipole moment changes from 3.5 to 7.1 Debye with a change in direction of 20 °. This change in magnitude and direction makes the 4AP molecule a candidate for a molecular probe of a polar solvent environment.

Ware et al.[11,12] used a nanosecond flash lamp and single-photon counting to do his studies on 4AP. A 5 ns pulse restricted his work to low temperatures and very viscous solvents. A time dependence of the maximum of the 4AP fluorescence in 1-propanol was first observed at -50 °C. Room temperature shifts of 4AP fluorescence could just be seen in the very viscous solvent glycerol. The shifts in time were attributed to an initial exciplex formation followed by the solvation of this newly formed exciplex. As evidence for an exciplex formation, *Ware et al.* noted large shifts and widening of the steady-state spectrum with only small amounts of 1-propanol added to solutions of 4AP in toluene. Exciplex formation would then take place during the subnanosecond relaxation that was observed. This relaxation was the shift from the maximum of fluorescence position of 4AP in 1-propanol at -196 °C to the first fluorescence maximum seen with the nanosecond time resolution. The observable spectral shift was then fit to a single exponential taking as the final fluorescence maximum the fluorescence of 4AP in 1-propanol at room temperature. These relaxation times as a function of temperature were then compared with the temperature dependence of the dielectric relaxation of the

1-propanol. The dielectric relaxation of 1-propanol was found to be longer than the measured relaxation times.

These results were the extent of the analysis of *Ware et al.*, but *Mazurenko*[23] chose to look at the data of *Ware et al.* in another way. He fit the data to three exponentials and then correlated these exponentials to the three dielectric relaxation times of 1-propanol. For this analysis, *Mazurenko* did not believe that exciplex formation was needed to explain the data.

By examining the spectral shift of 4AP with picosecond time resolution, these solvation processes can be followed at room temperature. Not only can what is occurring in the excited-state of 4AP be determined, but also a handle can be obtained on the excited-state solvation processes mentioned earlier.

B. Steady-State Spectra

Before examining the picosecond dynamics of 4AP, several questions involving the steady-state properties need to be answered. *Ware et al.*[12] and *Bakshiev et al.*[20] obtained different fluorescence maxima for 4AP in 1-propanol. After repeating these experiments, we agreed with the results of *Ware*. The steady-state fluorescence spectra for 4AP in toluene and in 1-propanol are shown in Figure 3.1. The spectrum is seen to shift nearly 100 nm from 429 nm in the lesser interacting solvent toluene to 525 nm in 1-propanol. The absorption spectrum also shifts. Figure 3.2 shows the corresponding fluorescence excitation spectra for 4AP in 1-propanol and toluene. The shift in the maximum here is from 351 nm in toluene to 373 nm in 1-propanol. The energy shift in the excitation spectra is 1680 cm^{-1} compared with 4262 cm^{-1} in the emission spectra, indicating that the red shift in the emission is not all due to a systematic shift of the electronic energy levels. Peak maxima and widths of fluorescence spectra of 4AP in a series of solvents are listed in Table 3.1.

Some information about the cause of this large shift in the fluorescence of 4AP can be obtained from steady-state emission and absorption spectra. Comparing spectral shifts

Figure 3.1 Steady-State Emission Spectra for 4AP in 1-Propanol and Toluene

Both spectra were taken with an excitation wavelength of 355 nm. The maximum in toluene is 429 nm and in 1-propanol, 525 nm. This shift is 4264 cm^{-1}. Emission maxima for the fluorescence of 4AP in other solvents are listed in Table 3.1.

Figure 3.1

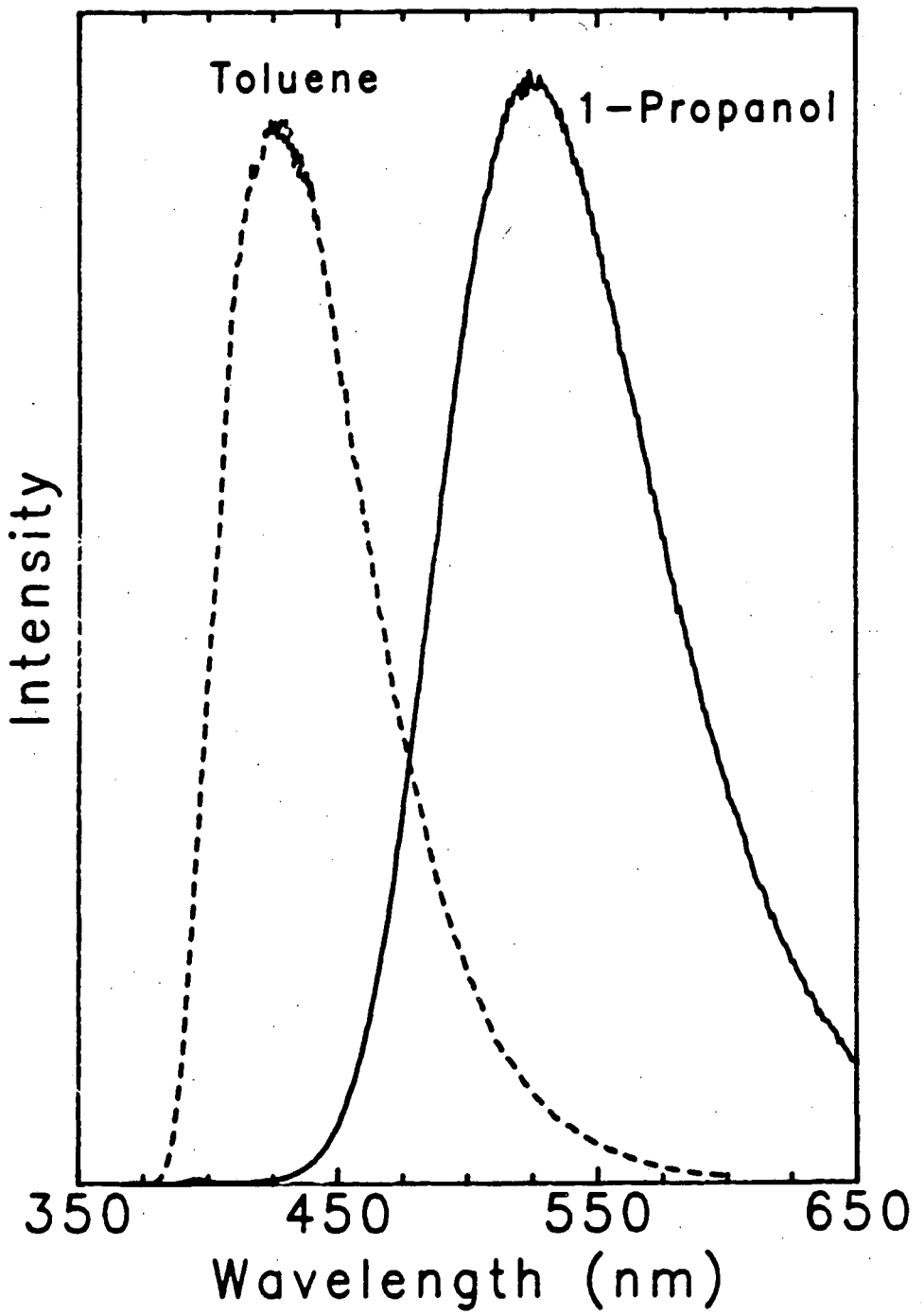

Figure 3.2 Steady-State Excitation Spectra of 4AP in 1-Propanol and Toluene

The excitation spectra were taken with the emission wavelength set at the maximum of 4AP in the solvent used. The maximum of the lowest energy absorption for 4AP is 351 nm in toluene and 373 nm in 1-propanol. This shift is 1680 cm^{-1}. Absorption maxima of 4AP in other solvents for this peak are listed in Table 3.1.

Figure 3.2

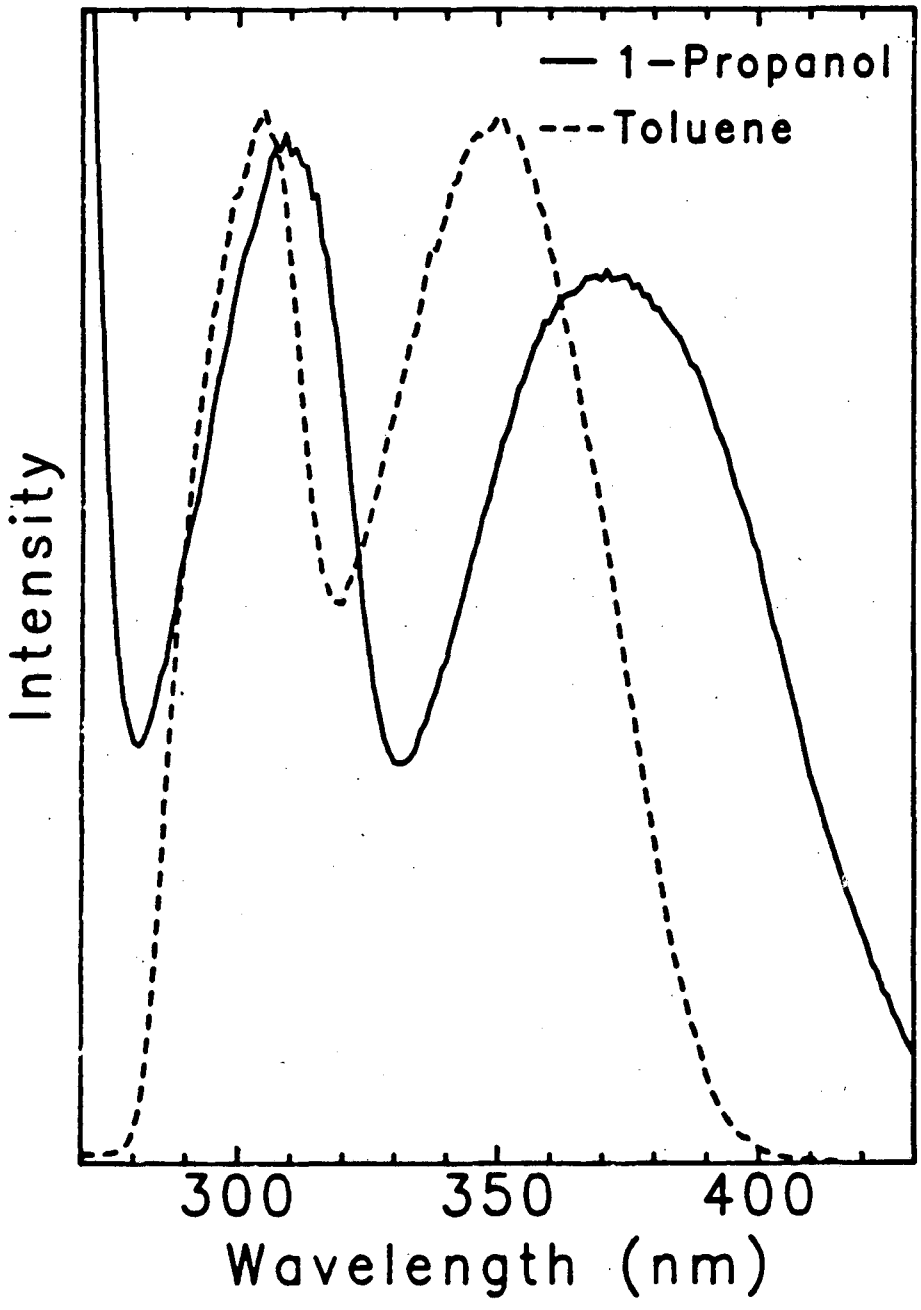

Table 3.1

Fluorescence Emission and Excitation Maxima for 4AP in Various Solvents

Solvent	Emission Maximum (nm)	Emission FWHM (cm^{-1})	Excitation Maximum (nm)
Toluene	429	3655	351
Dioxane	450	3269	354
THF	453	3608	360
Acetonitrile	474	4104	357
DMSO	483	3269	375
N-Methylformamide	517	4137	370
1-Octanol	519	3489	371
1-Pentanol	521	3476	372
1-Butanol	522	3885	369
2-Propanol	520	3442	371
1-Propanol	525	3538	373
Ethanol	525	3913	371
Methanol	532	4050	369

of solutes to physical properties of the solvent such as dielectric relaxation constant, viscosity, or dipole moment is often fruitless. Although comparisons show trends, alone, a single physical property of a solvent cannot address solvent-solute interactions. An empirical solvent polarity parameter, $E_T(30)$, has been developed to take into account any dipole-dipole interactions, hydrogen-bonding effects, self association of the solvent, etc.[24,25] For a given solvent, this $E_T(30)$ value is determined by taking the peak of the $\pi - \pi^*$ absorption of pentaphenyl pyridiniumphenolate dye (Figure 3.3). The $E_T(30)$ value for a solvent is obtained from the maximum of absorption of this molecule:

$$E_T(30)(kcal/mole) = 2.859 \times 10^{-3}/\lambda_{max}(cm)$$

This molecule has one of the largest shifts in absorption maximum with a change in solvent polarity and is soluble in different kinds of solvents. For a polar, hydrogen-bonding solvent, the ground state of the dye is significantly lowered by solvation of the separated charge, so absorptions are of higher energy when compared with absorptions of the dye in a nonpolar solvent. These $E_T(30)$ values are available for many pure solvents as well as mixed solvents.[26,27]

Kosower et al.[28,29] used these $E_T(30)$ parameters to propose a two state model for the mechanism of red shift of the emission of 6-N-4-methylphenylamino-2-naphthalene-sulphonic acid N,N-dimethylamide (TNSDMA) (Figure 3.4). In a nonpolar solvent, the ground state geometry prevails in the excited state: the aryl ring is out of the plane of the naphthalene ring. *Kosower* refers to this excited state as the $S_{1,np}$ state. In a polar solvent, the aryl group conjugates with the lone pair on the N and transfers an electron to the naphthalene ring, the $S_{1,ct}$ state. A plot of emission maximum versus $E_T(30)$ for dioxane:water mixtures gave two distinct lines (Figure 3.5). The line at low $E_T(30)$ values (low polarity of the solvent) represents the emission from the $S_{1,np}$ state, and the higher $E_T(30)$ values represent the $S_{1,ct}$ state. A plot of emission quantum yield versus $E_T(30)$ shows similar effects. Since the charge transfer state has a lower quantum yield than the S_1, np state, a sudden drop off in quantum yield is seen where the emission begins

Figure 3.3 Structure of Pentaphenyl Pyridinium Phenolate Dye

The absorption peak for this molecule is used to determine $E_T(30)$ values for solvents.

Figure 3.3

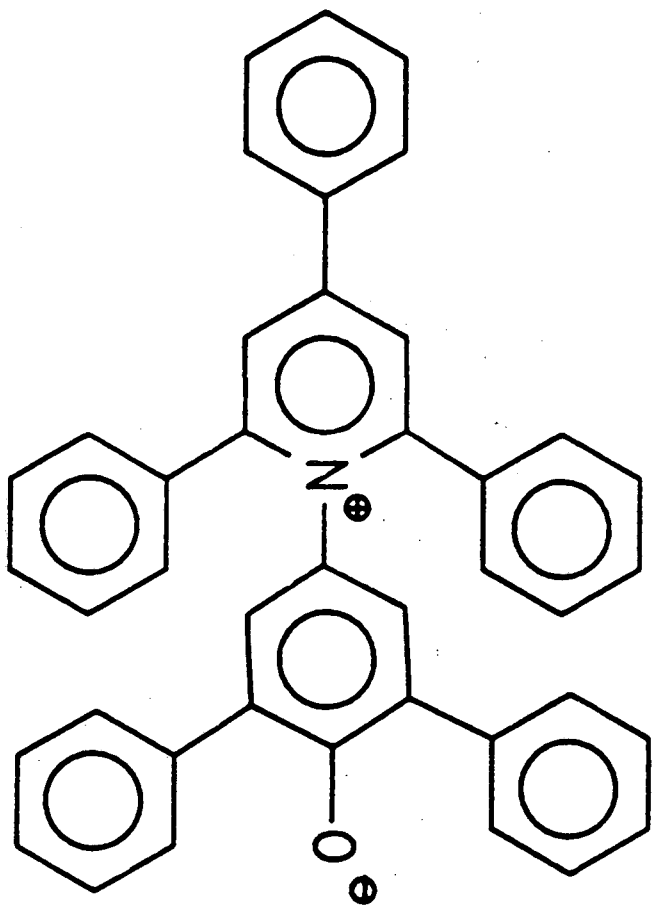

coming mainly from the twisted charge transfer state (Figure 3.6).

This type of $E_T(30)$ plot was done for 4AP in dioxane:water mixtures to ensure that the red shift was not due to a two state emission. Table 3.2 contains $E_T(30)$ values and 3AP and 4AP emission peaks for these mixtures along with the relative quantum yields for the 4AP emissions. Plots of the emission maxima versus $E_T(30)$ are shown in Figure 3.7 for 4AP and in Figure 3.8 for 3-aminophthalimide (3AP). Neither solute molecule displays the two state behavior seen in TNSDMA by *Kosower*. Nor are the functions linear indicating that the emissions are not from a single state, but perhaps from a continuum of states as would be seen in a solvation process. The curvature of the plots are opposite from the curvature of the plot for TNSDMA. This curvature implies that as water molecules are added, the solute molecule becomes less sensitive to them. Thus, the environment around the solute molecule is probably richer in the polar solvent than the bulk solution. This result will be discussed in detail in Chapter 4. The relative quantum yields versus $E_T(30)$ for 4AP in these mixtures are shown in Figure 3.9. For 4AP, a continual drop in the quantum yield is seen instead of the sudden drop off observed by *Kosower* for TNSDMA. The time dependence of the fluorescence will give further evidence of a continuum of emitting states.

C. Fluorescence Lifetimes

Fluorescence lifetimes for 4AP have been measured in many solvents[30]; results are listed in Table 3.3. No wavelength dependence for the fluorescence lifetime was seen for any solvent. Examples of the fluorescence lifetime data at both the blue and red side of the steady-state fluorescence spectrum of 4AP in 1-propanol are shown in Figure 3.10. The long lifetime is the same at all detection wavelengths and is easily obtained by taking the slope of the log plot of the data in Figure 3.10. The result of 11.0 ± 0.5 ns for 4AP in 1-propanol is shown in Figure 3.11.

Figure 3.4 Structure of 6-N-4-methylphenylamino-2-naphthalenesulphonic Acid N,N-Dimethylamide (TNSDMA)

According to *Kosower et al.*[28,29] the TNSDMA molecule has two excited states which can change relative energies of emission depending on the solvent. In the ground state the aryl group is out of the naphthalene plane. In a nonpolar solvent in the excited state, the excited-state geometry is no different from the ground-state geometry, the $S_{1,np}$ state. In a polar solvent the aryl group of the excited molecule can conjugate with the lone pair on the N and transfer an electron to the naphthalene ring, the $S_{1,ct}$ state.

Figure 3.4

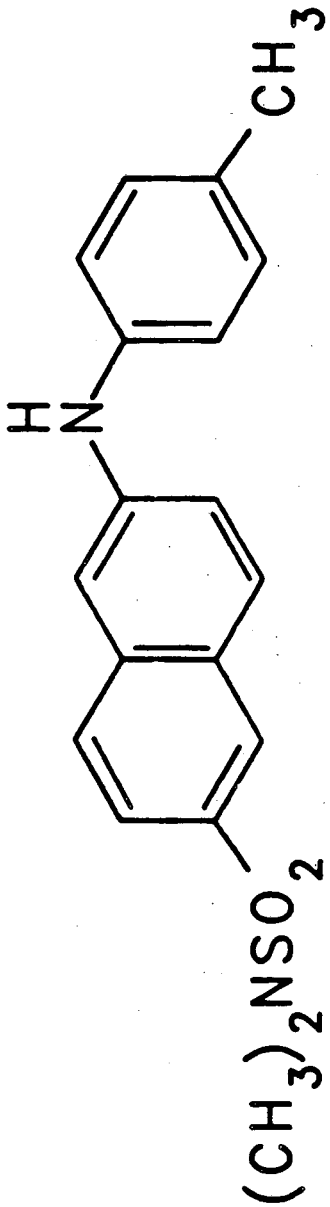

Figure 3.5 The Two State Emission from TNSDMA: Emission Maxima as a Function of $E_T(30)$ Values for Dioxane:H_2O Mixtues

The solid line is emission from the $S_{1,np}$ state of TNSDMA described in the text, and the dashed line is emission from the $S_{1,ct}$ state. The data are from reference 28.

Figure 3.5

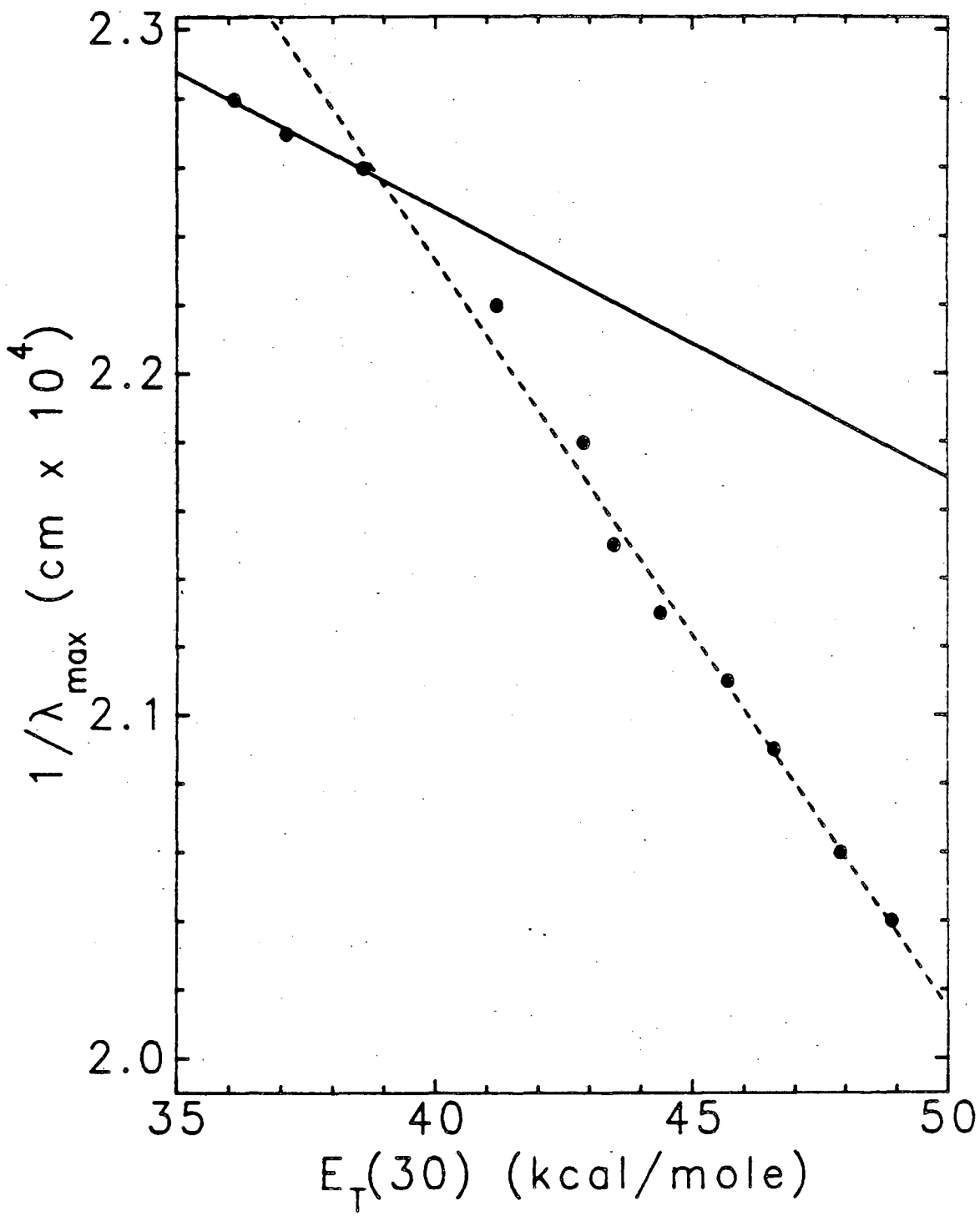

Figure 3.6 Quantum Yield of TNSDMA Emission as a Function of $E_T(30)$ for Dioxane:H_2O Mixtures

The quantum yield of the emission falls off after the formation of the $S_{1,ct}$ state becomes favored. Data are from reference 28.

Figure 3.6

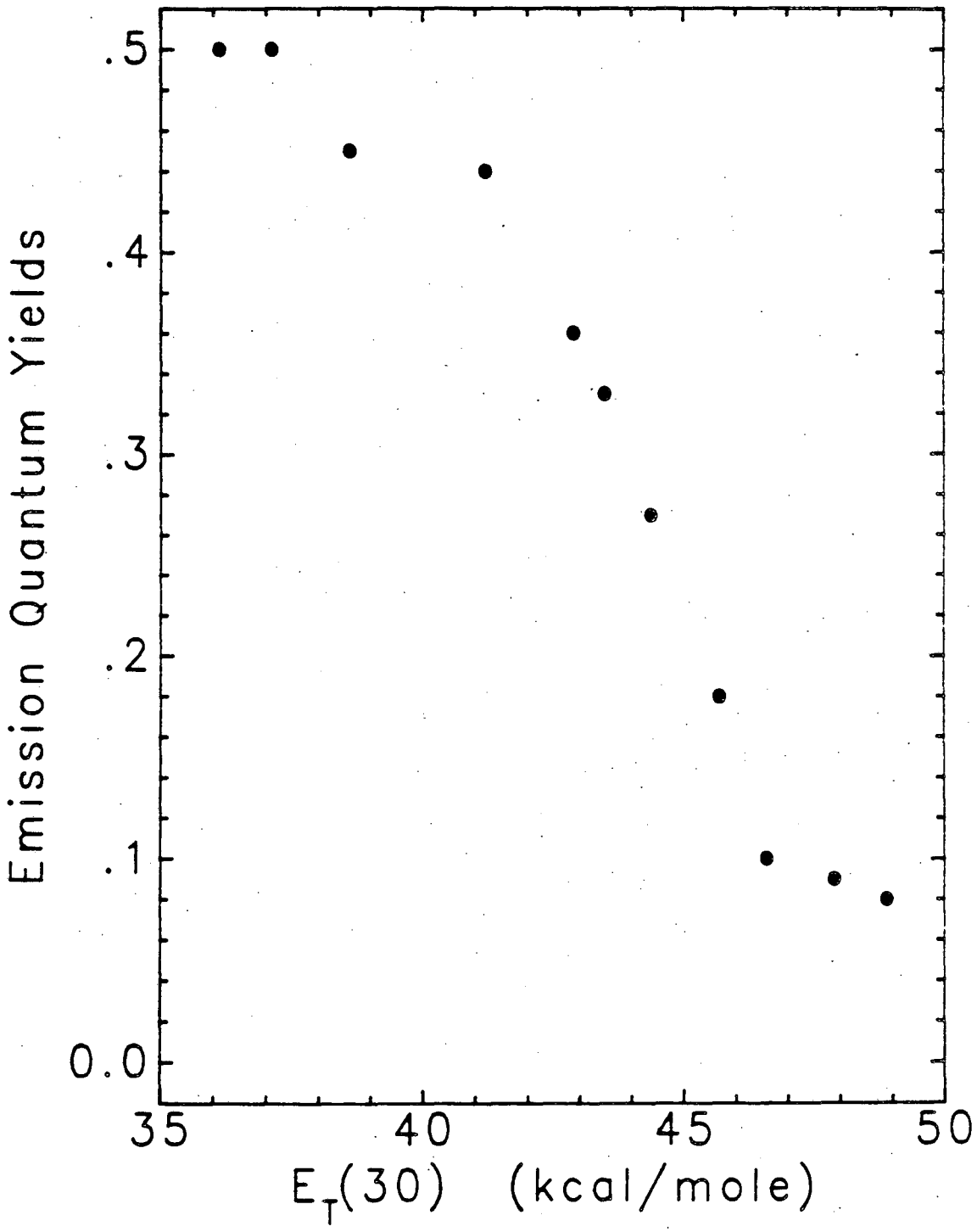

Table 3.2

Fluorescence Maxima and Quantum Yield versus $E_T(30)$ for Dioxane:Water Mixtures

Dioxane:H_2O % by volume	$E_T(30)$ * kcal/mole	λ_{max}(nm) 4AP	Relative Quantum Yield of 4AP	λ_{max}(nm) 3AP
100:0	36.0	450	2.57	448
98:2	41.4	484	2.12	461
96:4	42.9	495	1.79	468
94:6	44.5	504	1.50	471
92:8	45.9	508	1.39	474
90:10	46.7	512	1.26	476
80:20	49.0	521	0.89	482
70:30	50.9	528	0.73	487
60:40	52.3	532	0.53	490
50:50	53.6	537	0.39	493
40:60	55.6	543	0.31	494
30:70	57.1	549	0.21	498
20:80	58.6	554	0.15	500
10:90	61.1	558	0.11	504
0:100	63.1	560	–	507

* These values are from reference 28.

Figure 3.7 Emission Maxima of 4AP versus $E_T(30)$ Values for Dioxane:H_2O Mixtures

This plot does not show the two state behavior observed in the fluorescence of TNSDMA, Figure 3.5. See text for explanations of the curvature of this plot. Data for this plot are listed in Table 3.2.

Figure 3.7

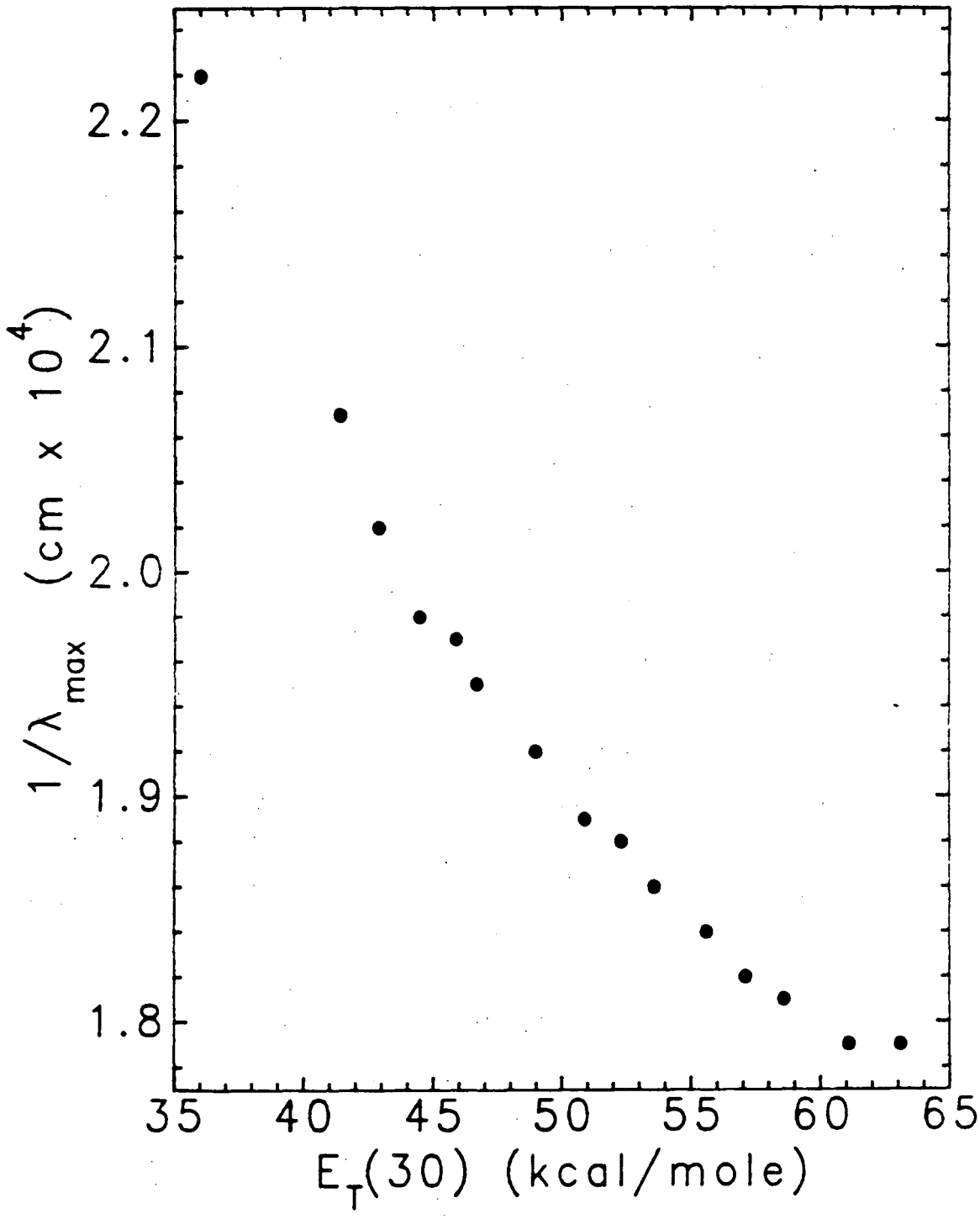
2.2
2.1
2.0
1.9
1.8
$1/\lambda_{max}$ (cm x 10^4)
35
40
45
50
55
60
65
$E_T(30)$ (kcal/mole)

Figure 3.8 Emission Maxima of 3AP versus $E_T(30)$ Values for Dioxane:H_2O Mixtures

This plot does not show the two state behavior observed in the fluorescence of TNSDMA, Figure 3.5. See text for explanations of the curvature of this plot. Data for this plot are listed in Table 3.2.

Figure 3.8

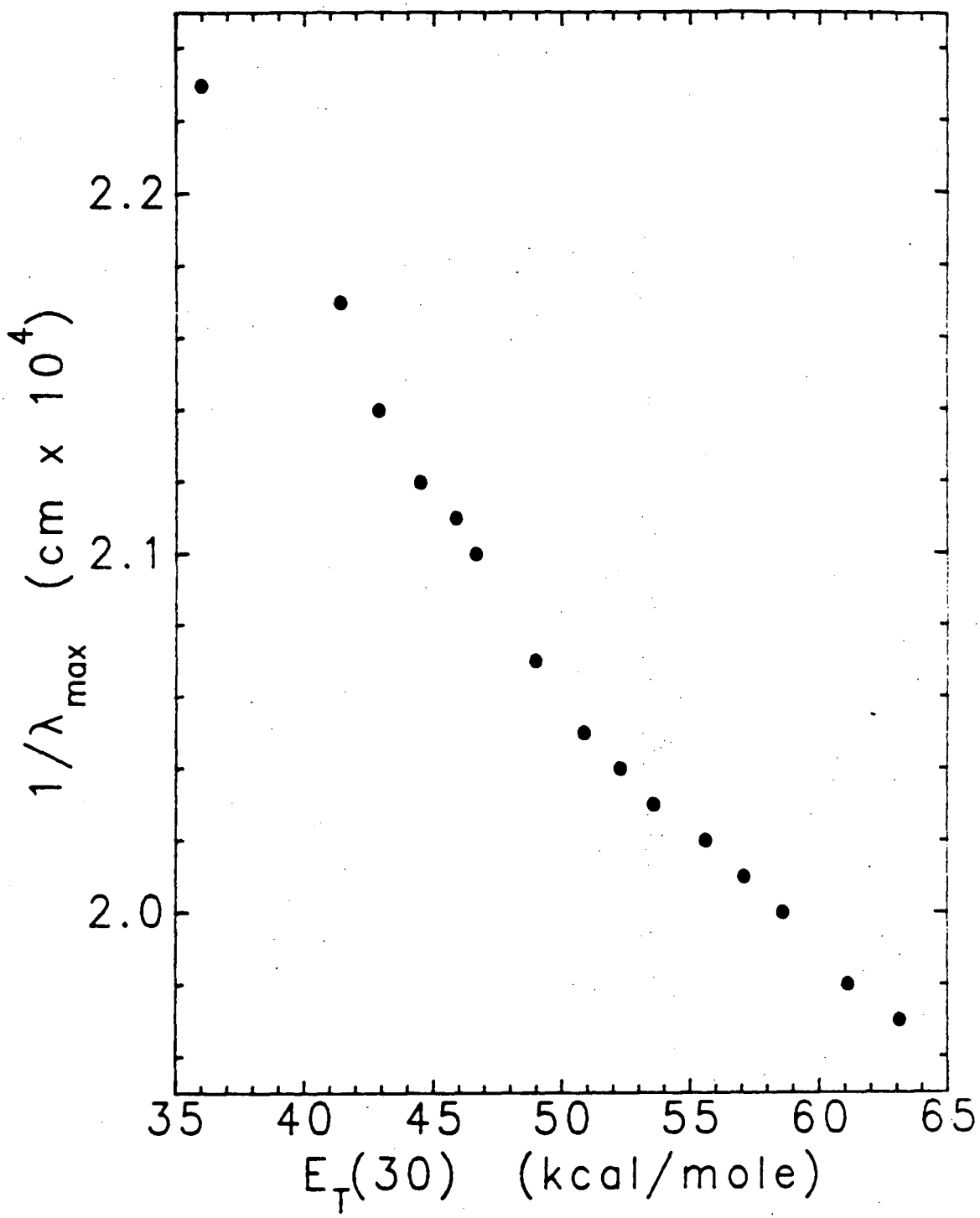

Figure 3.9 Relative Quantum Yield of Emission of 4AP versus $E_T(30)$ Values for Dioxane:H_2O Mixtures

This plot does not show the sudden drop of Figure 3.6, the quantum yield dependence on solvent polarity for TNSDMA. Data for this plot are listed in Table 3.2.

Figure 3.9

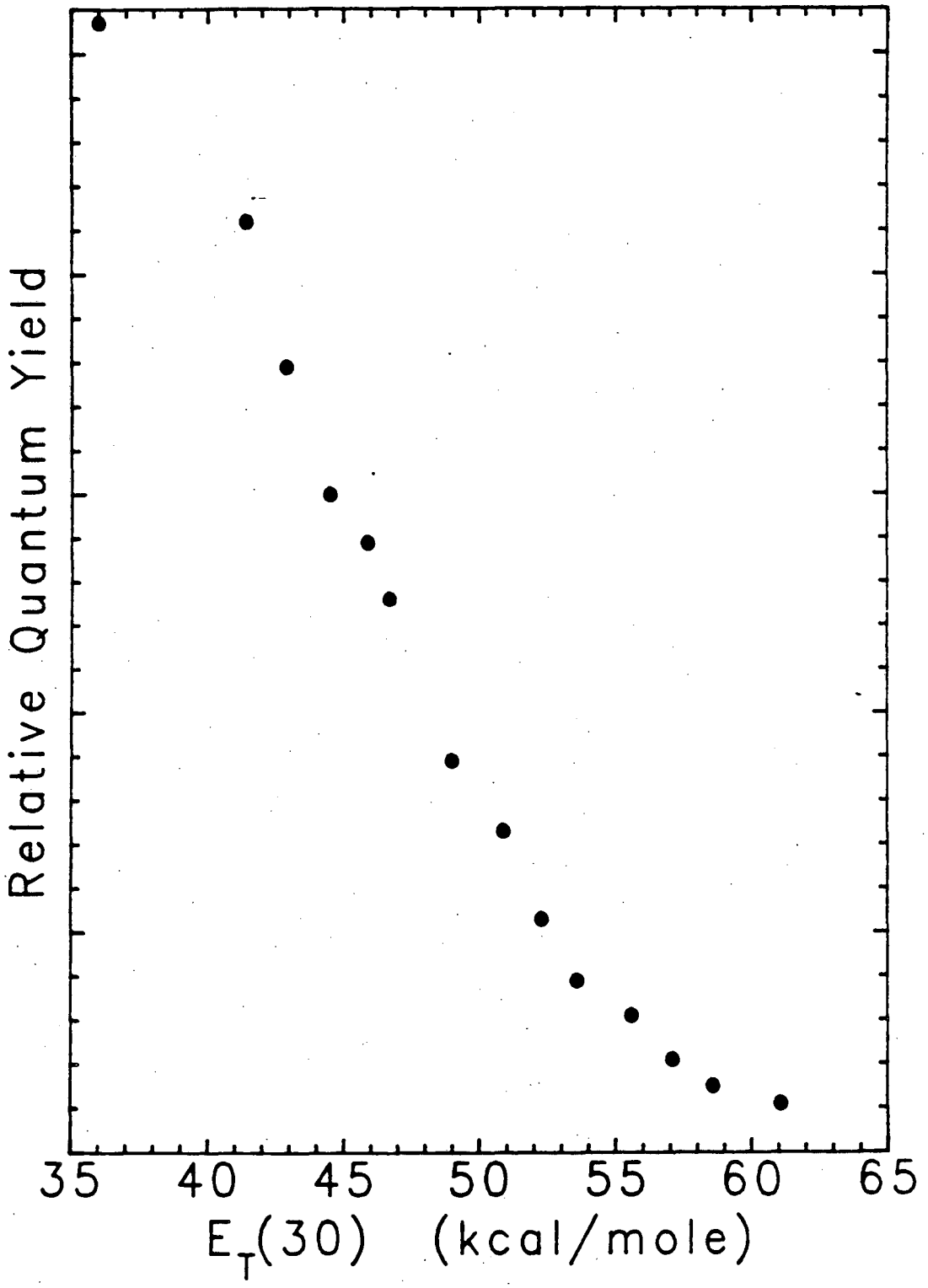

Table 3.3

Fluorescence Lifetime* of 4AP in Various Solvents

Solvent	Fluorescence Lifetime (ns)
Methanol	6.72 ± .29
Ethanol	10.26 ± .71
1-Propanol	11.00 ± .50
2-Propanol	12.13 ± .80
1-Butanol	11.58 ± .13
1-Octanol	12.80 ± .60
DMF	17.42 ± .73
Acetonitrile	15.00 ± .40
Dioxane	17.34 ± .64
Toluene	20.00 ± 1.6

* Results for solvents other than toluene and 1-propanol were obtained from reference 30.

Figure 3.10 Fluorescence Lifetime Data for 4AP in 1-Propanol

The solid line represents the lifetime data for 4AP in 1-propanol at 500nm, and the dashed line is the data for 4AP in 1-propanol at 620nm.

Figure 3.10

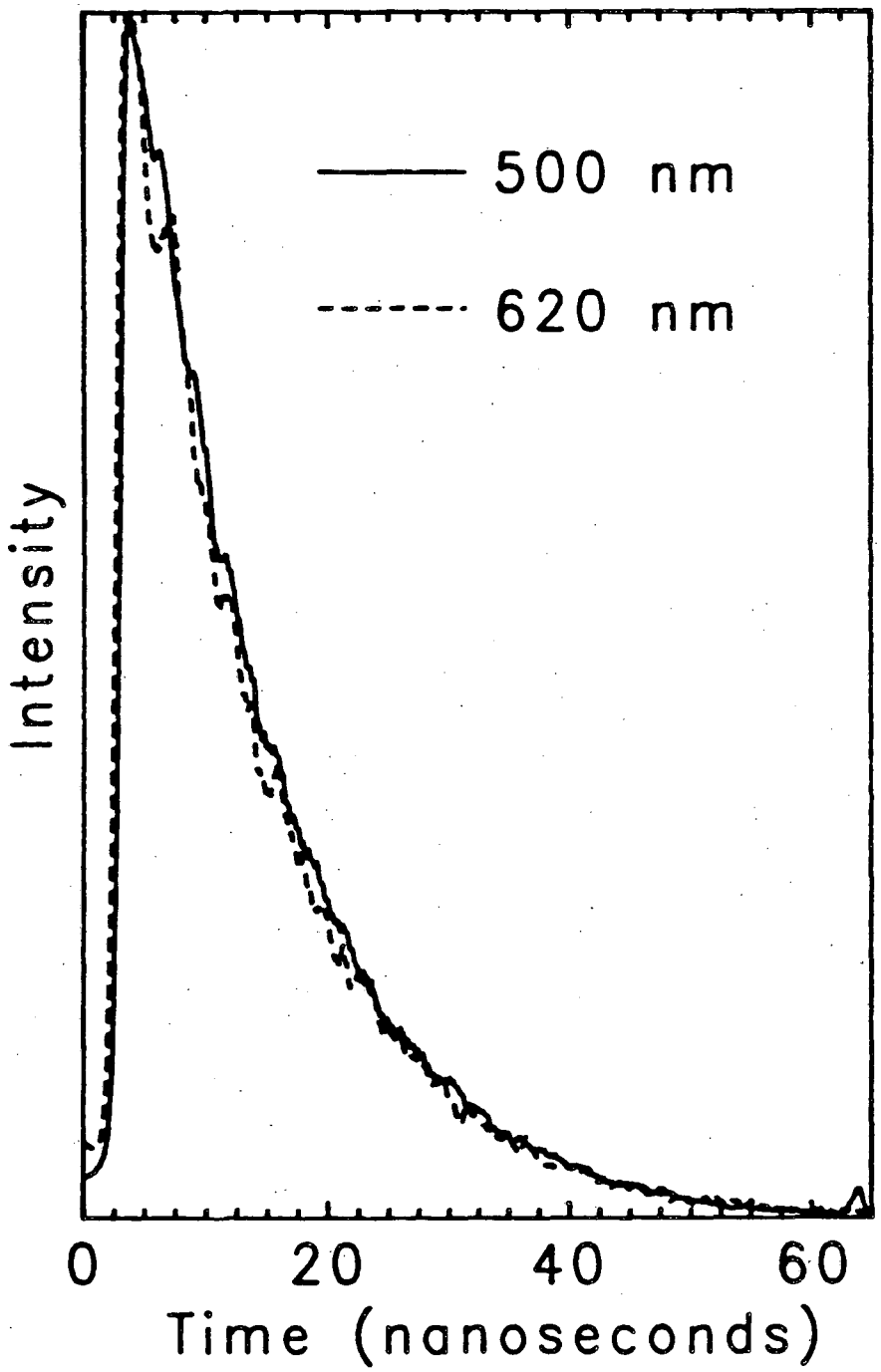

Figure 3.11 Log of the Fluorescence Lifetime Data for 4AP in 1-Propanol

The solid line represents the log of the lifetime data for 4AP in 1-propanol at 500nm and the dashed line is the data for 4AP in 1-propanol at 620nm. The lifetime of 4AP was found to be the same at all detection wavelengths. The slope of the line gives a lifetime of 11.0 ± 0.5 ns.

Figure 3.11

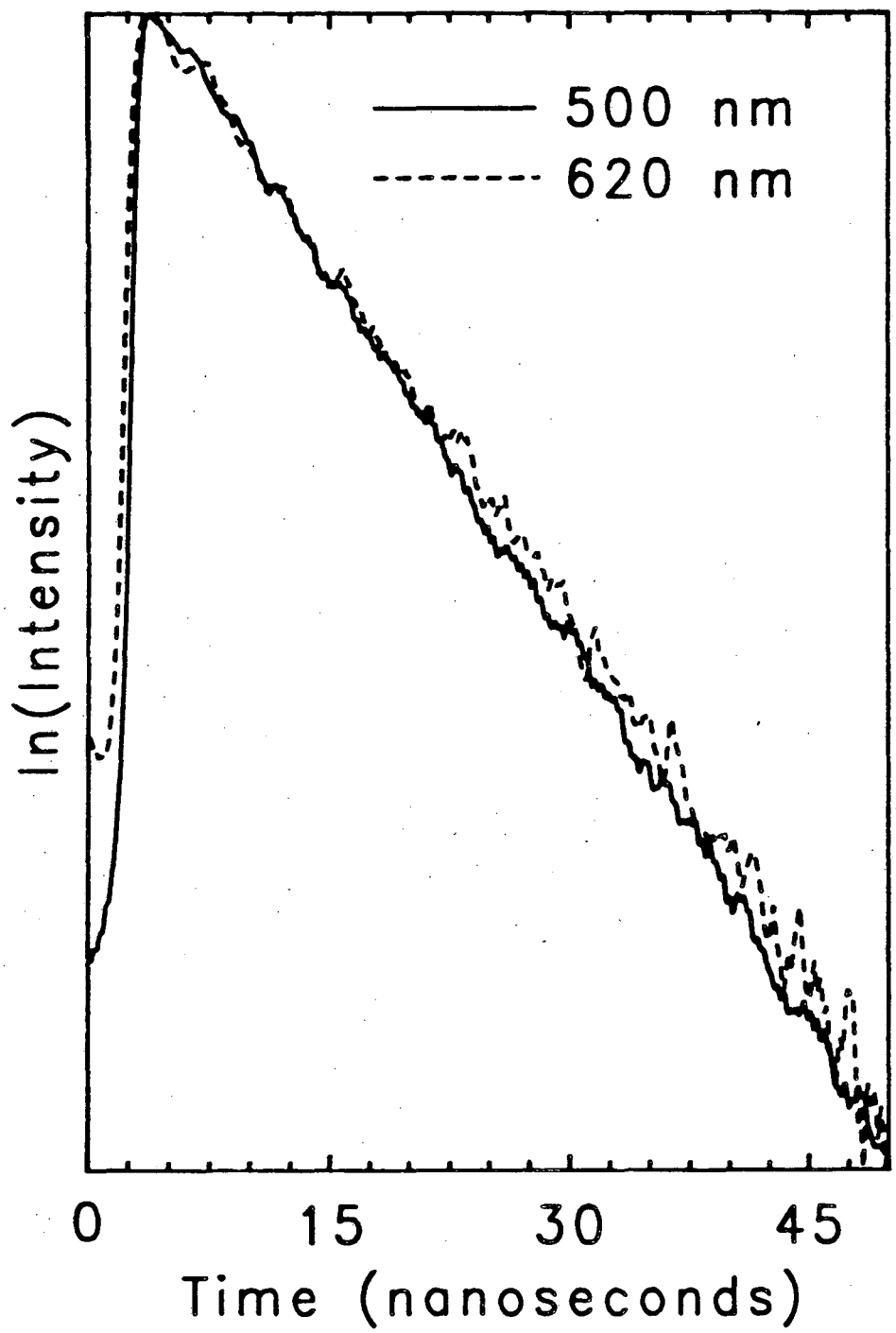

D. Fast Time Dynamics

1. 4-Aminophthalimide in 1-Propanol

Although both the red and blue edges of the 4AP in 1-propanol fluorescence have the same lifetimes, their fast time dynamics are vastly different. Figure 3.12 shows time-resolved spectra at these two wavelengths on an expanded time scale. The fast rise on the blue edge (500 nm) indicates an initial population at this wavelength, which decays at a rate of 142 ps. However, on the red edge (620 nm) there is a risetime of 96 ps. This type of red-shifted behavior is consistent with the model in Figure 1.2. The steady shift of the entire spectrum is easily seen in Figure 3.13. The numerical fit parameters for all of the wavelengths in Figure 3.13 are listed in Table 3.4. It is difficult to glean any physical information from these numbers, but the intensity versus wavelength dimension is very revealing (Figure 3.14). These spectra in time clearly show the gradual red shift of the emission spectrum. The shift occurs in about 200 ps, and the resulting population of excited molecules then decays away in time at a rate equal to the fluorescence lifetime of 4AP in 1-propanol.

Generating these time-dependent pictures of the fluorescence lifetime is a powerful tool for determining the nature of the emitting excited-state. The 4AP in 1-propanol spectra represent a continuum of emitting states as in Figure 1.2. If the same procedure is carried out for a known two state system such as the DMABN molecule[8,9] mentioned in the introduction, a completely different kind of behavior is seen. Figure 3.15 shows the intensity versus wavelength at various times for DMABN in acetonitrile which is capable of solvating the twisted internal charge transfer (TICT) state of DMABN. These spectra exhibit a definite isosbestic point with the decay rate on the blue side of the isosbestic point matched by the rate of rise of the spectrum on the red side. The time for this decay and rise is the time of formation of the TICT state. Although this time is easily measured by just the rise of one wavelength on the red edge, the spectra in Figure 3.15 give a better picture of the two state system. Certainly if the time dependence of the fluorescence of

Figure 3.12 Fast Time Dynamics of 4AP in 1-Propanol at the Red and Blue Edges of the Steady-State Spectrum

The 500 nm represents the blue edge of emission, and the 620 nm represents the red edge of the emission. The blue edge has a fall time of 142 ps, and the red edge has a rise of 96 ps.

Figure 3.12

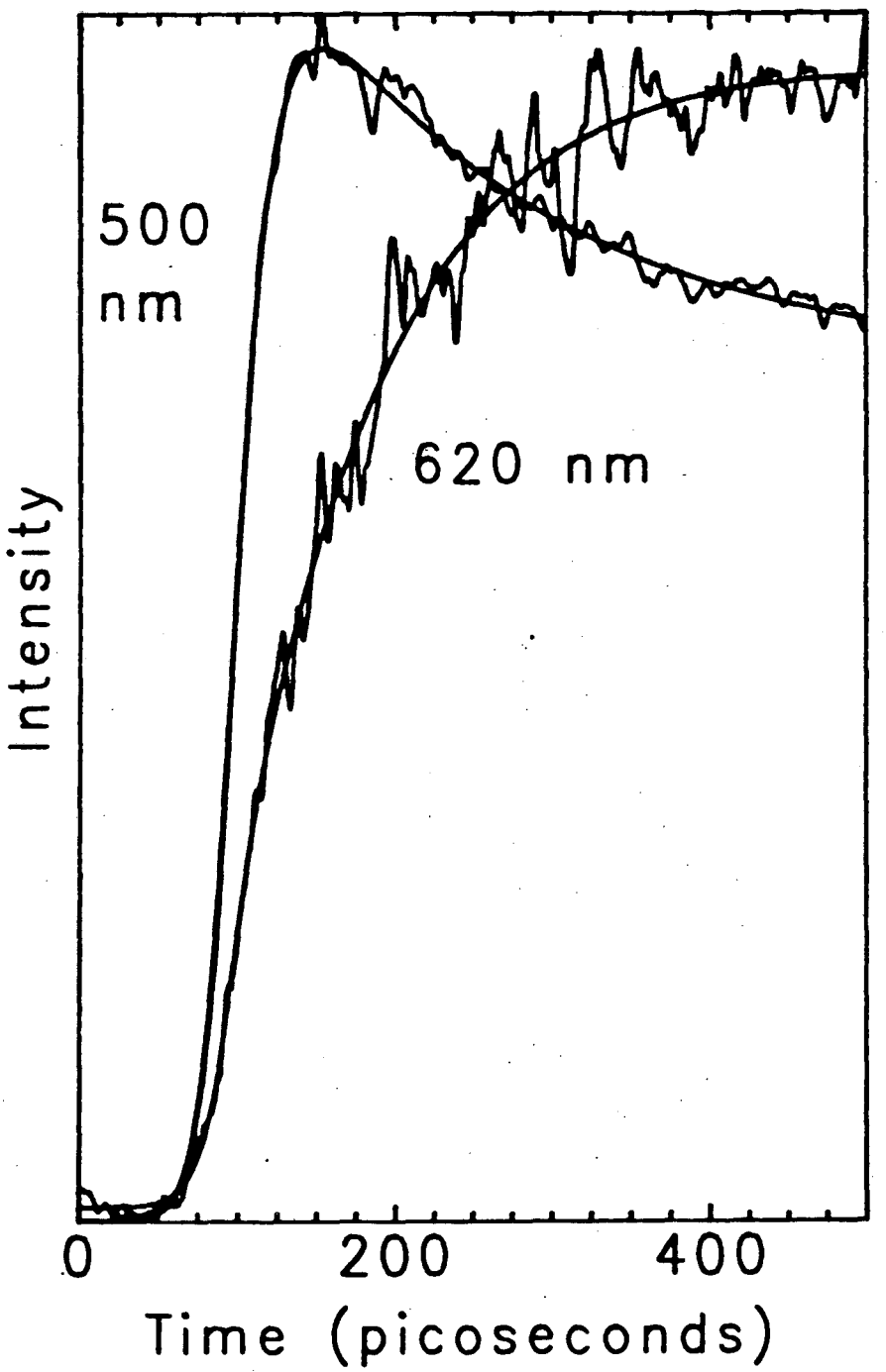

Figure 3.13 Fast Time Dynamics of 4AP in 1-Propanol for the Entire Spectrum

The fit parameters for this data are listed in Table 3.4.

Figure 3.13

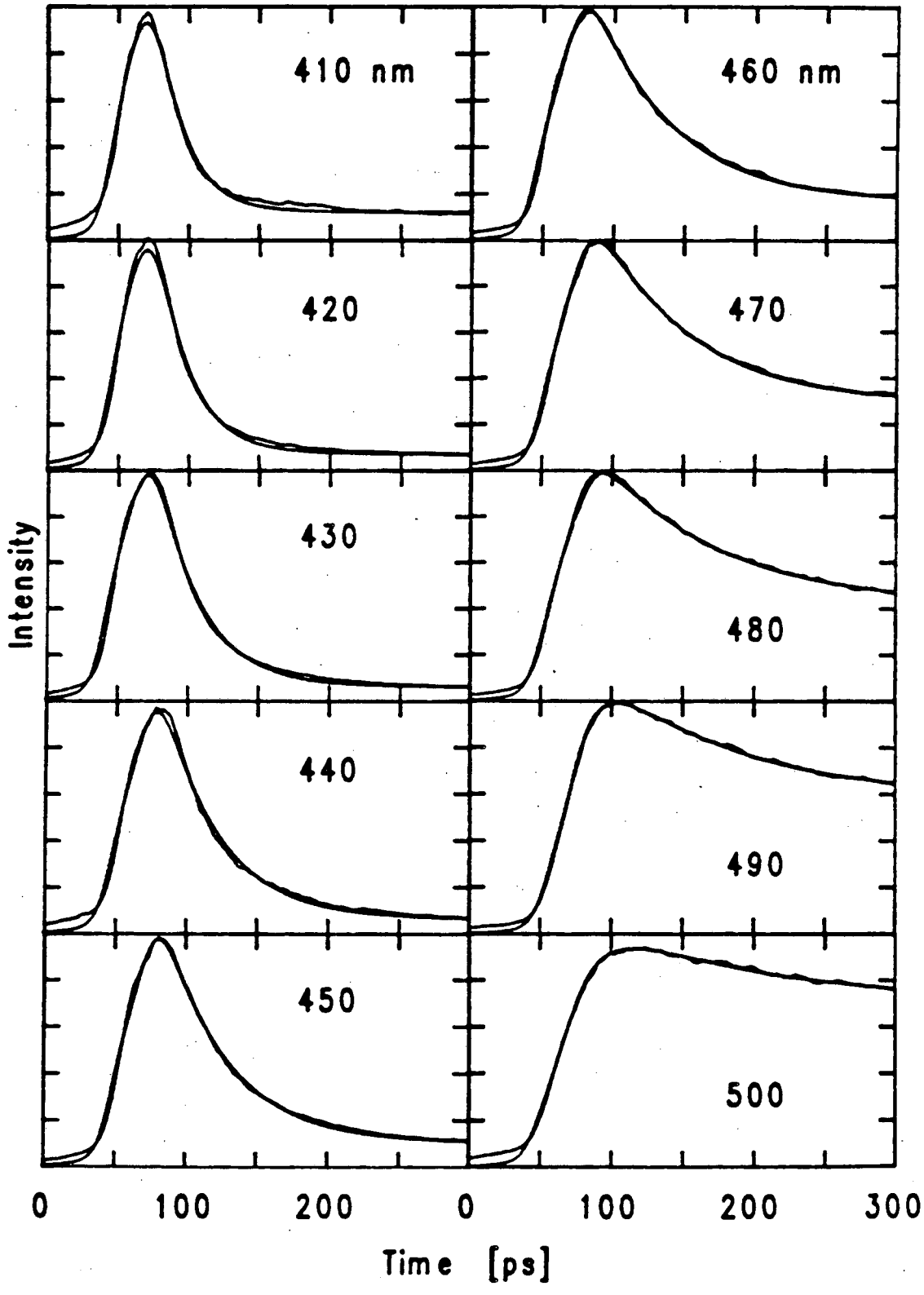
410 nm
460 nm
420
470
430
480
440
490
450
500
Intensity
0
100
200
0
100
200
300
Time [ps]

Figure 3.13 (cont.)

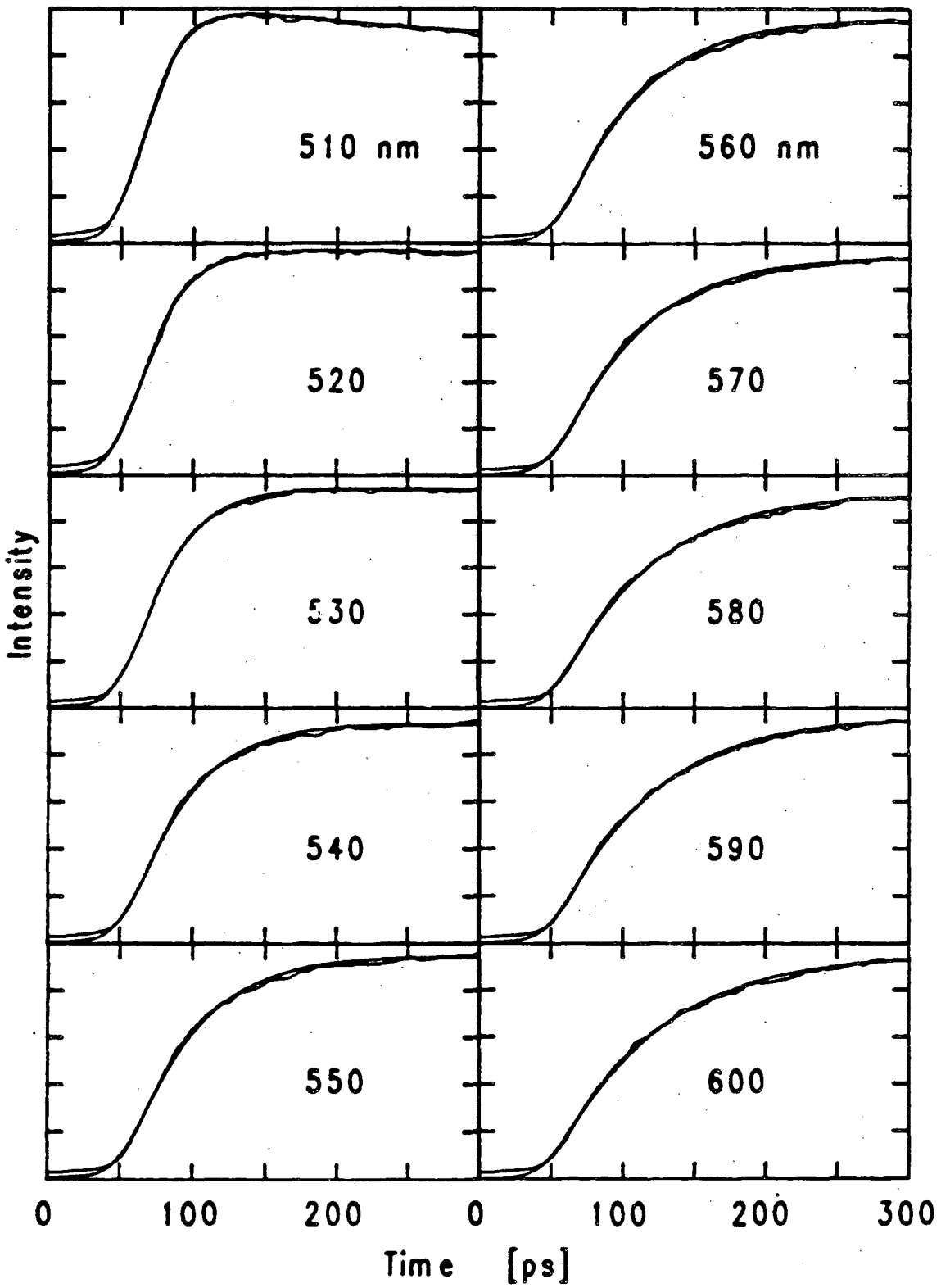

Table 3.4

Fit Parameters for 4AP in 1-Propanol

Negative amplitudes correspond to rises and postive amplitudes to falls.

Wavelength (nm)	$\tau(ps)$, α	Wavelength (nm)	$\tau(ps)$, α
420	0,-1. 12,1. 54,.14		
430	0,-1. 14,1. 64,2.	530	0,-1. 49,-1. 11000,1.
440	0,-1. 12,4. 70,1.	540	0,-.7 60,-1. 11000,1.
450	0,-1. 45,15. 11000,1.	550	0,-.6 65,-1. 11000,1.
460	.1,-1. 19,7.8 89,6.4 11000,1.	560	0,-.46 75,-1 11000,1.
470	.4,-1. 84,4.2 11000,1.	570	0,-.54 92,-1. 11000,1.
480	11,-1. 103,2.2 11000,1.	580	0,-.4 85,-1. 11000,1.
490	9,-1. 142,1. 11000,1.	590	0,-.5 104,-1. 11000,1.
500	16,-1. 143,.52 11000,1.	600	0,-.4 99,-1. 11000,1.
510	16,-1. 11000,1.	610	0,-.3 93,-1. 11000,1.
520	0,-.6 29,-1. 11000,1.	620	0,-.3 96,-1. 11000,1.

Figure 3.14 Time-Resolved Emission Spectra for 4AP in 1-Propanol

The spectrum shifts to the final position in about 200 ps. The population of excited-state molecules then decays at a rate equal to the fluorescence lifetime.

Figure 3.14

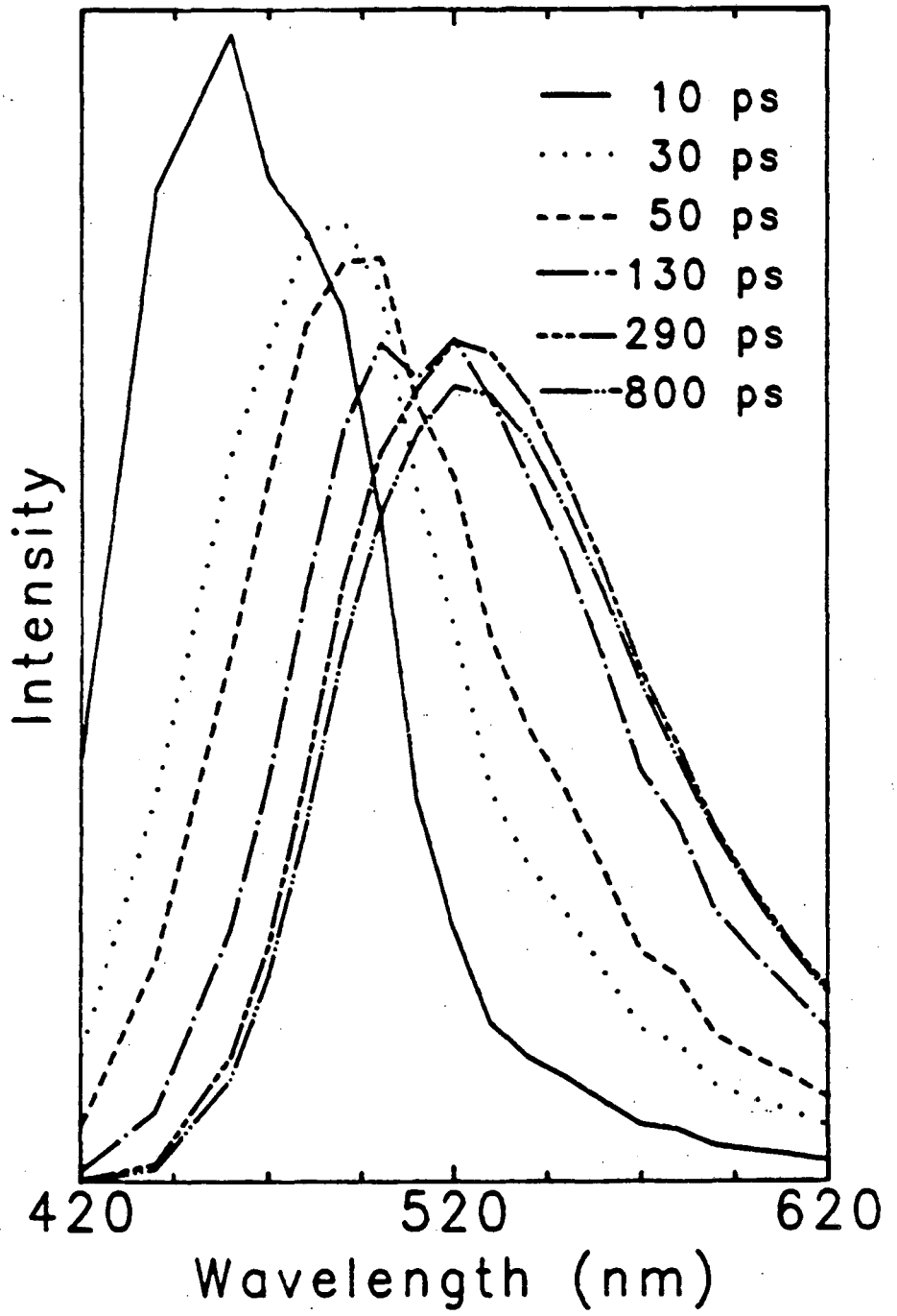
10 ps
30 ps
50 ps
130 ps
290 ps
800 ps
Intensity
420
520
620
Wavelength (nm)

4AP in 1-propanol was observed at just the right two wavelengths, the fall of the blue edge would match the rise of the red edge, and a two state system would be erroneously proposed (for example from Table 3.4, 480 nm has a fall of 103 ps, and 590 nm has a rise of 104 ps).

In order to get a more quantitative feel for the solvation process of 4AP in 1-propanol, the spectra as a function of time were fit to Gaussians in energy. Examples of these fits are shown in Figure 3.16. From these fits the fluorescence maximum versus time plot in Figure 3.17 is obtained. This plot was fit to two exponentials as described in Chapter 2 and the following times and amplitudes from Equation 2.1 were obtained: α_1=1.56, τ_1=15 ps; α_2=2.06, τ_2=90 ps. The width of the fluorescence band is an indication of the number of emitting states. Figure 3.18 shows a plot of the FWHM width of the spectra in Figure 3.16 versus time. The width is at a maximum after about solvation lifetime. This result is expected, since at this point fluorescence will still be coming from an entire array of different states from solute molecules with the solvent in the ground-state configuration to solute molecules with the solvent in the excited-state equilibrium configuration. After this maximum point the width decreases to the width of the steady-state fluorescence spectrum as fluorescence begins to come solely from the lowest energy solvated excited molecules.

2. Other Solvents

To understand the solvation times obtained for 4AP in 1-propanol, the emission from 4AP was examined in other solvents.

Aprotic Solvents

Acetonitrile has a high dipole moment of 3.44 Debye;[31] this solvent would thus be expected to rearrange around the newly created dipole moment of the 4AP excited state. Although the dipole moment of acetonitrile is higher than the dipole for 1-propanol, the steady-state spectrum is not as red shifted (Table 3.1). The blue and red edges of

Figure 3.15 Time-Resolved Emission Spectra for DMABN in Acetonitrile

This spectrum shows the two state behavior of the excited state of dimethyl-aminobenzonitrile. The state that emits at 400 nm is decaying into the state that emits at 500 nm. The isosbestic point at 460 nm distinquishes this two state system from the continuum behavior seen with 4AP in 1-propanol. The spectra are from reference 30.

Figure 3.15

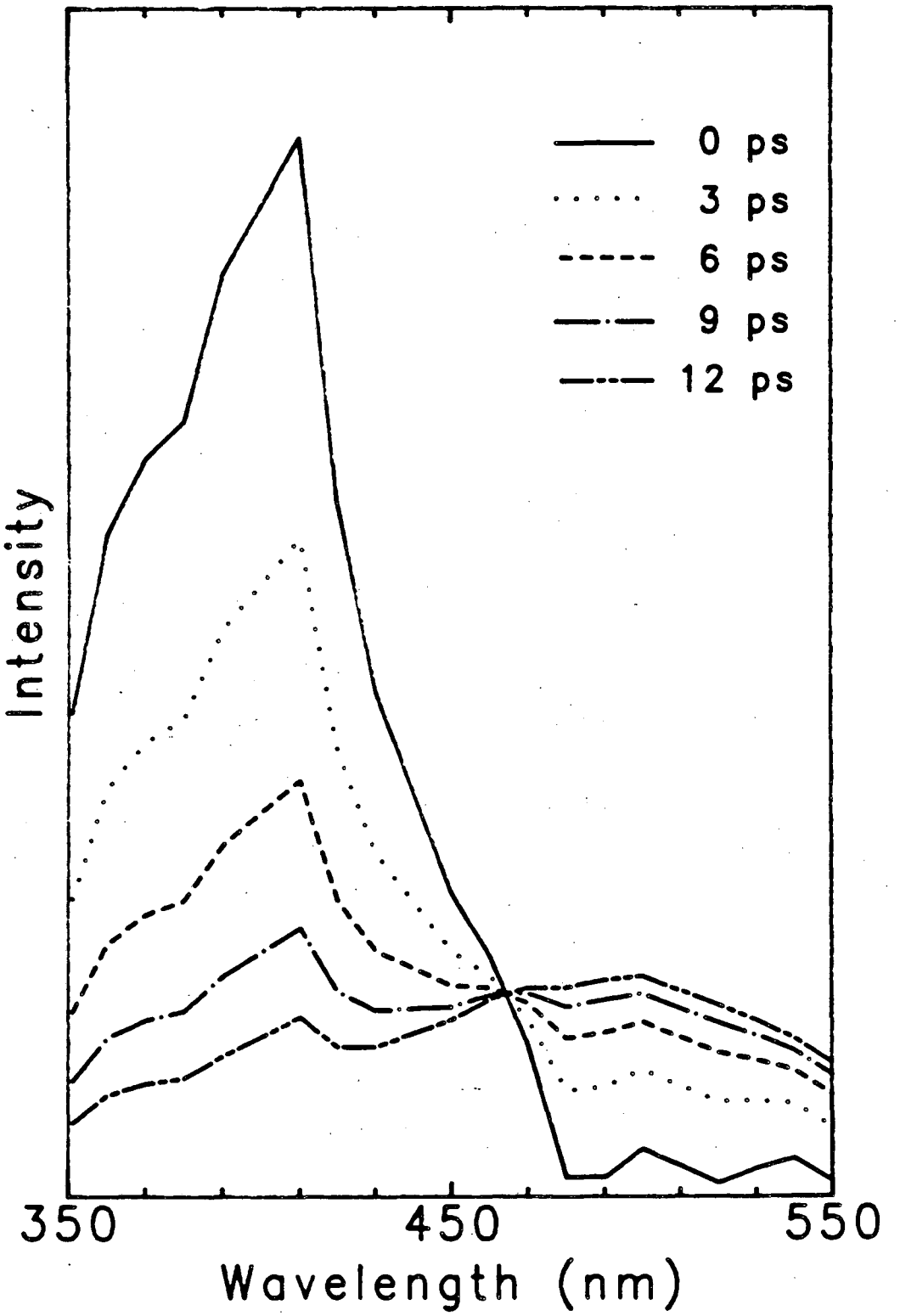

Figure 3.16 Gaussian Fits to Time-Resolved Emission Spectra of 4AP in 1-Propanol

These gaussian fits were used to obtain emission maxima and widths as functions of time. The dashed lines are the spectra and the solid lines are the Gaussian fits to the spectra.

Figure 3.16

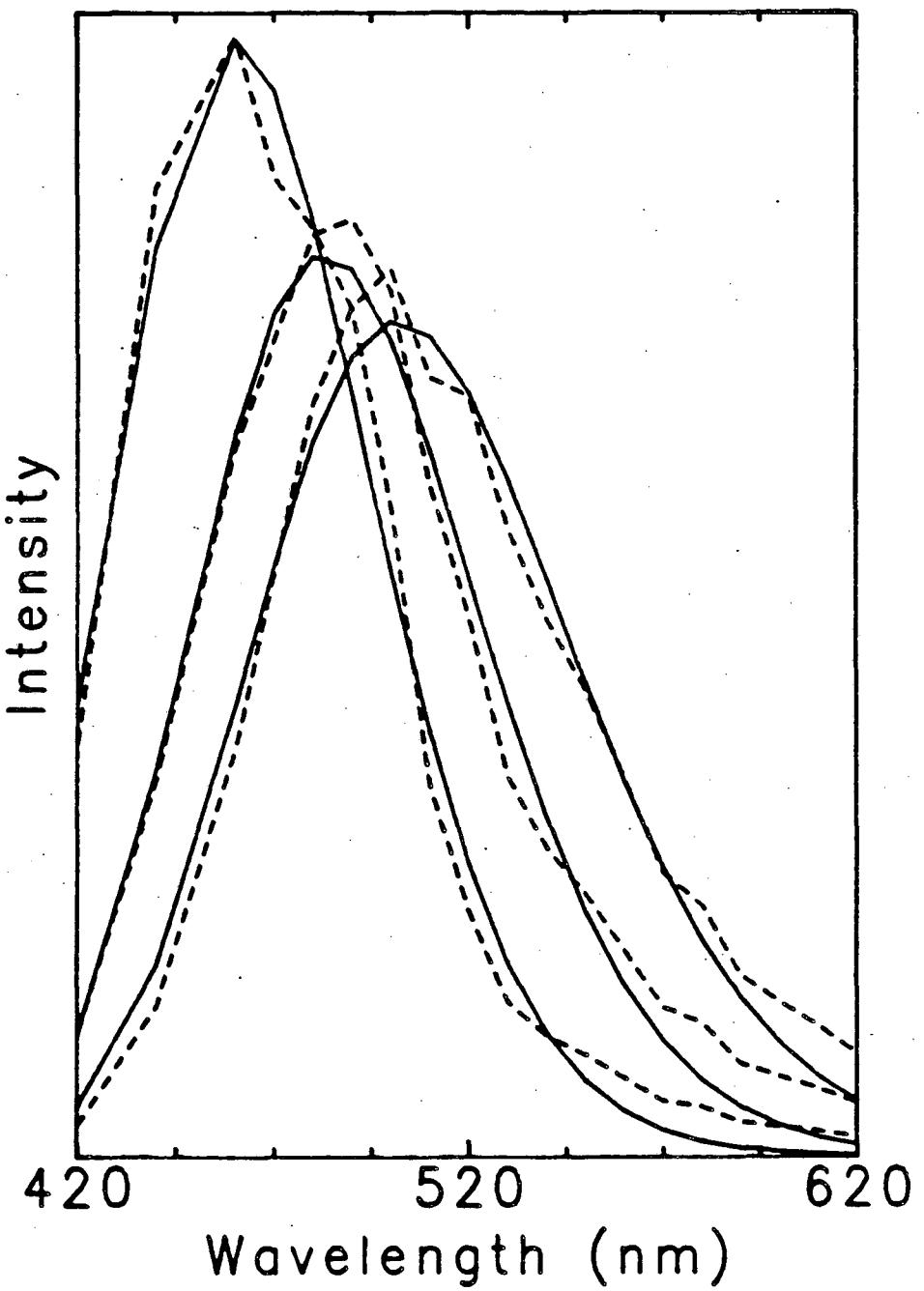

Figure 3.17 Emission Maximum as a Function of Time for 4AP in 1-Propanol

This peak position versus time plot was fit to two exponentials to obtain solvation times. The fit using Equation 2.1 had parameters of $\alpha_1 = 1.56$, $\tau_1 = 15$ ps; $\alpha_2 = 2.06$, $\tau_2 = 90$ ps.

Figure 3.17

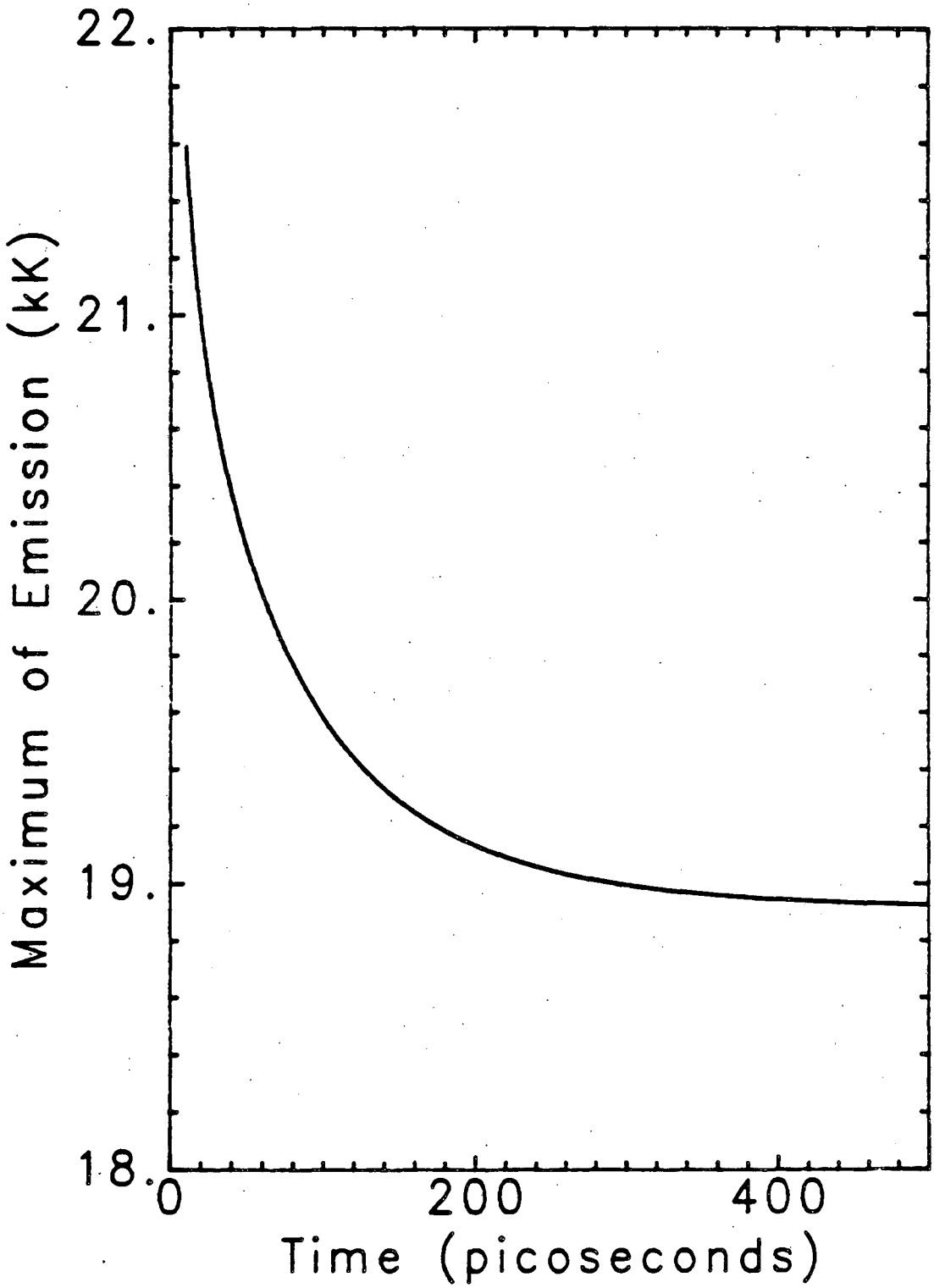
22.
21.
20.
19.
18.
0
200
400
Maximum of Emission (kK)
Time (picoseconds)

Figure 3.18 Spectral Width as a Function of Time for 4AP in 1-Propanol

The spectral width maximizes at 86 ± 15 ps, which is one solvation time for this solution. See text for an explanation of this phenomenon.

Figure 3.18

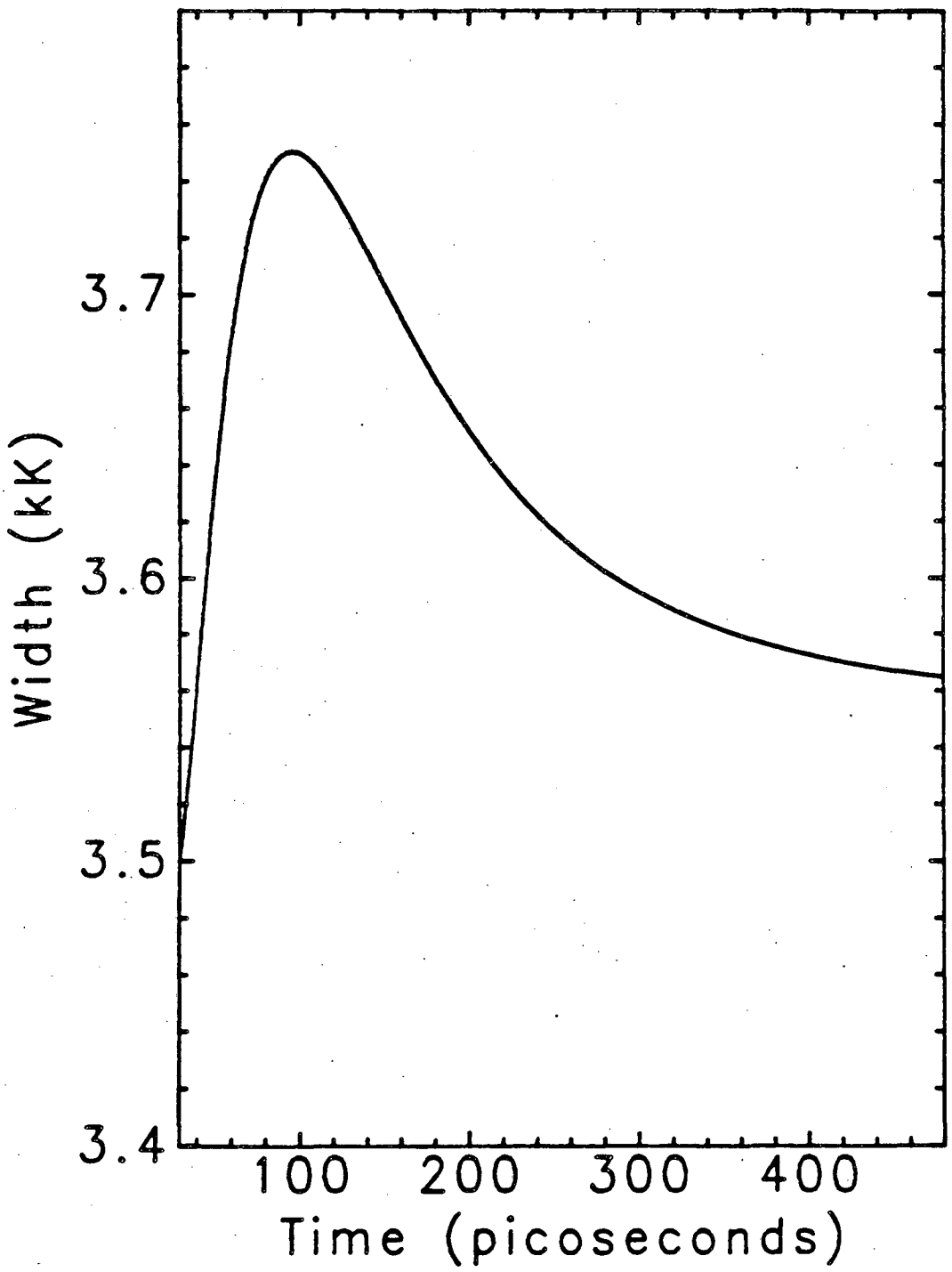

emission are shown in Figure 3.19. They both display instantaneous rises followed by a decay equal to the fluorescence lifetime of 4AP in acetonitrile. Any fast time dynamic shift of the fluorescence spectrum is occurring too fast for the time resolution of the instrumentation. No spectral shift was seen for any of the aprotic solvents THF, DMSO, toluene, or acetone. Since no time dependent shift was seen in these aprotic solvents, the reason for the shift could be hydrogen-bonding effects; therefore, protic solvents are examined.

Protic Solvents

A shift in time of the emission spectrum of 4AP was observed in all of the liquid alcohols listed in Table 3.5. Examples are given for ethanol, Figure 3.20, and 1-butanol, Figure 3.21. The shift in ethanol is faster than it is in 1-propanol; the time resolved spectrum shows the shift occurring in about 100 ps. For 1-butanol the shift takes about 400 ps, slower than in 1-propanol. The solvation times for these spectra were calculated along with other alcohols and are listed in Table 3.5.

Other H-bonding solvents are formamide and N-methylformamide. Both of these solvents shift the steady-state spectrum of 4AP as much as the alcohols did (see Table 3.1) with the same spectral width indicating a similarly strong interaction. The fast time dynamics for 4AP in formamide are shown in Figure 3.22. The red edge has an instantaneous rise. The blue edge has a spike which can be attributed to a Raman signal from the solvent. Thus, no fast time dynamics is observable in formamide, nor is any dynamic shift seen in N-methylformamide.

E. Dielectric Relaxation Times

If it is assumed that the solvation times measured are due to solvent rearrangement, they should be compared to a property of the solvent which describes solvent motion. Such a property is the dielectric relaxation time. The dielectric relaxation time measures the response of a molecule to an external electric field.[32] Debye theory describes this

Figure 3.19 Fast Time Dynamics of 4AP in Acetonitrile

The blue and red edges of emission are shown for 4AP in acetonitrile. Both sets of data show a rise time of zero with no fast fall component. Any time dependent shift occurring in this solvent is too fast to measure. Data were obtained from reference 30.

Figure 3.19

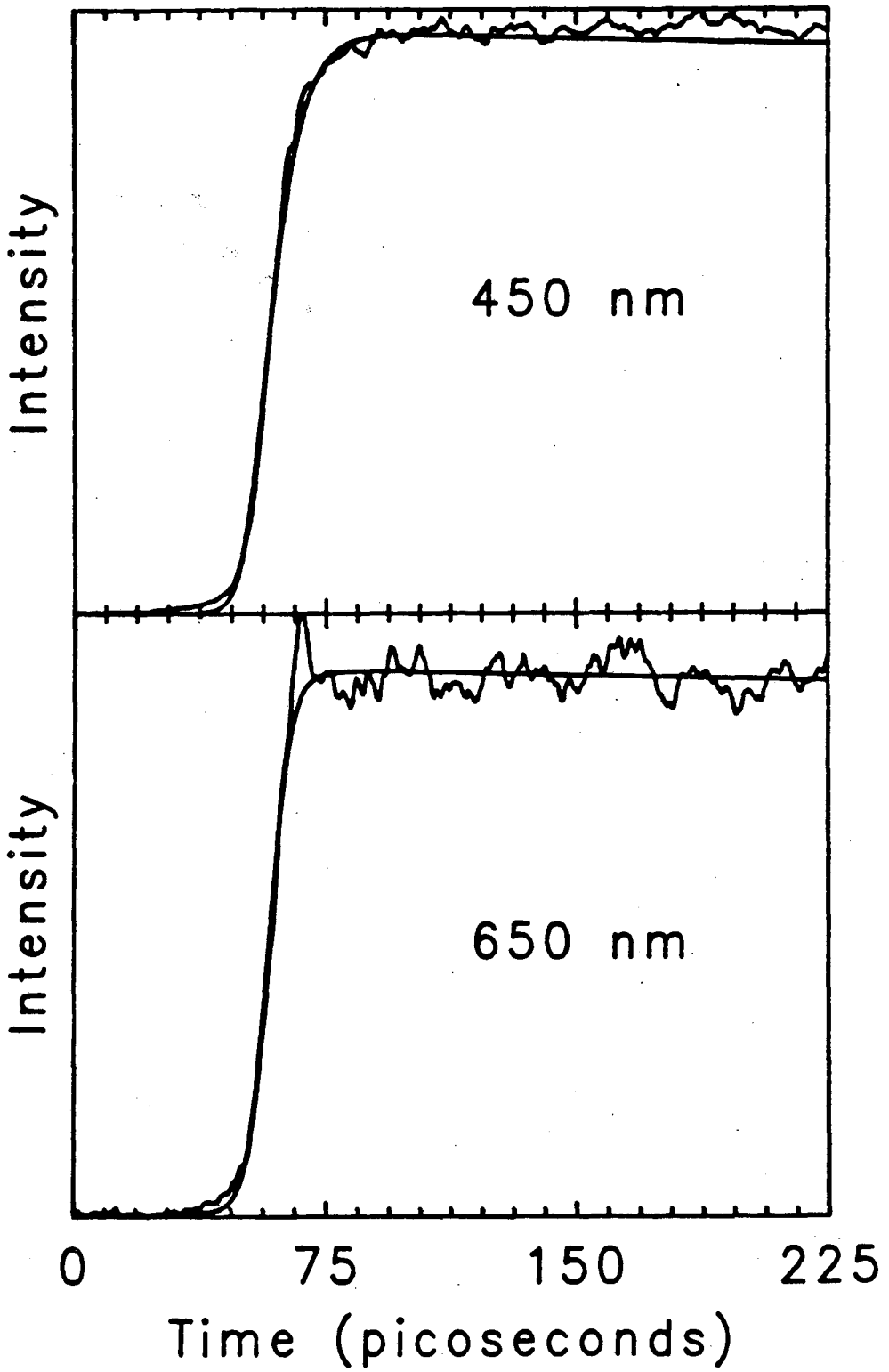
Intensity
450 nm
Intensity
650 nm
0
75
150
225
Time (picoseconds)

Figure 3.20 Time-Resolved Emission Spectra for 4AP in Ethanol

This shift occurs in about 100 ps, faster than the shift in 1-propanol. These spectra were obtained from reference 30.

Figure 3.20

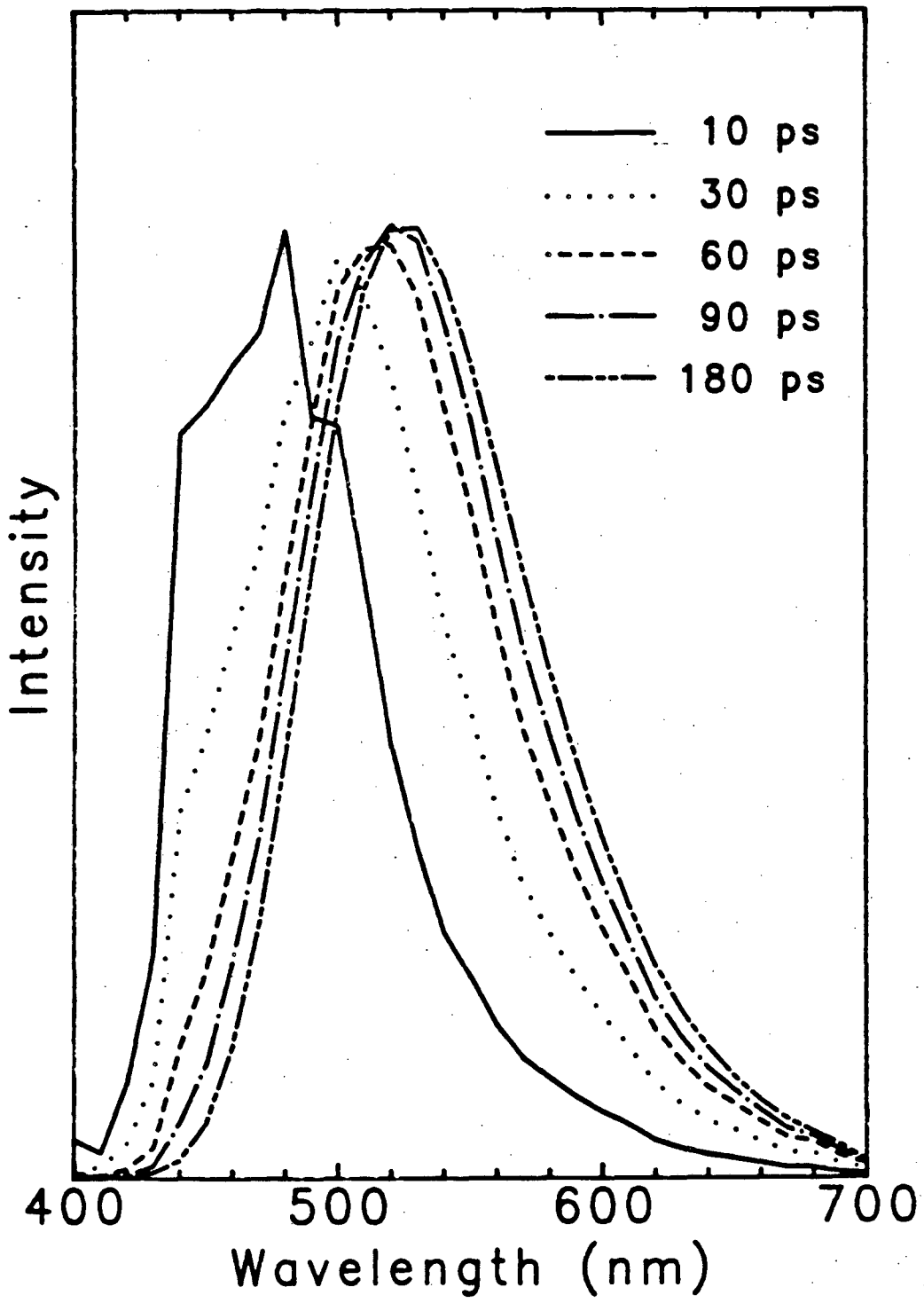
10 ps
30 ps
60 ps
90 ps
180 ps
Intensity
400
500
600
700
Wavelength (nm)

Figure 3.21 Time-Resolved Emission Spectra for 4AP in 1-Butanol

This shift occurs in about 400 ps, slower than the shift in 1-propanol. These spectra were obtained from reference 30.

Figure 3.21

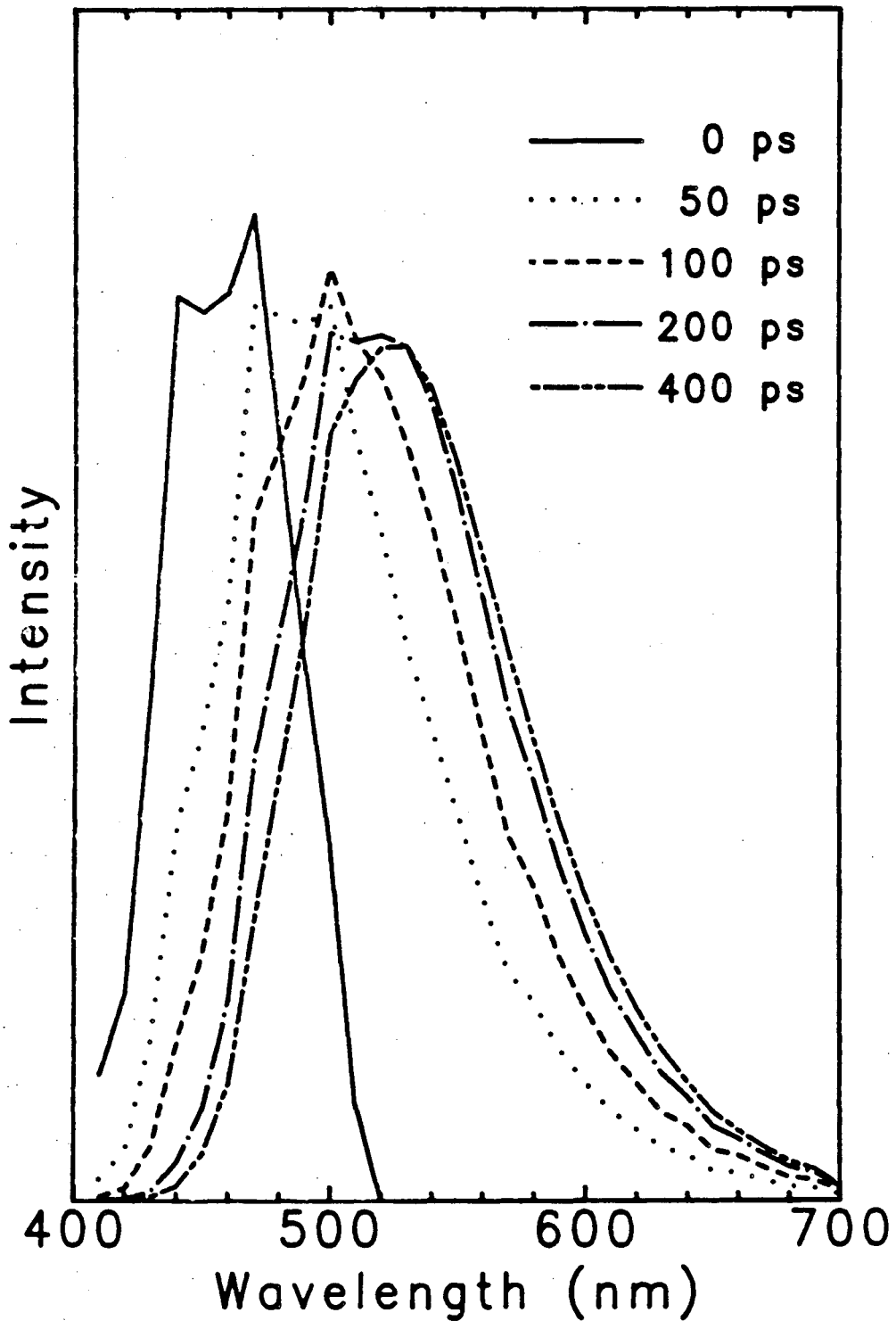
0 ps
50 ps
100 ps
200 ps
400 ps
Intensity
400
500
600
700
Wavelength (nm)

Table 3.5

Solvation Times* of 4AP in a Series of Alcohols at 20 °C

Alcohol	α_1	τ_1 (ps)	α_2	τ_2 (ps)	$\frac{\alpha_1 \times 100\%}{\alpha_1+\alpha_2}$
Ethanol	1.00	22	1.50	52	40%
1-Propanol	1.56	15	2.06	90	43%
2-Propanol	1.05	28	1.50	92	41%
1-Butanol	1.50	48	1.36	124	52%
1-Pentanol	1.15	63	1.32	203	46%

* Times for all of the alcohols except 1-propanol were calculated from data from reference 30. The parameters are fits of Equation 2.1 to peak position versus time data.

Figure 3.22 Fast Time Dynamics of 4AP in Formamide

Both the blue and red edges of emission show a rise time of zero picoseconds. The fast fall seen on the blue edge of emission can be attributed to the Raman signal from the solvent; thus no spectral shift is seen in formamide.

Figure 3.22

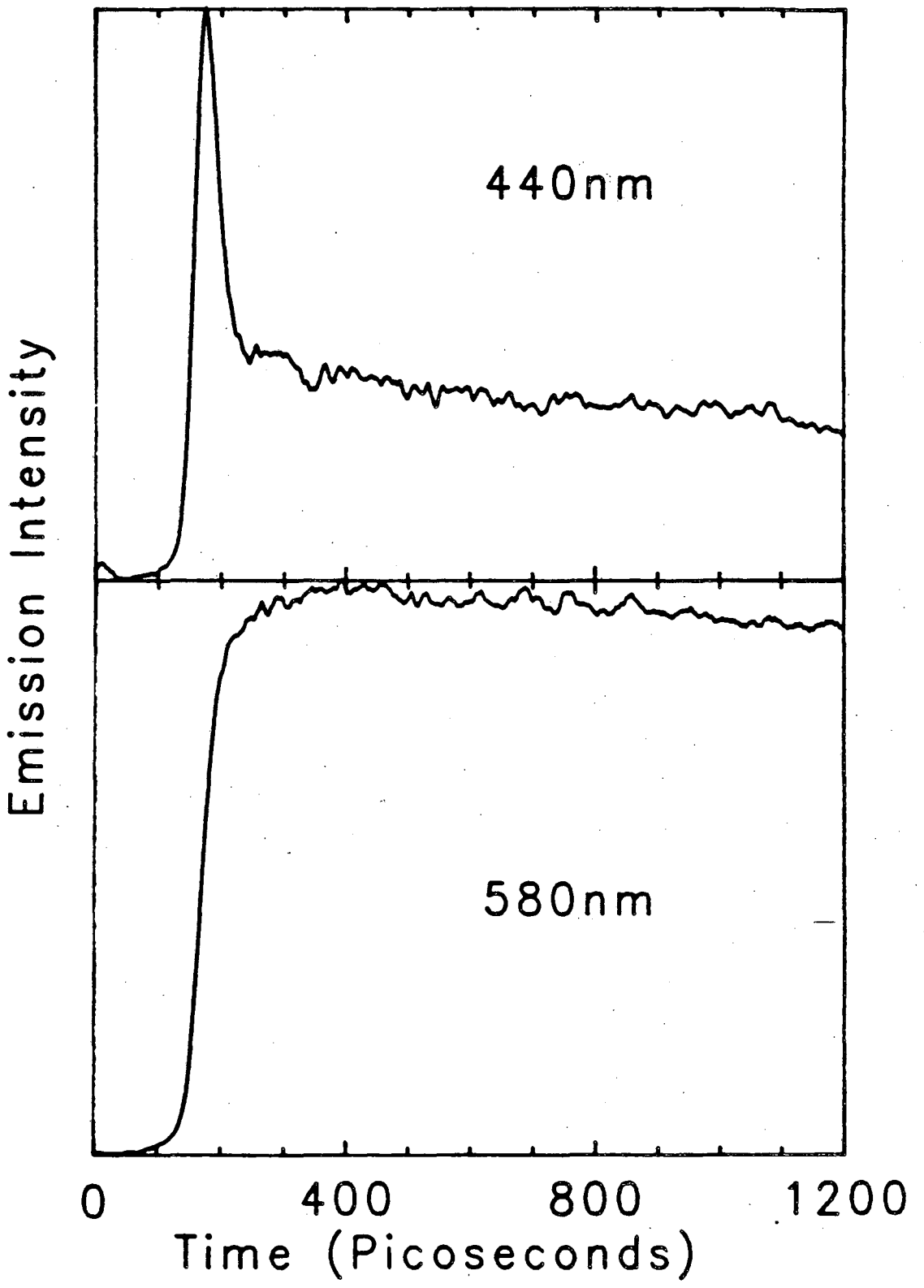
440nm
580nm
Emission Intensity
0
400
800
1200
Time (Picoseconds)

time as the lag of the dipole moment of a molecule behind an alternating electric field. These values are obtained by measuring the dielectric constant and dielectric loss of a solvent while varying the frequency of oscillation of the electric field. At low frequency, the solvent will have time to absorb the radiation from the field and use it as thermal energy to rearrange. At high frequency, since the dipoles of the molecule will not be able to rearrange fast enough, the solvent will appear transparent to the radiation. Using Cole-Cole plots,[32] the dielectric relaxation time is determined from the frequency of highest dielectric loss.

The dielectric relaxation times are thus measured under the condition of an alternating external charge; however, the situation of a solvent rearranging around a suddenly induced excited-state dipole moment is quite different. In the first case, the bulk solution is aligning to an external field and the field created by its own polarizability, while in the 4AP in 1-propanol case, a solvent shell is reacting to an internal constant charge. *Mozumder*[33] has computed the difference between the two relaxation times as follows.

The electric displacement, D, which is defined as being proportional to surface density of charge or polarization, can be expressed in terms of a time varying electric field, $E(t)$:

$$D(t) = \epsilon_\infty E(t) + \int_{-\infty}^{t} E(u)\alpha(t-u)du \qquad 3.1$$

where ϵ_∞ is the optical dielectric constant and α describes the decay of polarization. The decay function is assumed to be an exponential:

$$\alpha(t) = \alpha_0 exp(-t/\tau) \qquad 3.2$$

where τ is the relaxation time and α_0 is a constant. Substituting this exponential relationship into the expression for the electric displacement, the following derivative can be obtained:

$$\tau(d/dt)(D - \epsilon_\infty E) + (D - \epsilon_\infty E) = \tau\alpha_0 E. \qquad 3.3$$

For a static field, the change with time or d/dt will be zero and from the definition of the static dielectric constant, ϵ_0, $D = \epsilon_0 E$. Substituting these conditions in to the above

differential equation, the following expression for α_0 is obtained:

$$\alpha_0 = \frac{(\epsilon_0 - \epsilon_\infty)}{\tau}. \qquad 3.4$$

The equation relating D and E then becomes:

$$\tau(d/dt)(D - \epsilon_\infty E) + (D - \epsilon_\infty E) = (\epsilon_0 - \epsilon_\infty)E. \qquad 3.5$$

For the case of a constant charge suddenly introduced into a solution, D is a constant, so $dD/dt = 0$. A time dependent dielectric constant, $\epsilon(t)$, can be defined as:

$$E(t) = \frac{D}{\epsilon(t)}; \qquad 3.6$$

and consequently

$$\frac{dE}{dt} = D\frac{d}{dt}[\epsilon(t)]^{-1}. \qquad 3.7$$

Substituting the time dependent dielectric constant for the electric field, Equation 3.5 becomes

$$\frac{d}{dt}[\epsilon(t)]^{-1} = (\epsilon_\infty \tau)^{-1}(1 - \epsilon_0[\epsilon(t)]^{-1}). \qquad 3.8$$

This equation can be integrated under the conditions that $\epsilon(t) \rightarrow \epsilon_\infty$ as $t \rightarrow 0$:

$$[\epsilon(t)]^{-1} = \epsilon_0^{-1} + (\epsilon_\infty^{-1} - \epsilon_0^{-1})exp(-t/\tau'), \qquad 3.9$$

where

$$\tau' = \frac{\epsilon_\infty}{\epsilon_0}\tau. \qquad 3.10$$

In general, $\epsilon_0 > \epsilon_\infty$, so relaxation under this condition of constant charge will be faster than relaxation under the condition of a constantly applied field. Any times measured in a solvation process should be proportional to τ'.

For the alcohols, *Garg* and *Smyth*[34] found three distinct dielectric relaxation times, known as the three dispersion regions of the alcohols. The first and slowest time is attributed to the breakage of a hydrogen-bond, rotation of the molecule and formation of

a new hydrogen-bond. The middle time is the rotation of a monomeric alcohol molecule, and the fastest time is the rotation of a OH group around the CO bond. Because of the slow and fast relaxation times, the middle region is hard to measure and, reported values are not very accurate.

Table 3.6 lists these three relaxation times for some linear alcohols. Table 3.7 contains the slowest relaxation time, available static and optical dielectric constants for this region, and corrected relaxation times. For the other dispersion regions, the dielectric constants are not available, so corrected relaxation times can not be calculated. However, the corrections for the other regions would be less than a factor of 2 because of the small frequency range that they occupy[34]. The corrected value for the middle region can thus be taken as slightly shorter than the literature relaxation time. For 1-propanol, the two solvation times correlate well with the slowest and middle corrected dielectric relaxation times. Some of the 1-propanol molecules are free to rotate and orient themselves with the new dipole moment of 4AP; whereas, other alcohol molecules must break hydrogen-bonds with other alcohols or the 4AP molecule before realignment with the excited-state dipole. The fast solvation times for the longer chain alcohols are not as close to the middle relaxation times, but a large error occurs in both measurements. The slower solvation times plotted against the slowest dielectric relaxation times is shown in Figure 3.23. Within experimental error, the solvation time is found to correlate to the dielectric relaxation time of the solvent. The line has a slope equal to one.

Included in Table 3.5 is an indication of what percentage of the shift is due to the faster relaxation of Equation 2.1. Amplitudes can not be compared directly because the alcohols have different magnitudes of spectral shifts. The amount of the spectral shift due to τ_1 is calculated from:

$$\frac{\alpha_1 \times 100\%}{\alpha_1 + \alpha_2}.$$

A value of one would represent total relaxation by τ_1. As can be seen from Table 3.5, within experimental error, all of the alcohols relax a little over 40% by the rotation of

Table 3.6

Dielectric Relaxation Times* for Linear Alcohols

Alcohol	τ_1 (ps)	τ_2 (ps)	τ_3 (ps)
1-Propanol	2.12	22	430
1-Butanol	2.35	27	668
1-Pentanol	2.65	28	927

* Values obtained from reference 34.

Table 3.7

Dielectric Data for a Series of Alcohols at 20 °C

Alcohol	Reference	Dielectric Relaxation Time (ps) τ	Static Dielectric Constant ϵ_0	Optical Dielectric Constant ϵ_∞	Corrected Relaxation Time (ps)† $\tau' = \frac{\epsilon_\infty}{\epsilon_0} \times \tau$
Ethanol	35*	203	25.1	4.7	40
	36*	232	25.0	4.3	40
1-Propanol	34	430	21.1	4.0	82
	37	382	20.5		75
2-Propanol	36*	647	19.9	3.4	112
	38	588			111
1-Butanol	34	668	17.7		125
	35*	612	18.0	3.3	112
	37	631	18.0		117
1-Pentanol	34	927	15.2	3.0	183

* Values were extrapolated from data in these references.

† Error on these corrected values is assumed to be ± 10 ps or ± 10% depending on which is larger. Errors on the data used to calculate these values were not generally available.

Figure 3.23 Corrected Dielectric Relaxation Time versus Solvation Time for 4AP in a Series of Alcohols

The solvation times used are the slow components from Table 3.5. The line has a slope of 1.

Figure 3.23

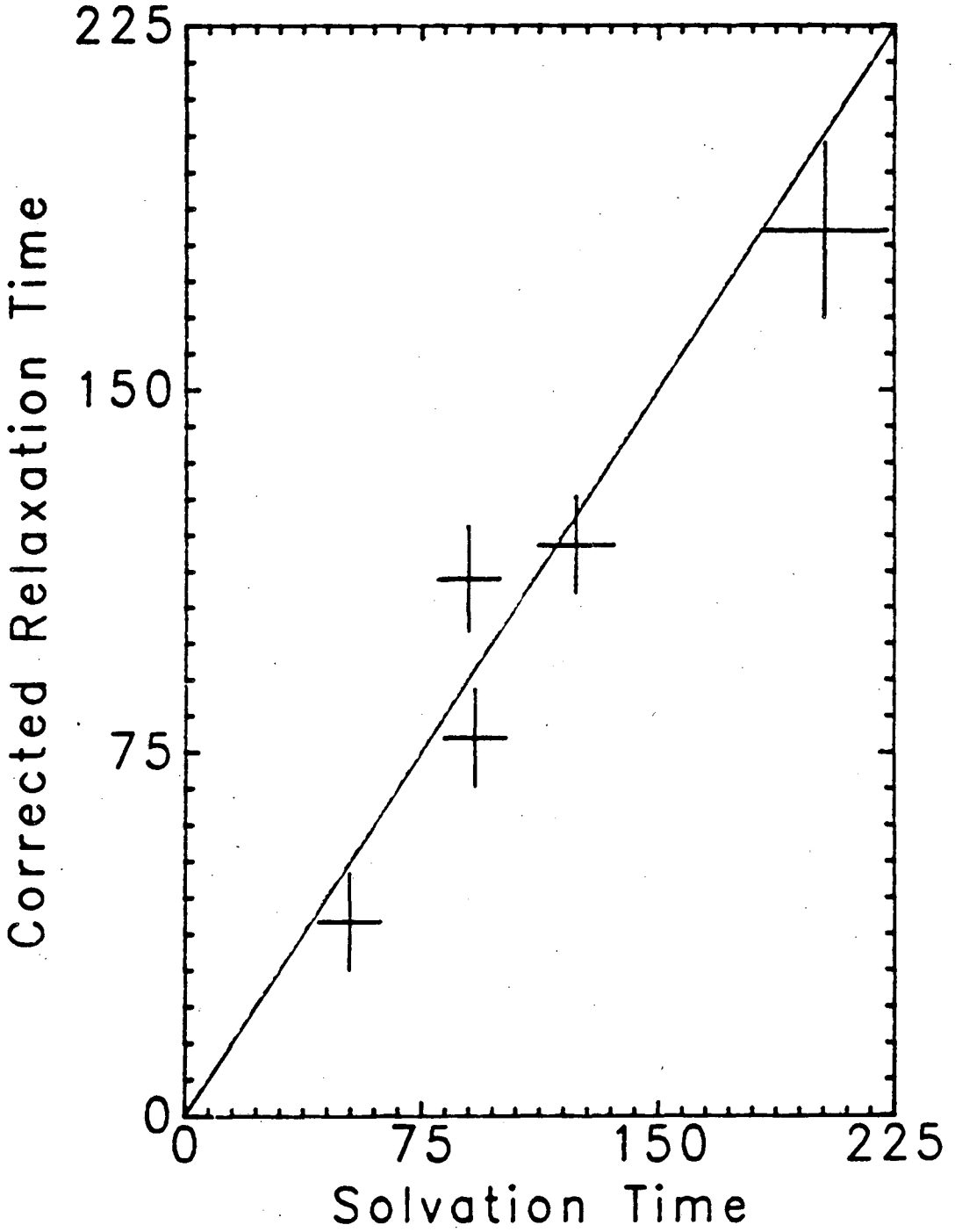
225
150
75
0
Corrected Relaxation Time
0
75
150
225
Solvation Time

a single molecule with the rest of the relaxation involving the making and breaking of hydrogen-bonds.

The solvation time being proportional to the corrected dielectric relaxation time is not surprising considering the theoretical results discussed in Chapter 1. The equation of *Bagchi et al.*[5] is approximately equal to Equation 3.10. *Zwan* and *Hynes*[6] claimed that the time dependent shift should be proportional to the longitudinal dielectric relaxation time; $\tau_L = \frac{\epsilon_\infty}{\epsilon_0}\tau_d$ where τ_d is the measured dielectric relaxation time. They further say that for an alcohol solvent the shift will be nonexponential because of the three dielectric relaxation times of these solvents. The above data are in fact not single exponential but need two exponentials to fit them.

The results of other solvents can be explained by examining their corrected dielectric relaxation times. Table 3.8 lists these values for the solvents mentioned earlier. All of the solvents that showed no time dependent shift in the 4AP fluorescence spectrum have fast dielectric relaxation times. Although formamide and N-methylformamide are both H-bonding solvents, their high static dielectric constants[39] correct the alternating field dielectric relaxation time to a value which is too fast for the time resolution of the picosecond instrumentation used in this work.

In order to strengthen the theory that the solvation dynamics are controlled by the dielectric relaxation times of the solvent, temperature and solute changes were studied. Table 3.9 lists solvation times for temperature studies of 4AP in 1-propanol along with the corrected slowest dielectric relaxation times of 1-propanol at these temperatures. The long time solvation times agree very well with the corresponding dielectric relaxation times. The temperature dependence of the middle region dielectric relaxation time is not available. The fast solvation times are slower with a decrease in temperature. The middle region of the dielectric response of the solvent corresponds to the rotation of a monomer. This rotation time is expected to be slower at lower temperatures. At high temperature, the extensive hydrogen-bonding of the alcohol is expected to be less than

Table 3.8

Dielectric Relaxation Times for Other Solvents at 20 °C

Solvent	Reference	Dielectric Relaxation Time (ps)	Corrected Dielectric Relaxation Time (ps)
Acetonitrile	40	6	<1.0
DMSO	41	19.6	2.3
Formamide	39	45	2.9
	41	37	2.4
N-Methylformamide	41	123	3.6
N,N-Dimethylformamide	39	18	2.2
	41	11	1.3

at lower temperatures. This decrease in the cluster sizes of the alcohols should create an increase in the amount of solvent relaxation that occurs by the faster solvation time, τ_1. Although the percent of relaxation from τ_1 in Table 3.9 shows this trend from 0 °C to 20 °C, the 40 °C value is much too low. This discrepancy could be due to the closeness of the two solvation times at this temperature. The best fit was obtained with values of 21 ps for τ_1 and 43 ps for τ_2. Constraining τ_2 to a slightly higher value would cause a decrease in both τ_1 and α_2 and an increase in α_1 without changing the fit by much. Small changes in the amplitudes would cause large changes in the ratio $\alpha_1/(\alpha_1 + \alpha_2)$.

The other solutes studied were 3-aminophthalimide and 4-amino-N-methyl-phthalimide; their structures are shown in Figure 3.24. Each of these solute molecules has a different steady-state spectral shift from that of 4-aminophthalimide; Figure 3.25 shows these excitation and emission spectra for the phthalimides in 1-propanol. The fit parameters of the fast time dynamics of all of these molecules are listed in Table 3.10. For a given wavelength the fit parameters are different, but after calculating peak positions versus time by using the various steady-state spectra, all of the solutes give similar solvation times. These times are listed in Table 3.11 along with the dielectric relaxation times of 1-propanol. Within all of the experimental errors, the times for all of the solutes agree with the corrected dielectric relaxation times of the solvent. The percent of relaxation of 1-propanol by the mechanism represented by τ_1 for 3AP is a little large. The intramolecular bond which is possible between the amino group and one of the carbonyls[15] of this molecule could be responsible for this result. The alcohol would not be able to form a hydrogen-bond with this carbonyl, so fewer bonds need be broken and made for the solvent to relax. Although the time of the spectral shift may not be solute dependent, perhaps the contribution from each type of relaxation of the solvent is solute dependent.

Table 3.9

Solvation Times* and Corrected Dielectric Relaxation Times for 4AP in 1-Propanol at a Series of Temperatures

Temperature °C	Solvation Time (ps) α_1 , τ_1	Solvation Time (ps) α_2 , τ_2	Corrected Dielectric Relaxation Time (ps)	$\frac{\alpha_1 \times 100\%}{\alpha_1+\alpha_2}$	Reference
0	0.80 , 34	1.70 , 133	134	32%	37
20	1.56 , 15	2.06 , 90	78	43%	34,37
40	0.35 , 21	1.84 , 43	47	16%	37

* Solvation times for 0 °C and 40 °C were calculated from data from reference 30.

Figure 3.24 Structures of 3-Aminophthalimide (3AP) and 4-Amino-N-Methylphthalimide (4AMP)

Figure 3.24

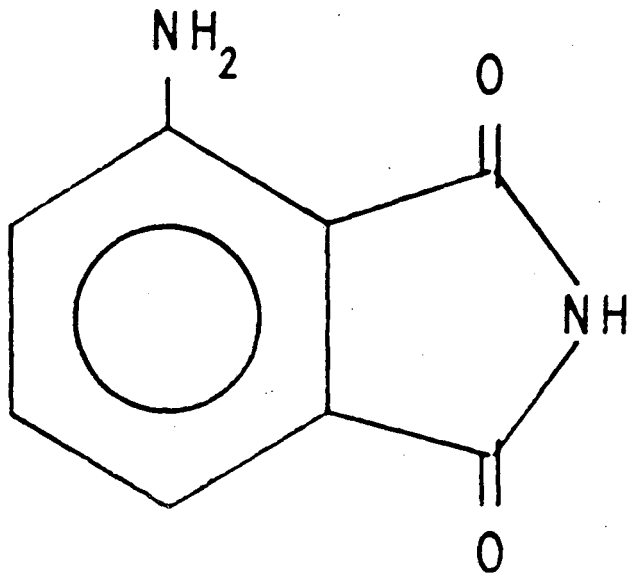

3-Aminophthalimide

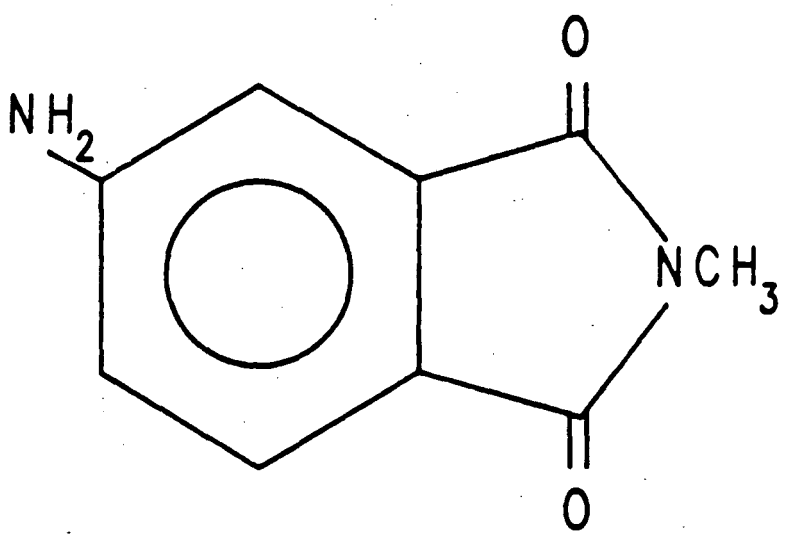

4-Amino-N-methylphthalimide

Figure 3.25 Steady-State Emission and Excitation Spectra for 4AP, 3AP and 4AMP in 1-Propanol

The maxima of emission are : 525 nm for 4AP, 487 nm for 3AP and 540 nm for 4AMP. The maxima of absorption are: 373 nm for 4AP, 387 nm for 3AP and 380 nm for 4AMP.

Figure 3.25

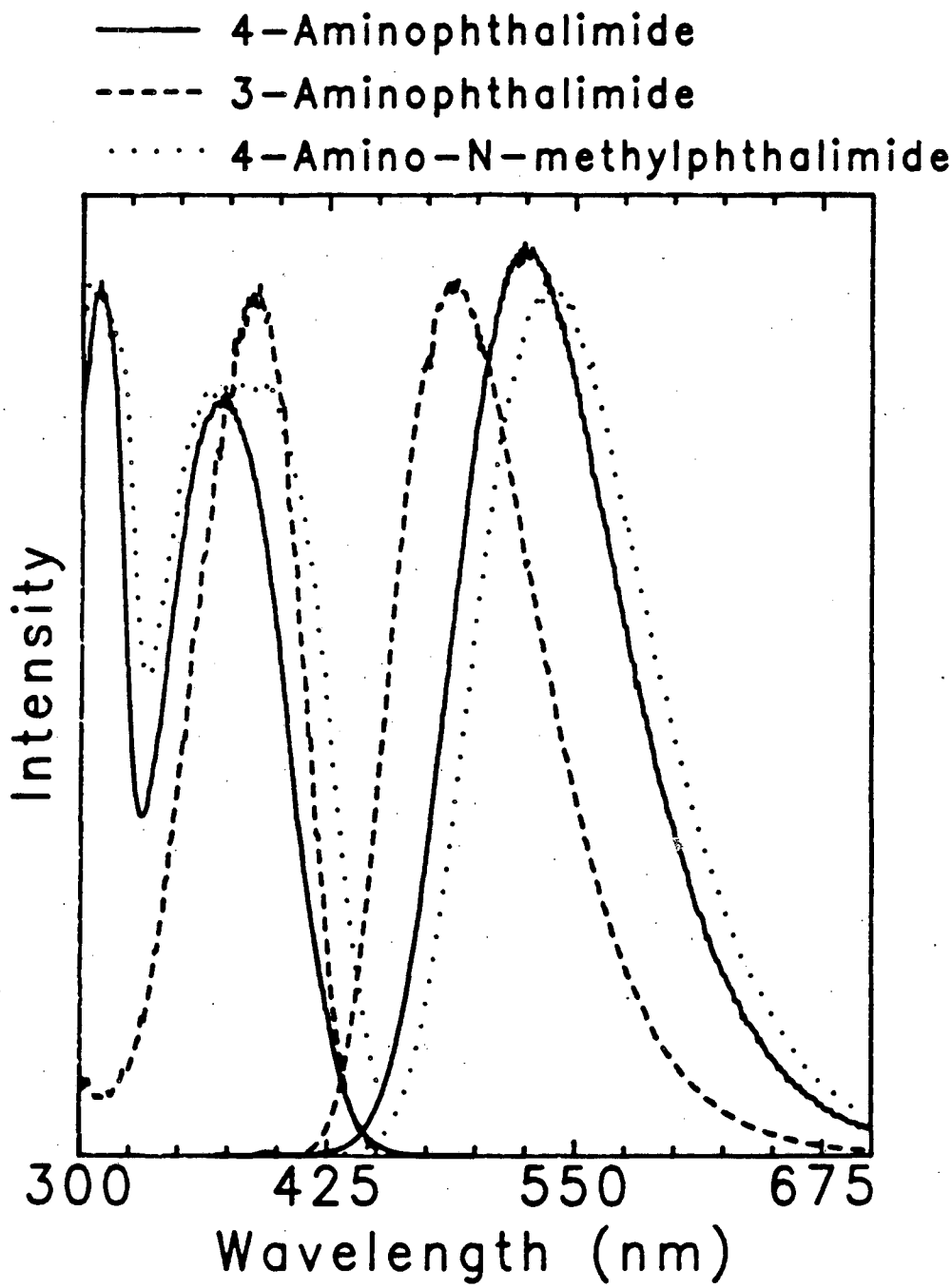
4-Aminophthalimide
3-Aminophthalimide
4-Amino-N-methylphthalimide
Intensity
300
425
550
675
Wavelength (nm)

Table 3.10

Fit Parameters for a Series of Solutes in 1-Propanol

Wavelength (nm)	4AP	3AP*	4AMP
420	0,-1. 12,1. 54,.14	0,-1. 31,8.6 14900,1.	0,-1. 16,10. 10600,1.
430	0,-1. 14,1. 64,2.	.4,-1. 42,6.7 14900,1.	0,-1. 20,11. 10600,1.
440	0,-1. 12,4. 70,1.	2,-1 54,3.2 14900,1.	0,-1. 29,12.2 10600,1.
450	0,-1 45,15. 11000,1.	7,-1 64,1.6 14900,1.	0,-1. 38,12. 10600,1.
460	.1,-1. 19,7.8 89,6.4 11000,1.	8,-1. 79,.7 14900,1.	0,-1. 48,9.5 10600,1.
470	.4,-1. 84,4.2 11000,1.	9,-1. 138,.26 14900,1.	0.,-1. 60,6. 10600,1.
480	11,-1. 103,2.2 11000,1.	12,-1. 14900,1.	0,-1. 75,3. 10600,1.
490	9,-1. 142,1. 11000,1.	18,-1. 14900,1.	10,-1. 85,1.5 10600,1.
500	16,-1. 143,.52 11000,1.	28,-1. 14900,1.	15,-1. 106,.8 10600,1.
510	16,-1. 11000,1.	32,-1. 14900,1.	29,-1. 69,.8 10600,1.

* Data for 3AP was obtained from reference 30.

Table 3.10 (cont.)

Wavelength (nm)	4AP	3AP	4AMP
520	0,-.6 29,-1. 11000,1.	41.,-1. 14900,1.	26.,-1. 64,.4 10600,1.
530	0,-1. 49,-1. 11000,1.	44,-1. 14900,1.	28,-1. 56,.2 10600,1.
540	0,-.7 60,-1. 11000,1.	46,-1. 14900,1.	40,-1. 60.,.1 10600,1.
550	0,-.6 65,-1. 11000	48.,-1. 14900,1.	38.,-1. 10600,1.
560	0,-.46 75,-1 11000,1.	52,-1. 14900,1.	48.,-1. 10600,1.
570	0,-.54 92,-1. 11000,1.	52,-1. 14900,1.	53,-1. 10600,1.
580	0,-.4 85,-1. 11000,1.	56,-1. 14900,1.	62,-1. 10600,1.
590	0,-.5 104,-1. 11000,1.	57,-1. 14900,1.	71,-1. 10600,1.
600	0,-.4 99,-1. 11000,1.	57,-1. 14900,1.	71.,-1. 10600,1.
610	0,-.3 93,-1. 11000,1.	57,-1. 14900,1.	72,-1. 10600,1.
620	0,-.3 96,-1. 11000,1.	60,-1. 14900,1.	75,-1. 10600,1.

Table 3.11

Solvation Times of Various Solutes in 1-Propanol

Solute	α_1	τ_1	α_2	τ_2	$\frac{\alpha_1 \times 100\%}{\alpha_1+\alpha_2}$
4-Aminophthalimide	1.56	15 ± 10	2.06	90 ± 10	43%
3-Aminophthalimide*	1.10	25 ± 10	0.90	68 ± 10	55%
4-Amino-N-methyl-phthalimide	0.90	25 ± 10	1.5	74 ± 10	38%
Corrected Dielectric Relaxation Times of 1-Propanol [34]		<20		78 ± 10	

* Solvation times for 3-aminophthalimide were calculated from the data from reference 30.

F. Rotations

The fast time dynamics of fluorescence of the 4AP molecule has been shown to depend on the motion of the solvent. To better understand this solvation process, the motion of the 4AP solute molecule was studied. The rotational diffusion time of a molecule can be monitored by doing time-dependent polarization studies. As described in Chapter 2, the sample is excited with vertically polarized light. Those 4AP molecules which have their absorption dipoles aligned vertically will absorb the light. If the emission dipole is parallel to the absorption dipole, initially most of the emission will be vertically polarized. As the solute molecule rotates, the percent of emission which is polarized horizontal will increase. The rotational anisotropy, r(t), is a measure of the degree of polarization of the emission from the molecules. The anisotropy is obtained at any one time by observing the fluorescence intensity vertical, $I_v(t)$, and horizontal, $I_h(t)$:

$$r(t) = \frac{I_v(t) - I_h(t)}{2I_v(t) + I_h(t)}$$

The derivation of this equation has been discussed in detail elsewhere.[13,42] The decay of rotational anisotropy can be related to the diffusional rotational reorientation time, τ_r, of the emitting molecule:

$$r(t) \propto exp\,(-t/\tau_r)$$

An example of the rotational data for 4AP in 1-propanol at 500 nm is shown in Figure 3.26. The vertical and horizontal components of emission are taken in two different datasets by changing the polarization of the prism on the detection side of the sample. The intensities of these datasets are compared at long times in order to normalize them to each other. This normalization process is called tail-matching; it eliminates any polarization dependence of the detection apparatus and optics, and takes into account excitation energy diferences that exist because the datasets cannot be taken at the same time. The rotational anisotropy function is calculated with these datasets and shown in Figure 3.27. The slope of a logarithm plot of r(t) gives a rotational reorientation time of 329 ps for 4AP in

1-propanol at 500 nm (see Figure 3.27). This rotational reorientation time becomes more significant after examining the theory of rotational diffusion.

The rotational reorientation time, τ_r, of a molecule can be described by the Stokes-Einstein-Debye equation:[43]

$$\tau_r = 4\pi a^3 \eta / 3kT$$

where a is the radius of the rotating molecule, η is the viscosity of the solvent, T is the temperature, and k is Boltzmann's constant. This equation describes motion of large solutes in a small non-interacting solvent. Since real molecules are nonspherical and since solvent-solute interactions exist, this equation does not hold true; however, for a solute in a series of solvents which have the same interaction with the solute, τ_r will be proportional to the viscosity. For a given solvent, rotation times are an indication of both the size of the rotating molecule and the interaction between the solvent and solute. For 4AP in 1-propanol, if solvent molecules are attaching themselves to the solute during the solvation process, the size dependence of the rotational reorientation time would dictate a longer time of rotation toward the red edge of the fluorescence spectrum. The rotational reorientation times of 4AP were thus obtained for a series of solvents and at a series of wavelengths.

The rotational reorientation time of 329 ps for 4AP in 1-propanol at 500 nm is large for a molecule of its size. P-terphenyl is of a comparable size to 4AP, but it does not have the oxygens and nitrogens for H-bonding with the solvent. It rotates in 113 ps in 1-propanol.[13] Because of 4AP's strong interaction with the propanol molecules, it does not rotate on its own but must drag along some of the solvent molecules. The rotational reorientation time for 4AP is longer than p-terphenyl because the rotating unit is larger and the interactions between the solvent molecules must be broken before the solute-solvent complex can rotate. The solvation time for 4AP in 1-propanol is 90 ps, so the solvent rearrangement around the excited-state is faster than the solute motion.

The rotational reorientation time for 4AP in 1-propanol was calculated every 10 nm

Figure 3.26 Rotational Data for 4AP in 1-Propanol at 500 nm

These data sets were tail-matched at 2000 ps. Initially fluorescence is seen mostly from the vertical component; fluorescence emission horizontal increases as the emitting molecule rotates. The anisotropy function for these datasets is shown in Figure 3.27.

Figure 3.26

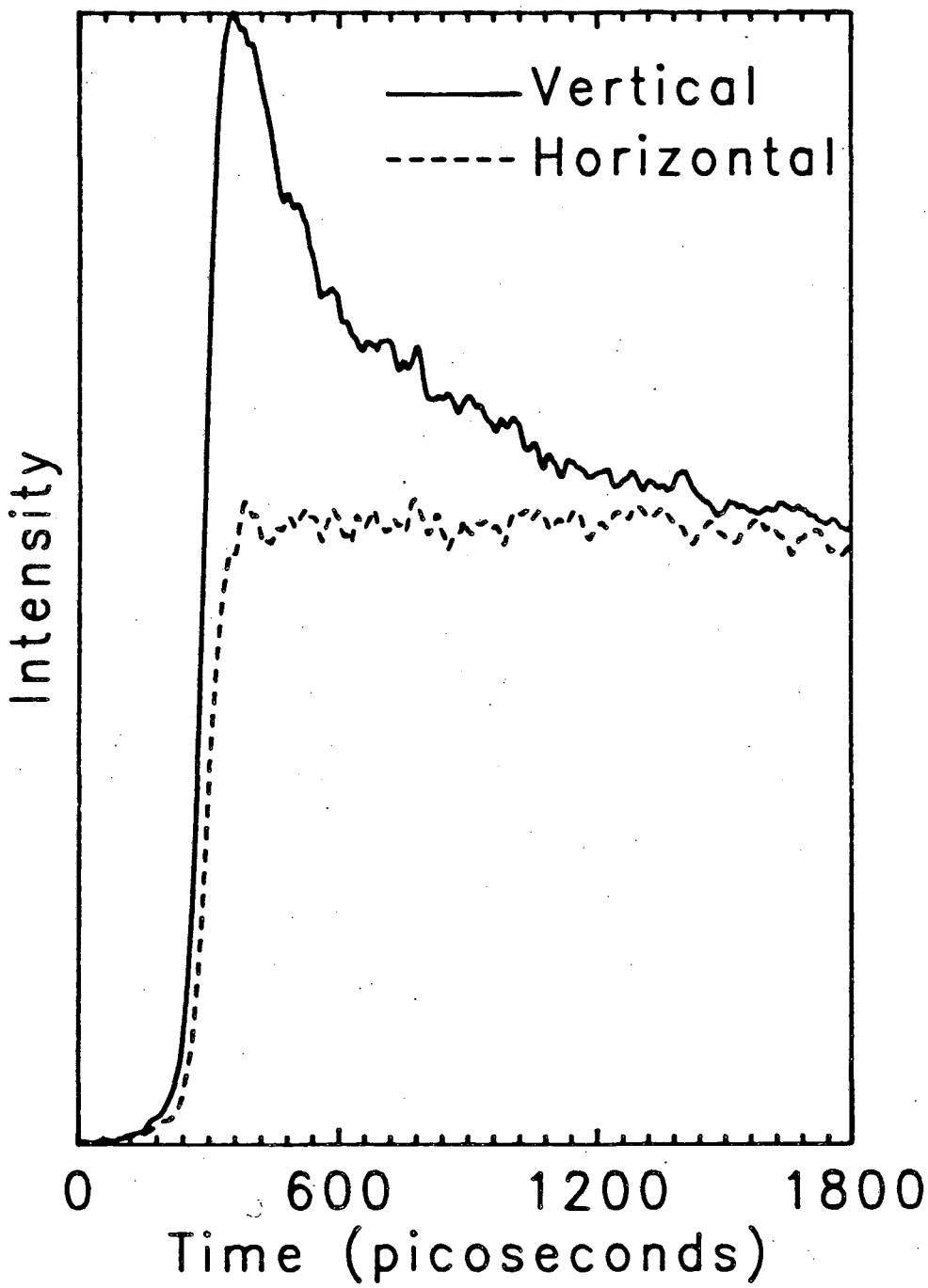
Vertical
Horizontal
Intensity
0
600
1200
1800
Time (picoseconds)

Figure 3.27 Rotational Anisotropy of 4AP in 1-Propanol at 500 nm

The slope of the log of the rotational anisotropy function gave a rotational reorientation time of 329 ps for 4AP in 1-propanol.

Figure 3.27

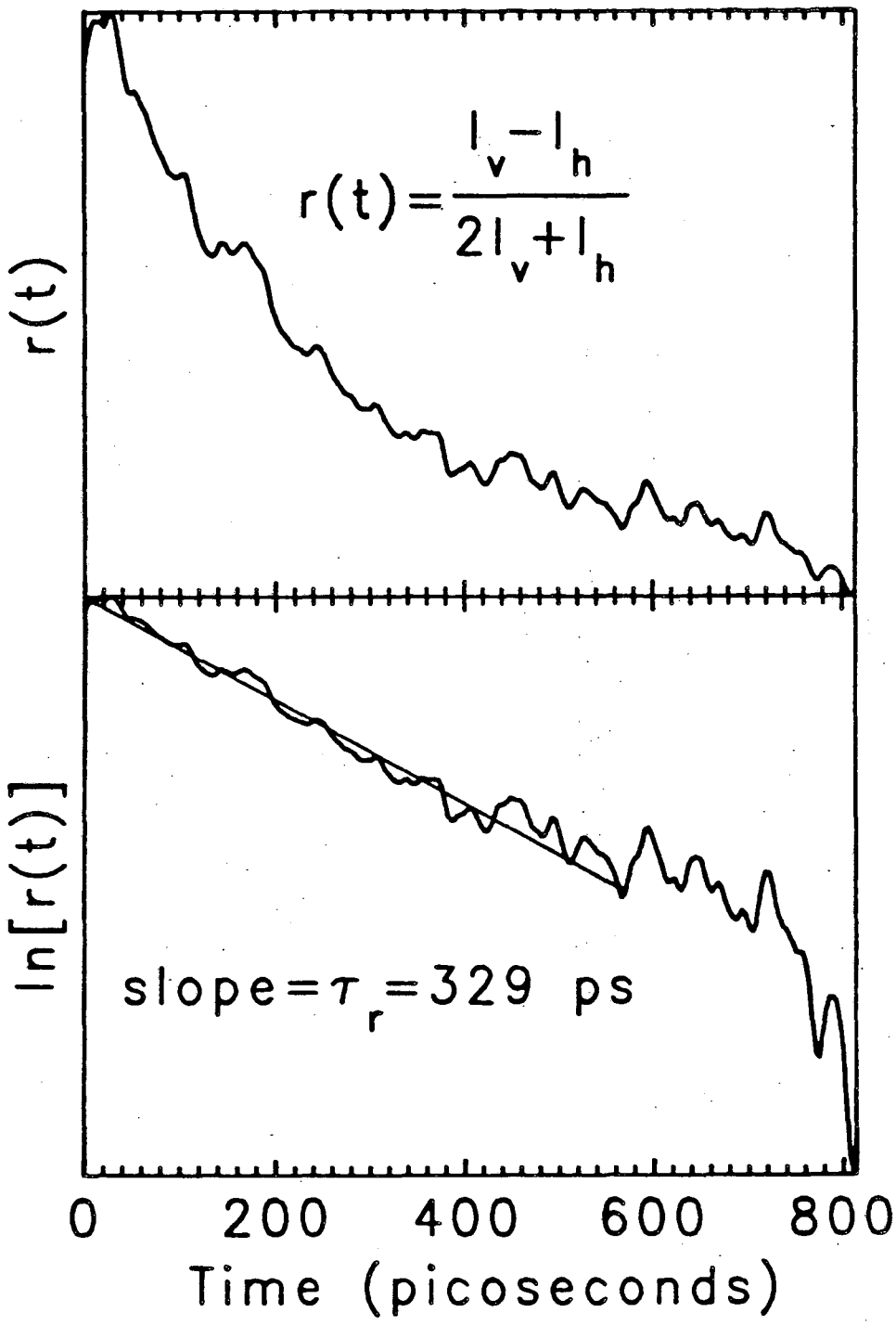
r(t)
$r(t)=\frac{I_v-I_h}{2I_v+I_h}$
ln[r(t)]
slope=τ_r=329 ps
0
200
400
600
800
Time (picoseconds)

from 420 nm to 620 nm, and no change in rotation time was seen. If alcohol molecules are bonding themselves to the 4AP molecule during the solvation process, the change in size was not large enough to see.

The rotational reorientation times for 4AP in a series of alcohols are listed along with the viscosities for the solvents in Table 3.12. The interaction of the 4AP molecule with the solvent is expected to be similar for all of the alcohols. The rotating unit made up of one solute and several solvent molecules may increase in size as the alcohol chain length increases. A plot of these rotation times versus viscosity is shown in Figure 3.28. Within the experimental error of the measurements, the relationship is linear. If the rotation unit is getting larger with chain length, it is not affecting the rotational reorientation time enough to observe a deviation from this linear behavior.

G. Conclusion

For all of the linear alcohols the rotational reorientation times of the 4AP solute are 3-4 times longer than the corresponding solvation times. The dominant source of the relaxation of the excited 4AP molecule is the solvent motion, not the solute motion. The entire shift can be attributed to the dielectric relaxation times of the solvent. The exciplex formation theory proposed by *Ware et al.*[12] is not necessary. These results agree with the extensive theory of *Zwan* and *Hynes*[6] and earlier workers[4,5] on the nature of the time dependent shift. These experiments bring to light the properties of the solvent that are most important in an excited-state relaxation process. Changes in solvent, solute, and temperature support the theory that the dielectric relaxation times of the solvent predict solvation times.

The results obtained here can be applied to many experiments mentioned in the literature. Conclusions about the reason for a time dependent shift are often made with incomplete data. The study of Coumarin 102 by *Shapiro* and *Winn*[10] led to a proposal of a complex between a carbonyl oxygen and an alcohol solvent. The formation of the

Table 3.12

Rotation Times of 4AP in Various Alcohols at 20 °C

Alcohol Solvent	Viscosity * η (cp)	Rotation Time † τ_r (ps)
Methanol	0.55	81 ± 6
Methanol-d	0.55	83 ± 8
Ethanol	1.15	160 ± 12
Ethanol-d	1.18	162 ± 16
1-Propanol	2.15	329 ± 40
2-Propanol	2.30	326 ± 15
2-Propanol-d	2.40	347 ± 25
1-Butanol	2.86	414 ± 13
1-Pentanol	3.70	520 ± 10
1-Octanol	8.82	1390 ± 90

* Viscosities are from reference 31.

† All rotation values except for value for 1-propanol from reference 15.

Figure 3.28 Rotational Reorientation Time of 4AP in Alcohols as a Function of Viscosity

The line is a best fit to the data in Table 3.12. Rotational reorientation time of a molecule is linear with the viscosity for a series of solvents with the same type of interactions.

Figure 3.28

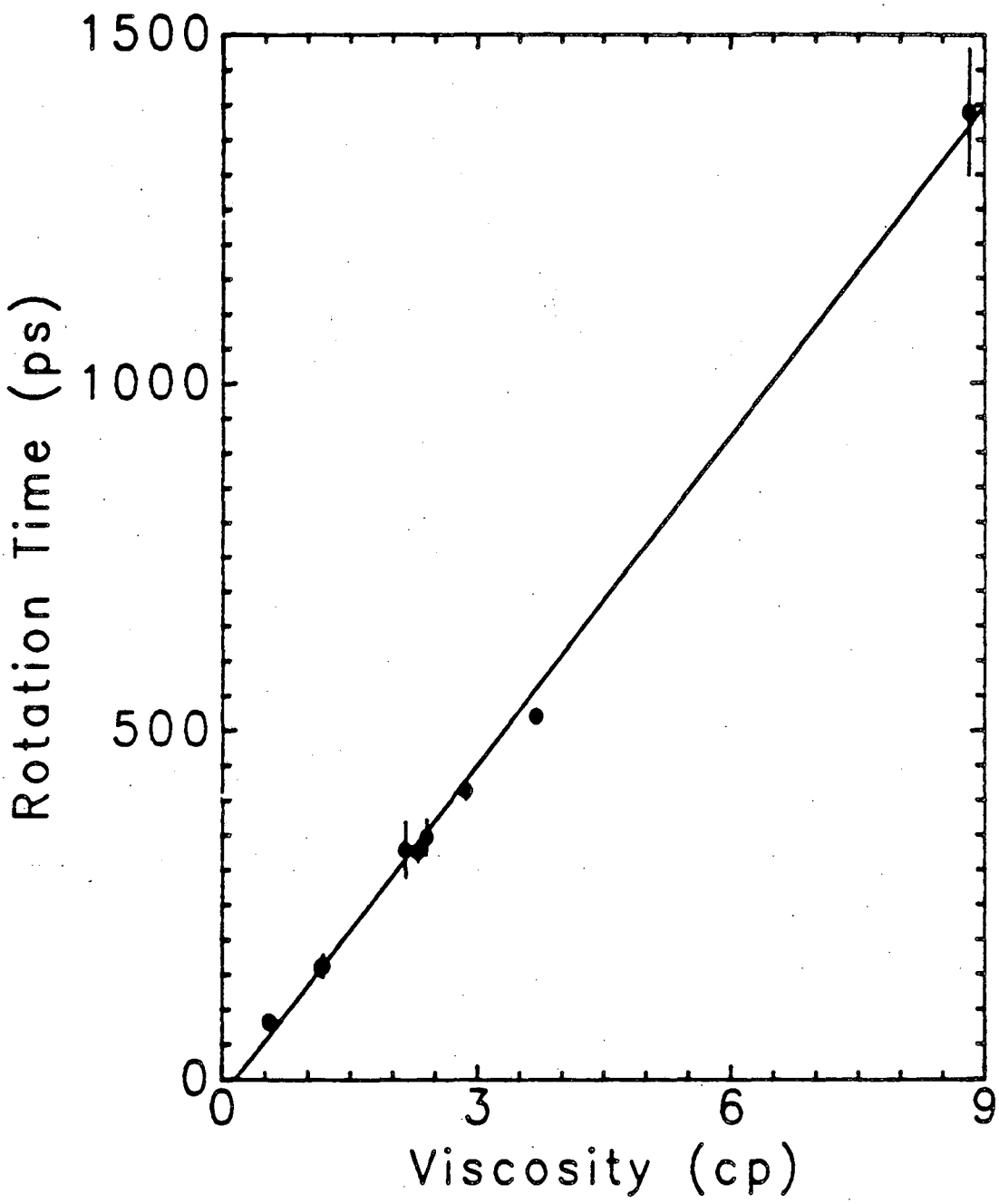

complex was dependent on the organizational time of the solvent. The authors obtained the fluorescence of this molecule at the blue and red edges of its fluorescence band and applied the falltimes of these two edges to a kinetic model of the formation of this complex. With a more complete spectral analysis, the difference between solvent rearrangement and an actual complex formation could probably have been observed. If both processes are occurring, the shape and position of the fluorescence spectrum as a function of time can be revealing. For DMABN in acetonitrile an isosbestic point is seen, whereas for 4AP in 1-propanol a continual shift is observed. If the spectra for DMABN in 1-propanol are examined, a clear isosbestic point is not seen.[30] This result can be explained by once again looking at the difference in dielectric relaxation times for acetonitrile and 1-propanol. After the DMABN charge transfers, the solvent will reorganize around the new charge distribution as the dimethylamino group rotates to form the twisted-internal-charge-transfer state. Because the dielectric relaxation time can be observed for 1-propanol and not for acetonitrile, shifts in the spectra due to the 1-propanol solvent rearrangement obscure the isosbestic point that is so clear in the acetonitrile solvent. Although the isosbestic point is not as clearly defined in 1-propanol, the time-resolved spectra for DMABN in this solvent indicate two components of fluorescence, one of which is slightly shifted. By knowing the relaxation time of the alcohol solvent, a kinetic model could be used to separate the solvent reorganization time from the twisting time of the DMABN molecule. A time for the formation of the TICT state could then be obtained with more accuracy than by measurement of the rise of the red edge or the fall of the blue edge, since both of these values would include a component from the relaxation of the solvent.

Molecules other than coumarin 102 whose excited-state behavior would become clearer with the complete spectral analysis introduced here include the following. *Hallidy* and *Topp*[44] examined the fluorescence shift of 2-amino-7-nitrofluorene in a solvent of 2-propanol. They attributed the time dependence of the shift to the relaxation of the

solvent but were unable to correlate their solvation times to the dielectric relaxation time of the 2-propanol molecule. This inability could be due to two separate problems. First, they were using the uncorrected dielectric relaxation times so the dielectric relaxation of the solvent appeared too long for their solvation times. Second, they only examined the decay of fluorescence at a few wavelengths, and an entire spectrum is needed to obtain the true solvation time of a fluorescing molecule. *Declemy et al.*[45] obtained emission maxima versus time plots for 7-amino-3-methyl-1,4-benzoxazine-2-one (AMBO) in alcohols and contributed to the observable shift to hydrogen-bond formation between the carbonyl of AMBO and the alcohol. They did not obtain quantitative solvation times from their plots, but the molecule looks similar to 4AP so the shift could be due entirely to the dielectric relaxation of the solvent. *Inoue et al.*[46] examined the solvent effects on the fluorescence of 1- and 2-substituted aminoanthraquinones, and *Flom* and *Barbara*[47] did similar studies on 1,5 dihydroxyanthraquinones. Depending on the substituents and position of the amino or hydroxyl group, these molecules can form intra- or inter- molecular hydrogen-bonds. Either formation can lead to a large change in electronic configuration for the solute. Neither author did complete spectral studies but both made predictions on the type of dynamics occurring with fast time data from just a few wavelengths. Complete spectral results like the ones mentioned here would reveal more information on the type of solvation processes which are important in each type of hydrogen-bond. Using nanosecond spectroscopy, *Detoma* and *Brand*[48] proposed a stoichiometric complex formation between 2-anilinonaphthalene and ethanol. However, using picosecond spectroscopy, *Okamura et al.*[49] contributed the fluorescence red shift of a similar molecule, 1-aminonaphthalene, entirely to a solvent relaxation around the excited molecule. The complex formation of *Detoma* and *Brand* was proposed because of a two-exponential decay time of fluorescence which was only seen at very low concentrations of ethanol in cyclohexane. Although complete spectral studies are needed to obtain accurate accounts of what is occurring in the solvation of these two molecules, the following chapter on

the solvation dynamics of 4AP in mixed solvents may explain the results of *Detoma* and *Brand*.

Chapter 4

4-Aminophthalimide Fluorescence in a Mixed Solvent System

A. Introduction

The information obtained from mixed solvent studies can be difficult to interpret due to differences between microscopic interactions and macroscopic observables. The solvation of 4AP needs to be examined on a microscopic level; the environment around the solute is most likely not the same as the environment of the bulk solution. However, mixed solvent work can help determine those processes that are important in a multicomponent solution. The mixed solvent data may answer some of the questions that were raised during the rotation of 4AP studies: how many alcohol molecules are necessary to solvate both the ground state and excited state of the 4AP molecule? In conjunction with this question, is solvent attachment noticeable during the solvation process?

As in the studies of 4AP fluorescence in pure solvents, *Mazurenko et al.*[50,51] examined steady-state and nanosecond fluorescence spectroscopy of aminophthalimides in mixed solvents. He was able to see a time-dependent shift of fluorescence of 4-amino-N-methylphthalimide at very low concentrations of 1-propanol ($\leq$1% by volume) in a decalin solution. He attributed these shifts along with the steady-state spectral shifts to a diffusional process. He says unit cells around the aminophthalimide molecule that contain nonpolar solvent molecules while the solute molecule has its ground-state electronic configuration are replaced by polar solvent molecules after excitation. When one of these unit cells become polar, the interaction energy between the solvent and excited solute molecule changes, bringing about a shift in the spectrum of the solute molecule.

Two more papers concern themselves with the steady-state fluorescence spectra of aminophthalimides in mixed solvents. *Veselova et al.*[52] and *Vlahovici et al.*[53] both studied various aminophthalimides in alcohol:nonpolar solvent mixtures. Both authors attributed the spectral shift and spectral widening to complex formation between nitrogen and oxygen atoms of the phthalimide and hydroxyl hydrogens of the alcohol. These steady-

state spectral shifts are inconclusive; fast time dynamics are needed to discover the time evolution of the shifted spectra.

B. Steady-State Spectra

4AP was studied in a 1-propanol:toluene mixed solvent. This mixture was chosen for the availability of certain properties in the literature: viscosities, dielectric relaxation times, and dielectric constants. Table 4.1 lists the concentrations of 1-propanol in toluene used; these concentrations are in varying units including the number of propanol molecules per 4AP molecule.

Examples of the steady-state spectra of these mixtures are shown in Figure 4.1. Fluorescence maxima for all of the solutions are listed in Table 4.2. As seen in Figure 4.1, only a small concentration, 20% by volume 1-propanol, is needed to shift the 4AP fluorescence spectrum to the position of the spectrum in pure 1-propanol. However, at this concentration, the absorption maximum is only shifted halfway to the maximum in 1-propanol. These results suggest that on the time scale of the fluorescence lifetimes of these molecules, the environment around the excited 4AP molecule is richer in propanol than the environment around the ground state 4AP molecule. With a polar molecule such as 4AP, the solvation by propanol molecules is expected to be preferred, so even in the ground state, the solvent environment around the 4AP molecule is probably richer in propanol than the bulk solution.

C. Fluorescence Lifetimes

Table 4.3 lists the fluorescence lifetimes of 4AP in these solvent mixtures. For those mixtures with large toluene concentrations ($\geq$50% by volume), degassing of the sample by freeze-pump-thawing was necessary to prevent quenching of the fluorescence lifetime by oxygen. The lifetimes become shorter with an increase in the amount of 1-propanol. If the solvent mixture is randomly arranged, the fluorescence lifetime would be inversely

Table 4.1

Concentrations of 1-Propanol used in 1-Propanol:Toluene Mixtures

Volume % of 1-Propanol	Concentration of 1-Propanol Moles/Liter	Mole Fraction of 1-Propanol	Concentration of 4AP Moles/Liter	Total Number of 1-Propanol molecules per 4AP molecule
100	13.37	1.0	1.2×10^{-4}	
90	12.03	.927	1.2×10^{-4}	100250
80	10.07	.851	1.2×10^{-4}	83920
70	9.36	.768	1.2×10^{-4}	78000
60	8.02	.681	1.2×10^{-4}	66833
50	6.68	.587	1.2×10^{-4}	55667
40	5.35	.489	1.2×10^{-4}	44580
30	4.01	.378	1.2×10^{-4}	33417
20	2.67	.263	1.2×10^{-4}	22250
12	1.60	.162	2.5×10^{-5}	64000
4.2	0.56	.056	2.5×10^{-5}	22400
1.0	0.13	.014	2.5×10^{-5}	5200
0.1	0.013	.0014	2.5×10^{-5}	520
0 (Toluene)	0	0	2.5×10^{-5}	0

Figure 4.1 Steady-State Fluorescence Spectra of 4AP in 1-Propanol:Toluene Mixtures

Concentrations of propanol are in % by volume. Only a small amount of propanol is necessary to shift the steady-state spectrum of 4AP fluorescence most of the way from its position of 428 nm in toluene to the position of 525 nm in pure propanol.

Figure 4.1

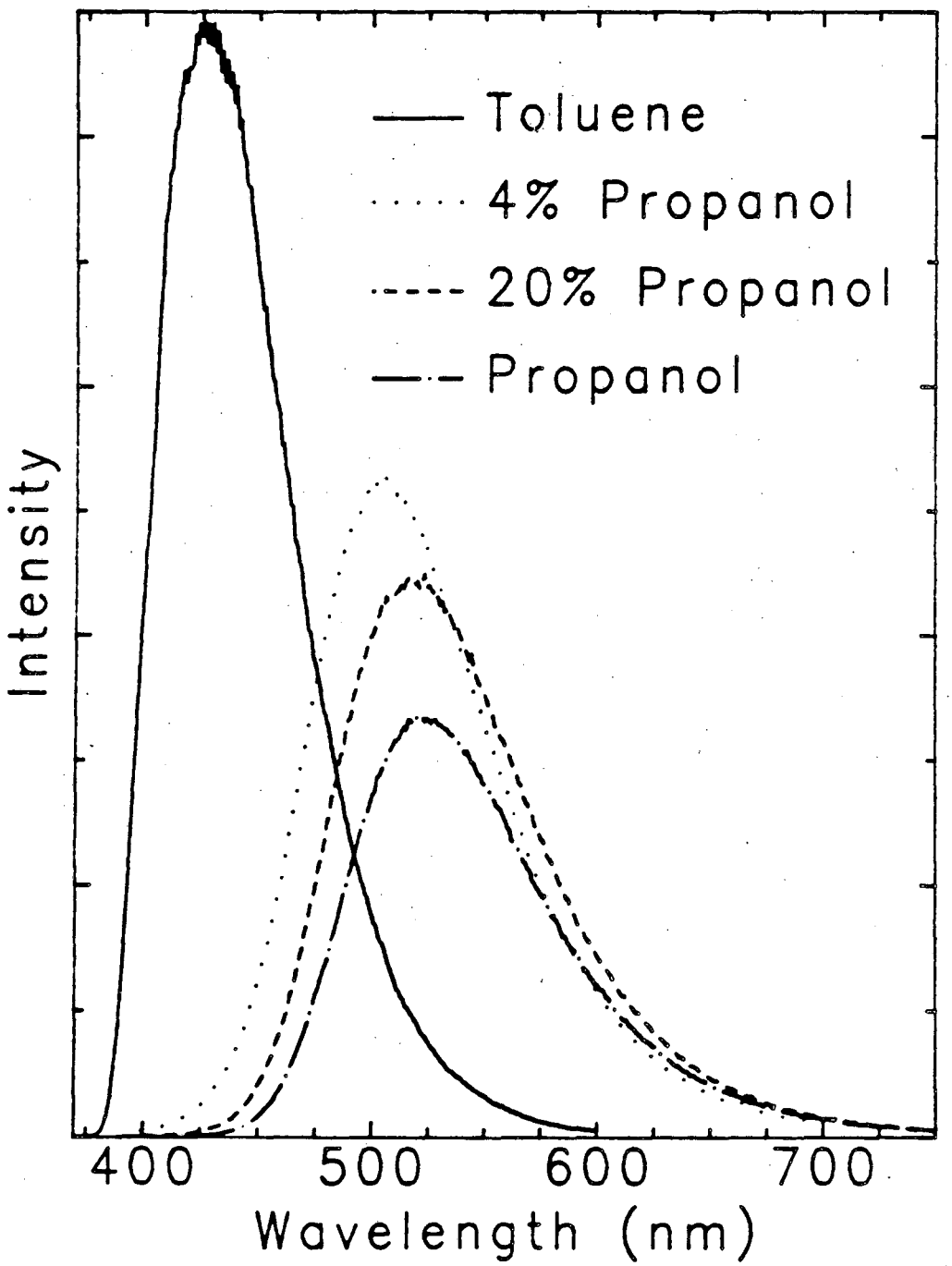
Toluene
4% Propanol
20% Propanol
Propanol
Intensity
400
500
600
700
Wavelength (nm)

Table 4.2

Steady-State Absorption and Fluorescence Data for 4AP in 1-Propanol:Toluene Mixtures

Volume % Propanol	Fluorescence Maximum(nm)	Absorption Maximum(nm)
100	525	373
90	525	372
80	525	371
70	523	370
60	523	369
50	522	369
40	520	367
30	520	366
20	520	363
12	513	361
4.2	506	356
1.0	479	352
0.1	440	351
0	428	351

proportional to the rate of relaxation by toluene, k_t, plus the rate of relaxation by 1-propanol, k_p:

$$\tau_{fl} \propto 1/(k_t\chi_t + k_p\chi_p + C)$$

where χ_t and χ_p are the mole fractions of toluene and 1-propanol respectively and C is a constant. Since $\chi_t + \chi_p = 1$, the fluorescence lifetime becomes inversely proportional to the mole fraction of propanol:

$$\tau_{fl} \propto 1/(k_t(1-\chi_p) + k_p\chi_p + C);$$

$$1/\tau_{fl} \propto \chi_p.$$

Figure 4.2 shows this linear relationship, obtained from the two pure solvent limits, along with the data points from Table 4.3. The data points fall above the line, indicating a shorter fluorescence lifetime than the theory would predict. This shorter lifetime is indicative of a larger 1-propanol population around the 4AP than the bulk solution concentrations would indicate.

D. Rotations

The rotational reorientation times reveal some of the same information as the steady-state and fluorescence lifetime data. These times plus the corresponding bulk viscosities of the mixed solvents are listed in Table 4.4. As described in Section F of Chapter 3, the rotational reorientation times of 4AP should be directly proportional to viscosity for a series of solvents with similar interactions. Figure 4.3 is a plot of the data in Table 4.4 along with some of the data from Figure 3.28 and a linear fit of the rotational reorientation times for 4AP in the pure alcohols. Above a 1-propanol concentration of 30% by volume, the rotational reorientation times are linear with the bulk viscosity of the solvent. Although a fit of the rotational reorientation times of 4AP in the solutions with a 1-propanol concentration above 30% by volume is almost parallel to the fit of the pure solvent rotations, it would not match the pure solvent fit. For a corresponding viscosity,

Table 4.3

Fluorescence Lifetimes of 4AP in 1-Propanol:Toluene Mixtures at 20 °C

Mole Fraction of Propanol χ_P	Fluorescence Lifetime τ_{fl} (ns)	(Fluorescence Lifetime)$^{-1}$ $1/\tau_{fl}$ (ns)$^{-1}$
1.0	11.0 ± 0.5	.0875 ± .0023
.927	11.6 ± 0.3	.0861 ± .0022
.851	11.8 ± 0.2	.0849 ± .0014
.768	11.9 ± 0.1	.0839 ± .0007
.681	12.2 ± 0.2	.0818 ± .0013
.587	13.0 ± 0.3	.0768 ± .0018
.489	13.2 ± 0.1	.0757 ± .0006
.378	13.4 ± 0.2	.0747 ± .0011
.263	14.0 ± 0.3	.0714 ± .0015
.162	14.2 ± 0.2	.0704 ± .0010
.056	15.4 ± 0.2	.0649 ± .0009
.014	17.5 ± 0.8	.0570 ± .0026
.0014	17.5 ± 1.2	.0570 ± .0039
0.0	20.0 ± 1.6	.0499 ± .0040

Figure 4.2 Fluorescence Lifetime Data for 4AP in 1-Propanol:Toluene Mixtures

Lifetime data is from Table 4.3. Theoretical line is defined by the lifetime of 4AP in pure toluene and pure 1-propanol. All of the lifetimes of the mixed solvents fall above the line, indicating a shorter lifetime than the theory in section C suggests. This result implies an alcohol rich environment around the 4AP molecule.

Figure 4.2

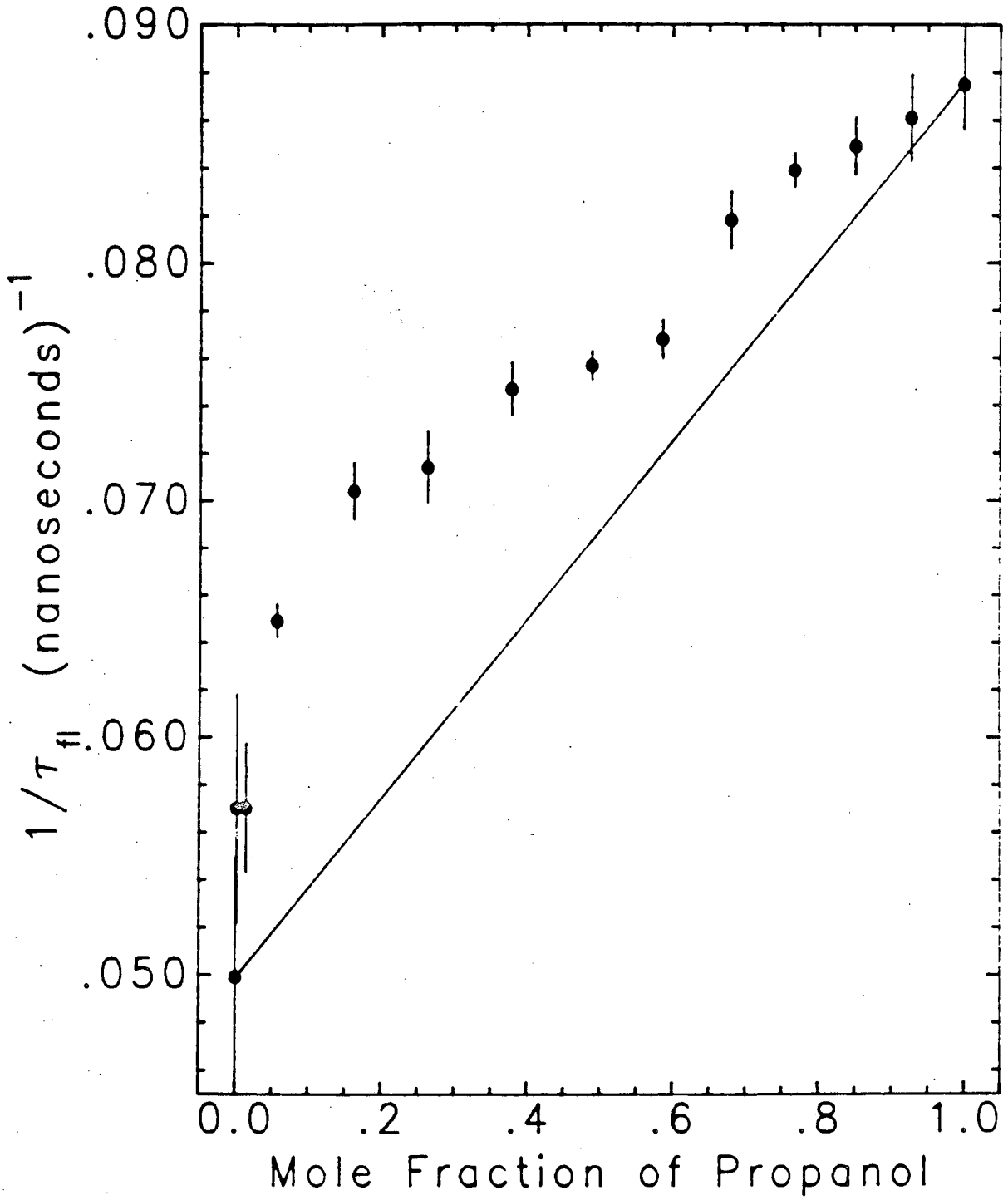
.090
.080
.070
.060
.050
$1/\tau_{fl}$ (nanoseconds)$^{-1}$
0.0
.2
.4
.6
.8
1.0
Mole Fraction of Propanol

the rotational reorientation time of 4AP in these mixed solvents is slow when compared to a pure alcohol. This trend suggests that the microscopic viscosity around the 4AP molecule is higher than the viscosity of the bulk solution. If a larger concentration of propanol molecules relative to the bulk solution is around the 4AP molecule, a higher microscopic viscosity is expected. For the lower concentrations of propanol in toluene, the rotational reorientation times are below any linear fit of the higher concentration data. At these concentrations, two different effects can be contributing: the microscopic viscosity around the 4AP molecule is closer to the bulk viscosity and the size of the rotating unit may be smaller. There may not be enough propanol molecules to create a significantly different microscopic environment around the solute molecule. If a large complex of 4AP and propanol molecules is rotating in the pure solvents, in these very dilute solutions of propanol the number of alcohol molecules rotating with the 4AP molecule may be less. These questions about the microscopic environment around the 4AP molecule are further addressed by considering the fast time dynamics of solvation.

E. Solvation Dynamics

The fast time dynamics were examined every 10 nm between 400 nm and 600 nm for all of the above mixed solvents. Some examples of the blue and red edges are shown in Figures 4.4 and 4.5 respectively. The blue edge shows a slower fall time as the amount of propanol is decreased. This result is reflected on the red edge, where the risetime is slower with lower concentrations of propanol. As with the pure solvents, peak positions and widths of spectral bands versus time plots can be obtained. The fluorescence peak positions versus time for the solutions in Figures 4.4 and 4.5 verify the slower solvation times with a decrease in propanol concentration, Figure 4.6. By fitting the peak positions versus time curves to two exponentials, the solvation times listed in Table 4.5 were obtained. For the most dilute solution, 0.1% by volume propanol, the solvation time was too slow to measure, although some solvation dynamics were occurring. Figure 4.7 shows the blue side of the fluorescence for 4AP in this solution and in pure toluene. The

Table 4.4

Rotation Times of 4AP in 1-Propanol:Toluene Mixtures at 20 °C

Volume % of Propanol	Viscosity * η (cp)	Rotation Time τ_r (ps)
100	2.15	329 ± 40
90	1.98	319 ± 19
80	1.74	276 ± 15
70	1.50	273 ± 19
60	1.28	255 ± 9
50	1.08	205 ± 29
40	0.93	202 ± 27
30	0.77	169 ± 27
20	0.69	130 ± 17
12	0.64	117 ± 17
4.2	0.60	88 ± 20
1.0	0.59	53 ± 15
0.1	0.59	40 ± 16
0	0.586	37 ± 19

* Values obtained from extrapolation of data in references 54 and 55.

Figure 4.3 Rotational Reorientation Times of 4AP in 1-Propanol:Toluene Mixtures

The * represents rotational reorientation times of 4AP in the mixed solvents from Table 4.4, and the • represents some of the rotational reorientation times of 4AP in pure alcohols from Table 3.11. The line is a best fit of all of the data of Table 3.11. Except for the low concentrations of 1-propanol, the rotations of 4AP in the mixed solvents are slower for a corresponding bulk solution viscosity than in the pure alcohols.

Figure 4.3

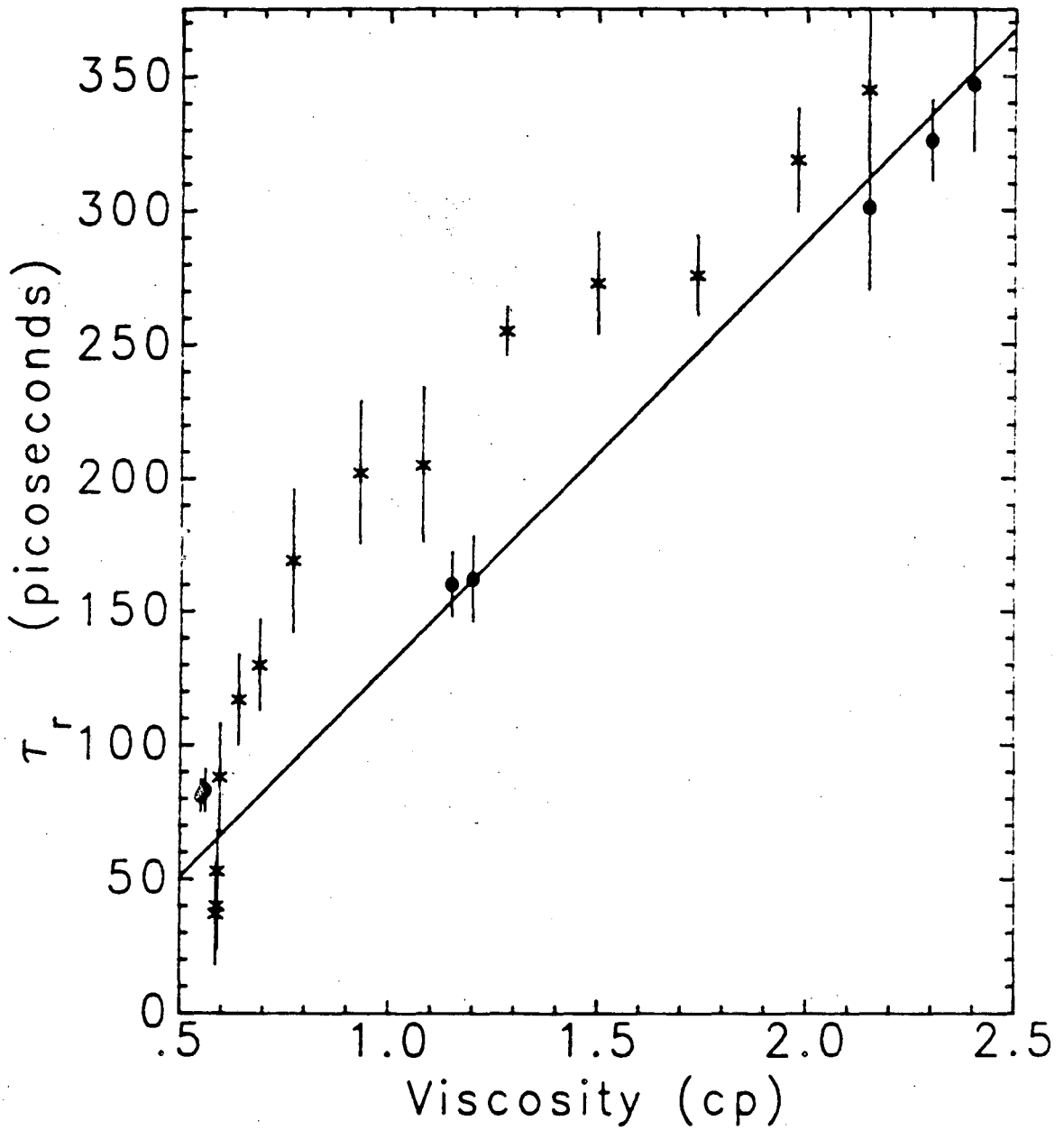
350
300
250
200
150
100
50
0
τ_r (picoseconds)
.5
1.0
1.5
2.0
2.5
Viscosity (cp)

slow fall for the 0.1% propanol solution is faster than the fluorescence lifetime of 4AP in this solvent mixture, but the falltime is close enough to the fluorescence lifetime that separating out the solvation time from the fluorescence lifetime would be difficult. In comparing all of the solutions, the long-time exponential becomes longer with a decrease in the amount of propanol whereas, within experimental error, the short time component does not change.

Examples of the width of the spectral band versus time are given in Figure 4.8. The shapes of these plots are the same as for the pure solvent work described in Figure 3.18. The ranges of the maxima for these plots, Table 4.6, once again fall in the range of the long time component of the solvation times obtained from the exponential fits of the peak position versus time plots. In order to parallel the pure solvent work, these solvation times were compared with the dielectric relaxation times of the mixed solvents.

F. Dielectric Relaxation Times

The long time dielectric relaxation times of mixed solvents have been measured for many mixtures. These times need to be corrected, so the dielectric constants and optical dielectric constants for the mixed solvents are also needed. The dielectric constants, ϵ_o, are found from extrapolating values in references 54 and 55. The optical dielectric constants, ϵ_∞, are not available for the mixed solvents. *Koshii et al.*[56] claim that ϵ_∞ does not change from the value in pure propanol for up to 50% benzene in 1-propanol, but the data of *Campbell et al.*[55] for 1-propanol and cyclohexane mixtures do not agree with this result. As in the pure solvents, the ϵ_∞ parameter will be the error limiting value in the corrected dielectric relaxation times. Table 4.7 contains the dielectric relaxation times, ϵ_o, and the corrected relaxation times for these mixed solvents using the ϵ_∞ value of pure 1-propanol. These corrected dielectric relaxation times are thus the highest values possible, since the ϵ_∞ for the mixtures is most likely lower than the value for 1-propanol.

Since no information is available about any other dispersion regions for mixed solvents, assigning the fast solvation time from Table 4.5 to a second relaxation time is

Figure 4.4 Fast Time Dynamics of 4AP in 1-Propanol:Toluene Mixtures at 450 nm

Concentrations of 1-propanol are in % by volume. The fall of the fluorescence at the blue edge of the steady-state spectrum becomes slower with a decrease in 1-propanol concentration. The time constants for the fast component of the falls shown here are 58 ps for propanol, 87 ps for 80% propanol, 100 ps for 60% propanol, 130 ps for 40% propanol and 205 ps for 20% propanol.

Figure 4.4

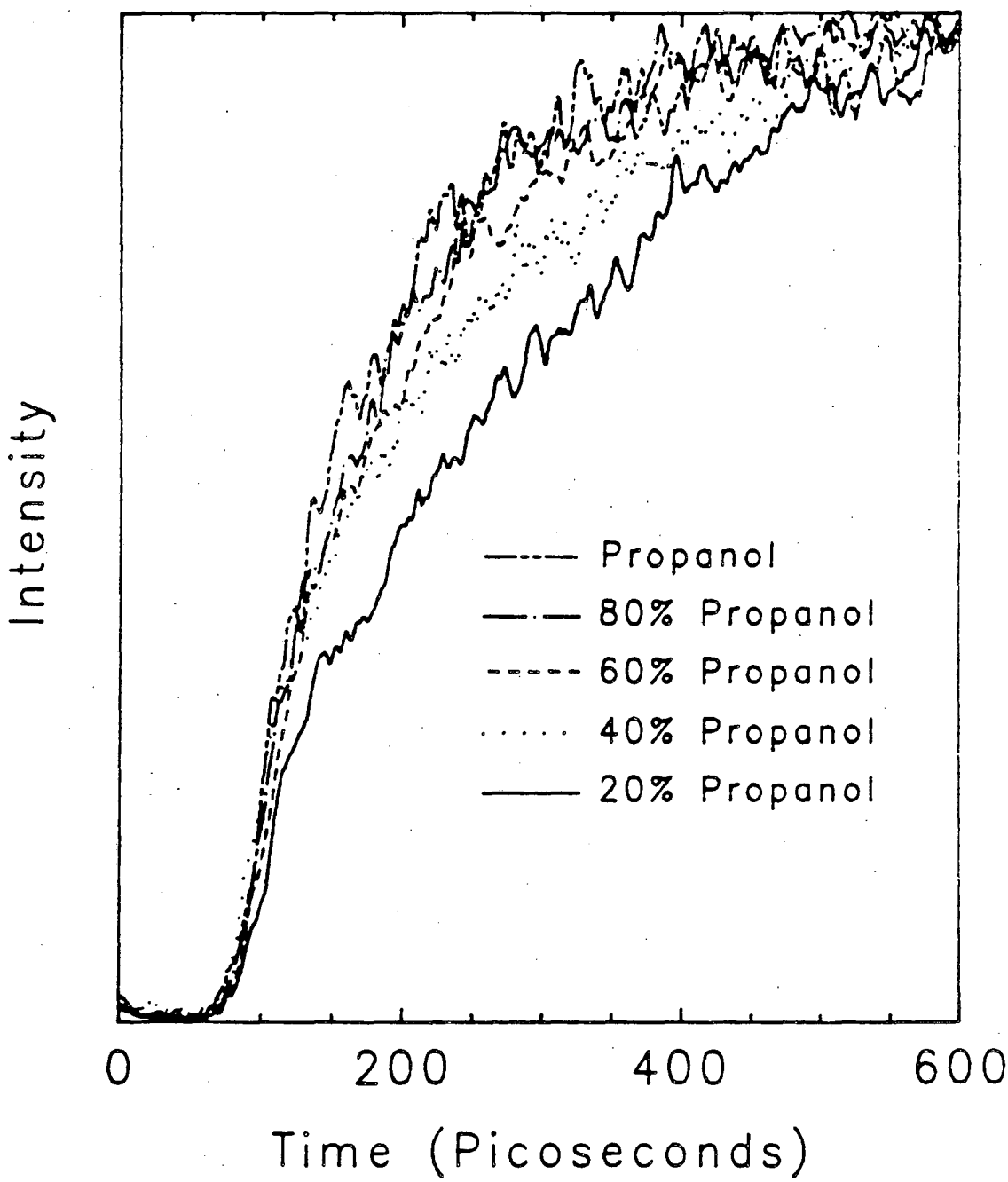
Intensity
Propanol
80% Propanol
60% Propanol
40% Propanol
20% Propanol
0
200
400
600
Time (Picoseconds)

Figure 4.5 Fast Time Dynamics of 4AP in 1-Propanol:Toluene Mixtures at 600 nm

Concentrations of 1-propanol are in % by volume. The rise of the fluorescence at the red edge of the steady-state spectrum becomes slower with a decrease in 1-propanol concentration. The time constants for the rise of the 4AP fluorescence in the solutions shown here are 110 ps for propanol, 119 ps for 80% propanol, 133 ps for 60% propanol, 200 ps for 40% propanol, and 305 ps for 20% propanol.

Figure 4.5

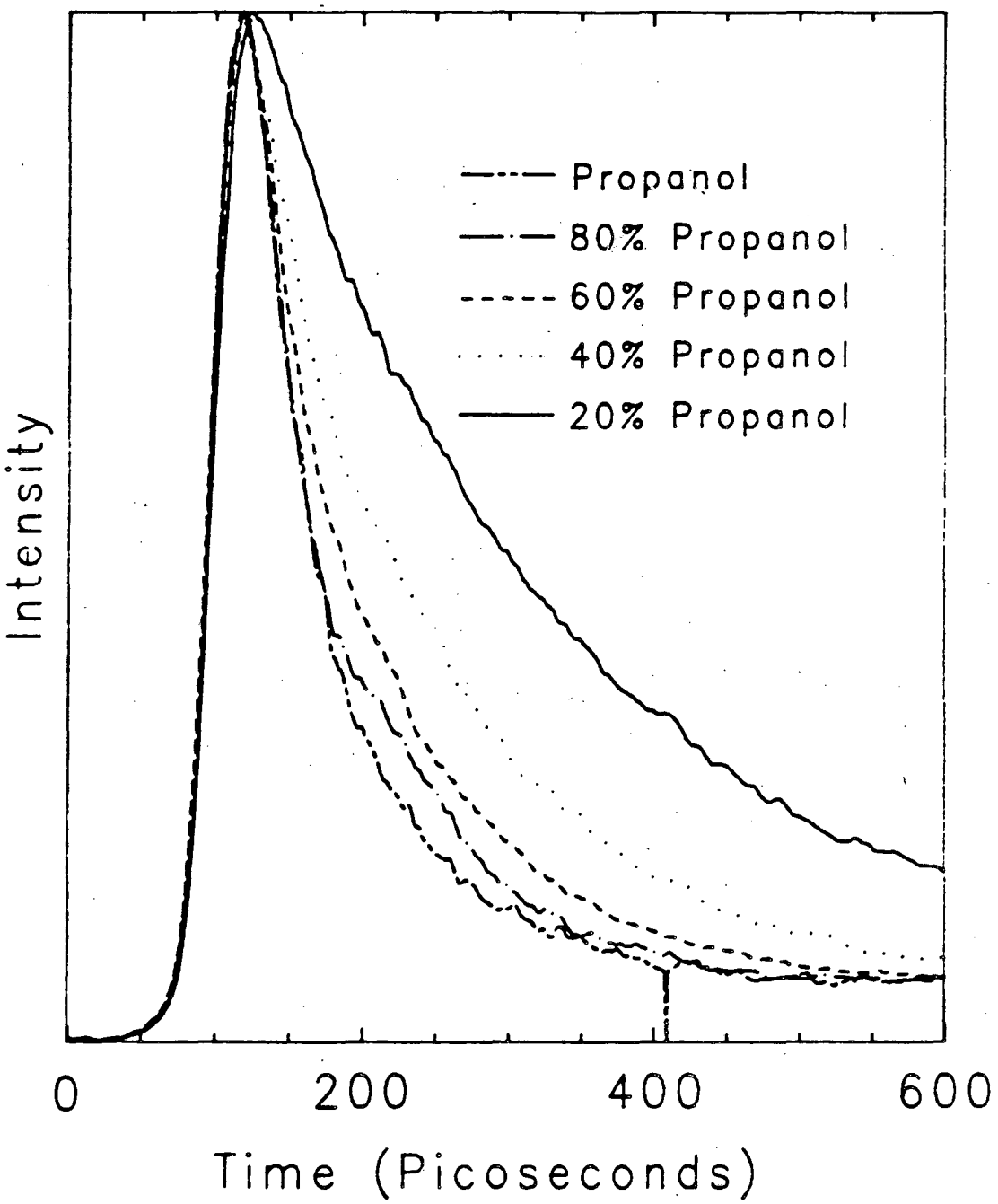
Propanol
80% Propanol
60% Propanol
40% Propanol
20% Propanol
Intensity
0
200
400
600
Time (Picoseconds)

Figure 4.6 Fluorescence Peak Positions versus Time for 4AP in 1-Propanol:Toluene Mixtures

Concentrations of 1-propanol are in % by volume. The rate of the shift of the fluorescence spectrum slows with a decrease in 1-propanol concentation. Two exponential fits to these plots are listed in Table 4.5.

Figure 4.6

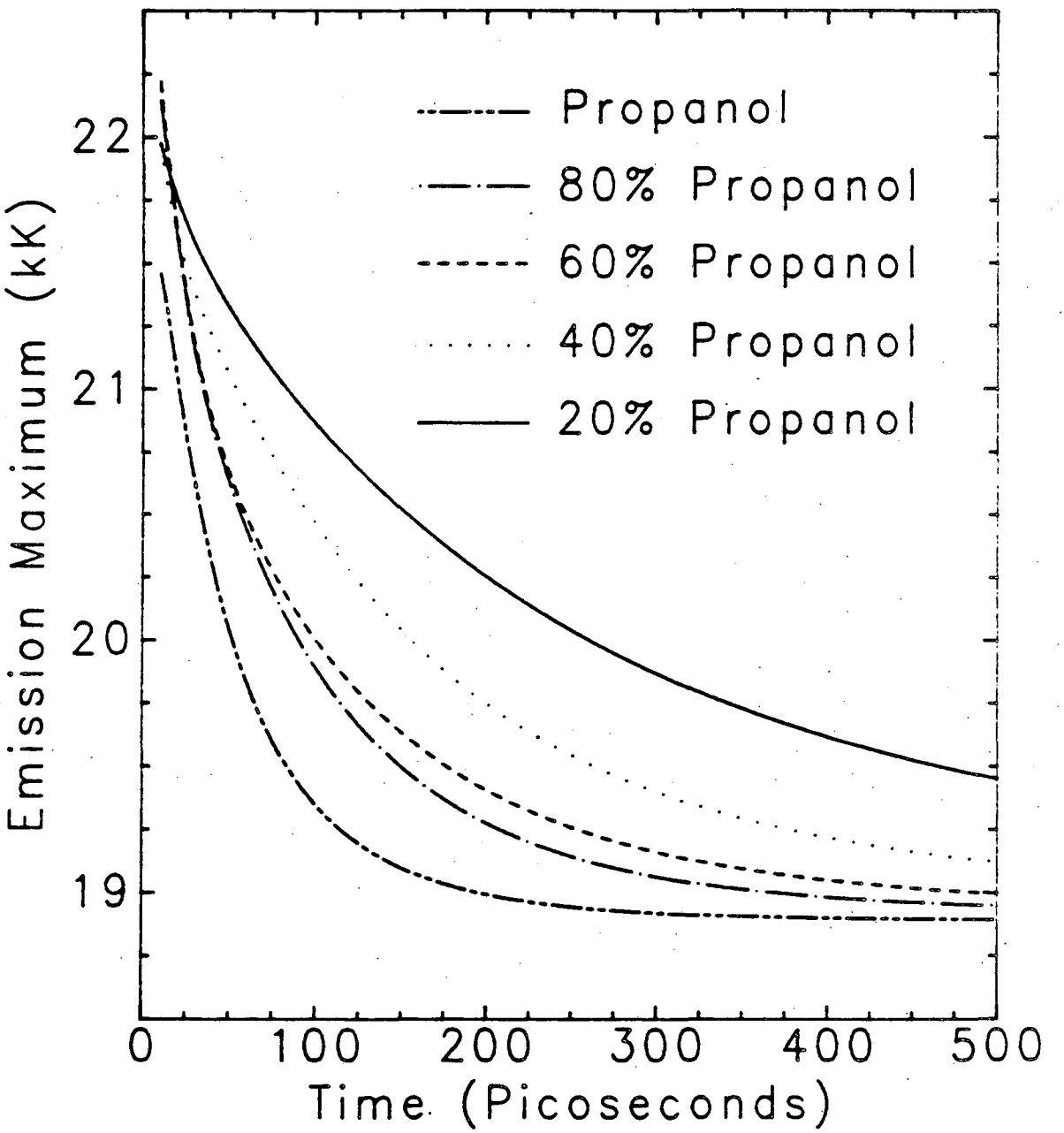
Propanol
80% Propanol
60% Propanol
40% Propanol
20% Propanol
Emission Maximum (kK)
22
21
20
19
0
100
200
300
400
500
Time (Picoseconds)

Table 4.5

Solvation Times of 4AP in 1-Propanol:Toluene Mixtures at 20 °C

Volume % of Propanol	α_1	τ_1 (ps)*	α_2	τ_2 (ps)†
100	1.56	15	2.06	90
90	1.50	19	2.25	104
80	1.47	19	2.61	100
70	1.50	20	2.53	115
60	1.90	21	2.27	129
50	1.24	25	2.48	144
40	0.61	18	2.27	157
30	0.70	40	2.28	217
20	0.58	54	2.45	265
12	0.20	20	2.33	498
4.2	0.03	20	2.74	1080
1.0	–	–	–	2700‡

* Error on these values is ± 10 ps.

† Error on these values is ± 10%.

‡ No second exponential was needed to fit the data.

Figure 4.7 Fast Time Dynamics of 4AP in Toluene and a Dilute 1-Propanol in Toluene Solution at 410 nm

Concentration of 1-propanol is 0.1% by volume. Both spectra have a rise time of 0 ps, but the sample with 1-propanol has a fall component, which is too slow to measure, different from the fluorescence lifetime.

Figure 4.7

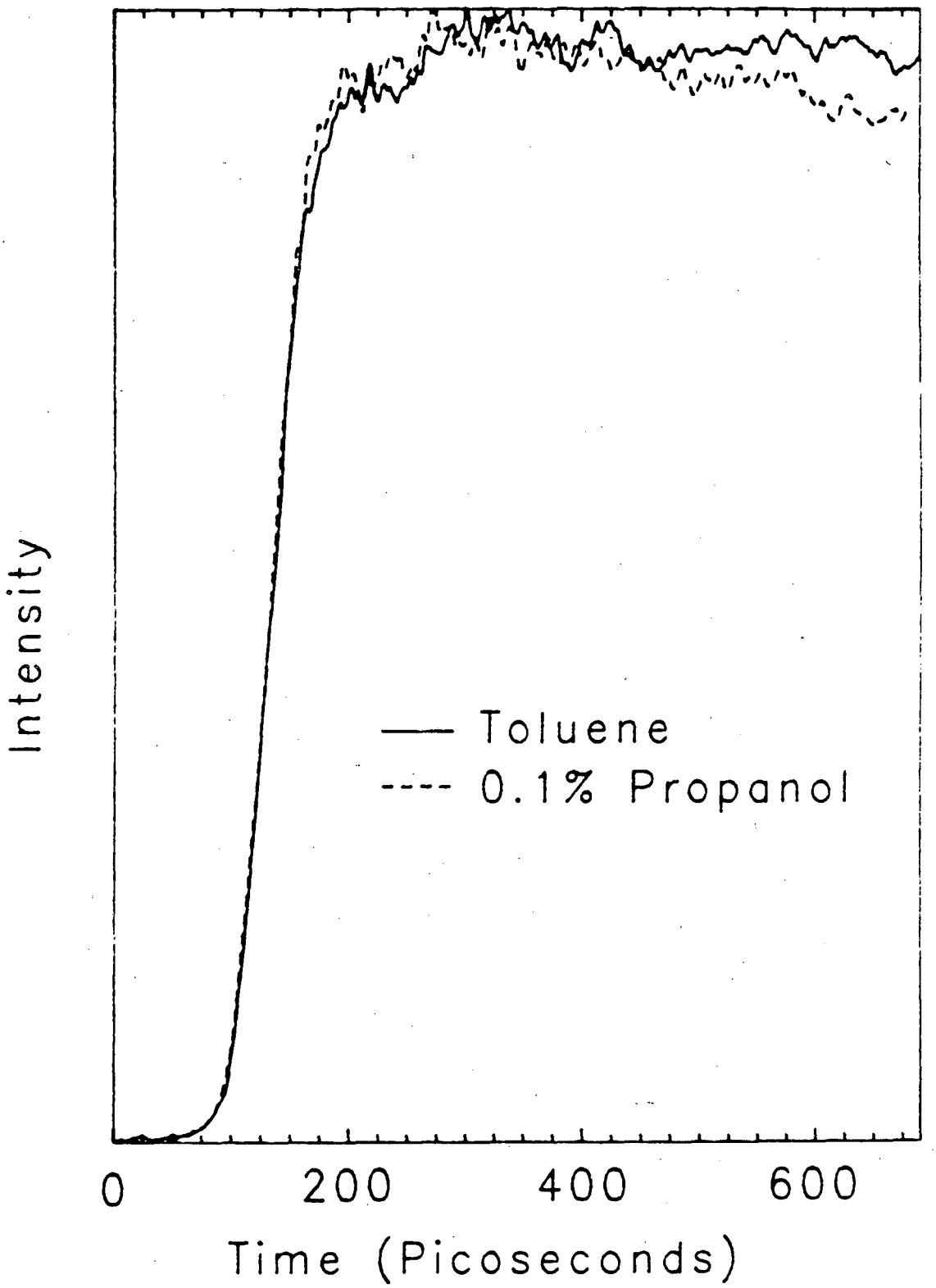
Intensity
Toluene
0.1% Propanol
0
200
400
600
Time (Picoseconds)

Figure 4.8 Spectral Width as a Function of Time for 4AP in 1-Propanol:Toluene Mixtures

Concentration of 1-propanol are in % by volume. The maximum of the spectral widths correspond to one solvation lifetime for all of the mixed solvents studied. The times for the maxima of the spectra shown here are given in Table 4.8.

Figure 4.8

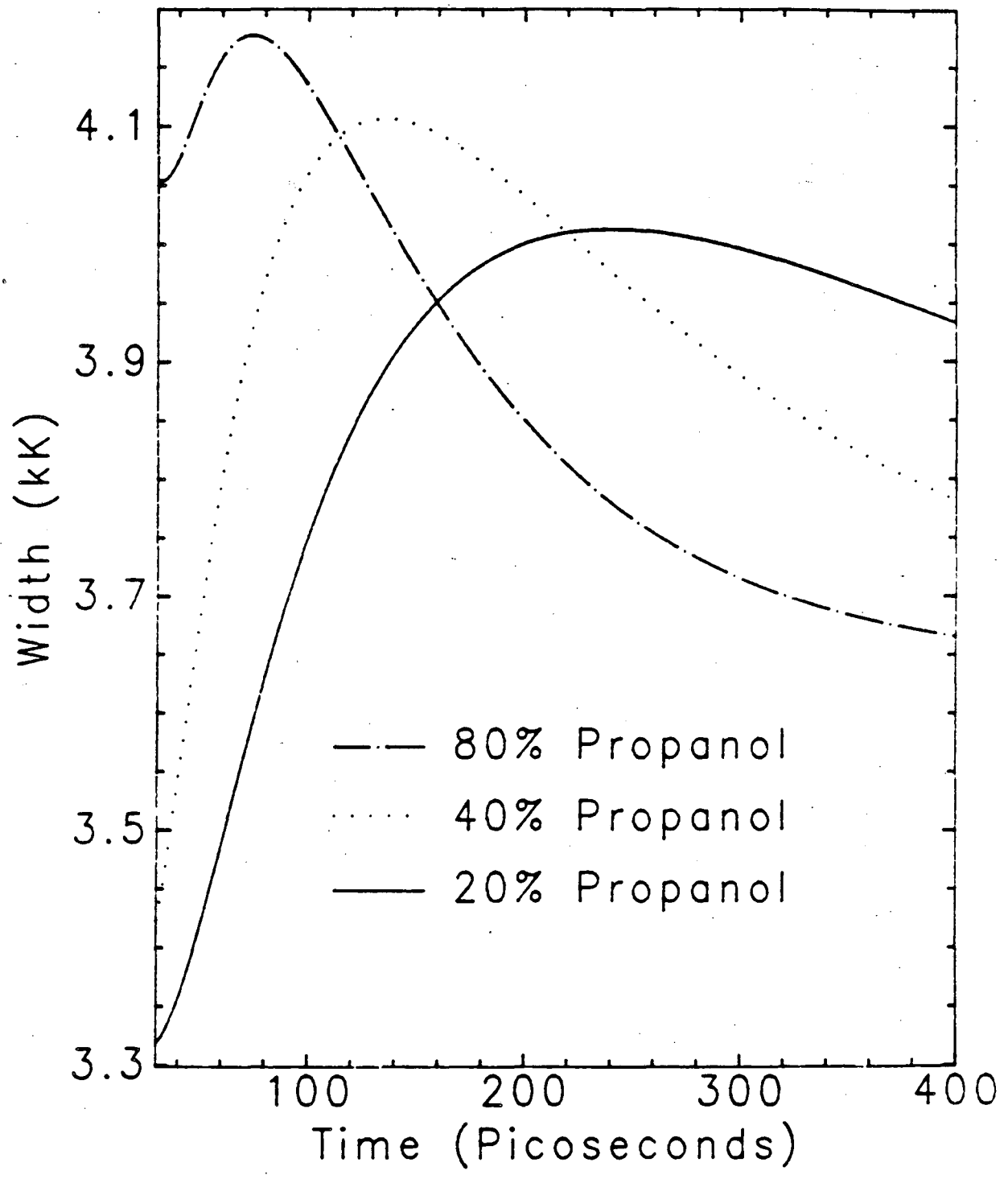
4.1
3.9
3.7
3.5
3.3
Width (kK)
100
200
300
400
Time (Picoseconds)
80% Propanol
40% Propanol
20% Propanol

Table 4.6

Time of Maximum Spectral Width versus Solvation Time for 4AP in 1-Propanol:Toluene Mixtures

Volume % of Propanol	Time of Maximum Spectral Width (ps)	Solvation Time τ_2 (ps)
100	86 ± 15	90 ± 10
90	89 ± 10	104 ± 10
80	74 ± 10	100 ± 10
70	93 ± 10	115 ± 12
60	94 ± 10	129 ± 13
50	108 ± 10	144 ± 14
40	136 ± 20	157 ± 16
30	211 ± 20	217 ± 22
20	244 ± 40	265 ± 26
12	558 ± 70	498 ± 50
4.2	1050 ± 100	1080 ± 108
1.0	2440 ± 200	2700 ± 270

Table 4.7

Dielectric Relaxation Times of 1-Propanol:Toluene Mixtures at 20 °C

Volume % of Propanol	Dielectric Relaxation Time τ (ps)**	Static Dielectric Constant $\epsilon_0^{\dagger}$	Optical Dielectric Constant $\epsilon_\infty^{\ddagger}$	Corrected Dielectric Relaxation Time $\tau' = \tau \times \epsilon_\infty / \epsilon_0$
100	380	20.7	4.24	78
90	367	19.3	*	≤80
80	330	17.6	*	≤79
70	295	15.0	*	≤83
60	265	11.8	*	≤90
50	230	9.0	*	≤102
40	190	7.0	*	≤109
30	150	5.2	*	≤115
20	105	4.0	*	≤105
12	70	3.1	*	≤90
Toluene		2.37	2.24	

* Value for 1-propanol was used to calculate the highest possible value for the corrected dielectric relaxation times.

** Value for 1-propanol is from reference 34; all other values are extrapolated from data in references 55 and 57.

† Values are extrapolated from data in reference 54 and 55.

‡ Value for toluene is from reference 31.

difficult. This region was attributed to the rotation of a propanol molecule which can still be occurring around the 4AP molecule. If many propanol molecules are around the 4AP molecule, the rotation time of the propanol molecule would not change much with dilution of toluene. Understanding the longer solvation time will help in unravelling the mysteries of this shorter time component.

The long time component of the solvation time is listed along with the corrected dielectric relaxation times in Table 4.8. All of the solvation times are greater than the highest possible dielectric relaxation times for each solvent mixture. Since the solvation times no longer correlate with the dielectric relaxation times, a new predictive theory is needed.

G. Diffusion

Since the 4AP molecule has a larger dipole moment in the excited state, the molecular environment can accomodate more of the polar alcohol molecules in the excited state than in the ground state. These alcohol molecules would have to diffuse in from the bulk solution. This diffusion rate of a molecule can be described by the Debye equation:[43,58]

$$\tau_d \propto a^3\eta/T.$$

Here a is the radius of the diffusing propanol molecules, τ_d is the time of diffusion, and η is the viscosity of the solution. The volume of a mole of the propanol molecules, V_n, can be expressed in terms of the radius of the molecule and Avogadro's number, N_A:

$$V_n = \frac{4\pi a^3 N_A}{3}.$$

The volume of a mole is inversely proportional to the concentration or moles per liter, so the diffusion rate, $1/\tau_d$, should be proportional to the concentration of propanol divided by the viscosity for a given temperature:

$$1/\tau_d \propto [propanol]/\eta.$$

Table 4.8

Solvation Times of 4AP versus Dielectric Relaxation Time of 1-Propanol:Toluene Mixtures

Volume % of Propanol	Dielectric Relaxation Time τ' (ps)	Solvation Time τ_2 (ps)
100	78 ± 10	90 ± 10
90	≤ 80	104 ± 10
80	≤ 79	100 ± 10
70	≤ 83	115 ± 12
60	≤ 90	129 ± 13
50	≤ 102	144 ± 14
40	≤ 109	157 ± 16
30	≤ 115	217 ± 22
20	≤ 105	265 ± 26
12	≤ 90	498 ± 50

Figure 4.9 is a plot of the inverse solvation time from Table 4.8 versus the volume % of propanol/viscosity. For low propanol concentrations, this plot is linear; however, at higher propanol concentrations the solvation times are too fast for this diffusional analysis.

Similar work done by *Hallidy* and *Topp*[54] compares with the the above work on 4AP in 1-propanol:toluene mixtures. They studied the time dependent shift of 2-amino-7-nitrofluorene (ANF) in a mixture of 2-propanol and benzene. By examining the decay of the red and blue edges of emission, a rate constant associated with a Stokes' shift process was obtained. After plotting this rate constant versus the function of propanol concentration divided by viscosity mentioned above, a similar plot to Figure 4.9 was obtained. The plot starts off linear at low 2-propanol concentrations and levels off after a 2-propanol concentration of 30% by volume; at this same concentration of 1-propanol in toluene, Figure 4.9 becomes nonlinear. *Hallidy* and *Topp* attribute this nonlinearily to a different microscopic viscosity around the solute than the bulk viscosity of the solution. In order to explain the direction of the deviation, a lower microscopic viscosity than the bulk solution had to be evoked. The rotational reorientation dynamics of the 4AP molecule showed that the microscopic viscosity around the solute is more likely to be greater than the bulk solution for these mixed solvents of alcohol:aromatic hydrocarbons. This study does not satisfactorily explain the results obtained for ANF or the above results for 4AP. A new approach to this problem follows.

H. Combined Mechanism of Relaxation

The solvation times at low propanol concentration were much too slow for dielectric relaxation, but at high propanol concentrations, they were too fast for a diffusional process. This result suggests that both relaxation mechanisms are occurring. The dielectric relaxation of the alcohols already around the 4AP molecule occurs, while other alcohol molecules, needed to completely relax the 4AP molecule, are diffusing into the solvent sphere surrounding the 4AP molecule. At low alcohol concentrations the rate limiting step to relaxation is the diffusion of the alcohol to the excited molecule. At higher con-

Figure 4.9 Debye Model for a Diffusional Process

The inverse of the long time solvation time is plotted against volume % of 1-propanol divided by the viscosity of the bulk solution. The line is the best fit from the five lowest concentrations of 1-propanol in Table 4.5. The high 1-propanol concentrations have solvation times which are too fast for this diffusional analysis.

Figure 4.9

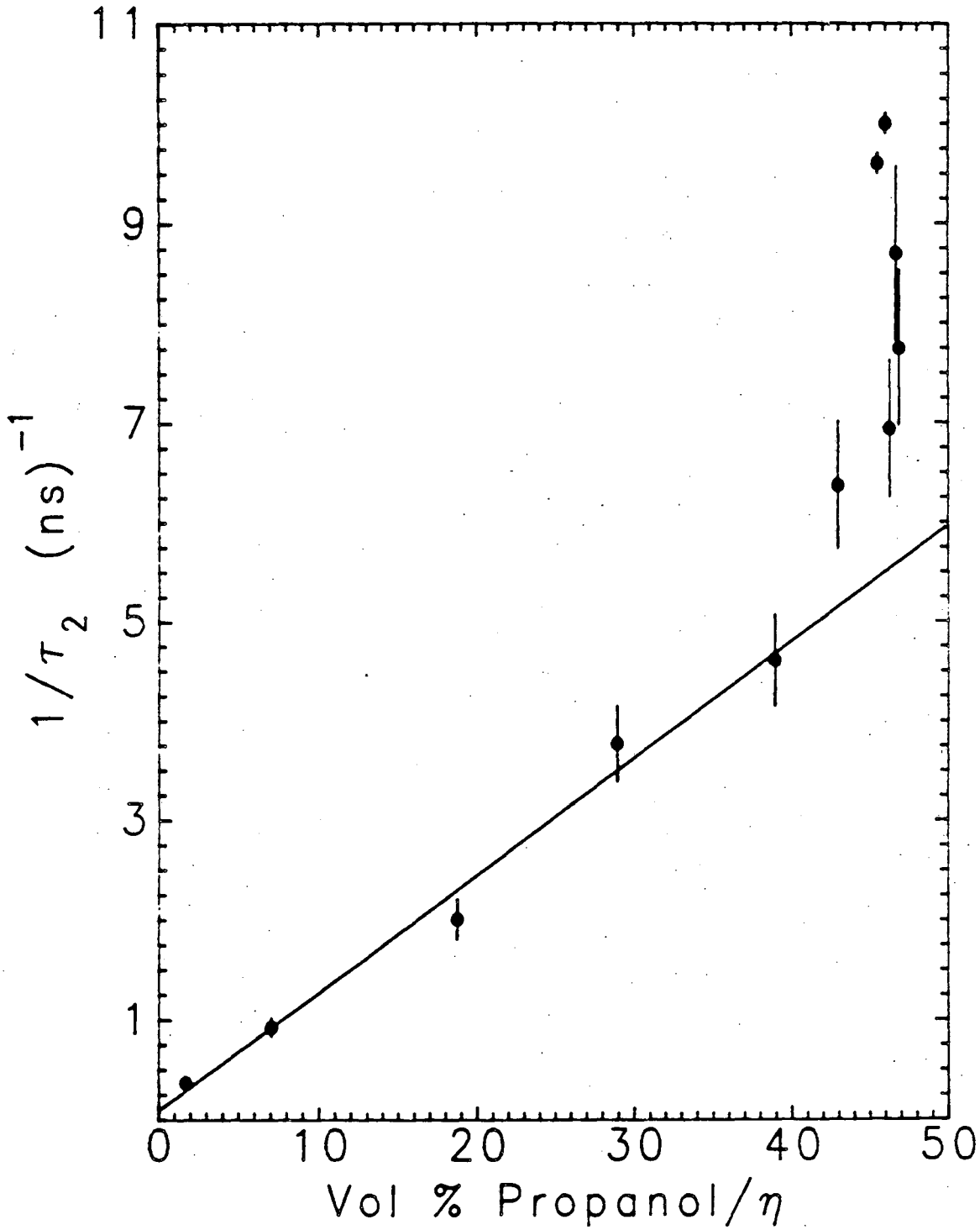

centrations, the diffusion rate and dielectric relaxation rate of the alcohol are about the same.

In order to find support for this theory, the peak position versus time spectra, examples of which were shown in Figure 4.6, were refit to three exponentials. One of these times was fixed to what should have been the diffusional time. This time is obtained from Figure 4.9 by extrapolating the times of the high propanol concentration solutions down to the diffusion line, which was determined by the low concentrations of propanol. The three solvation times obtained from this three exponential fit are listed in Table 4.9. The fastest exponential time is now more consistent than the numbers in Table 4.5. The contribution of this component, reflected in the alpha values, becomes less as the amount of propanol decreases. This trend is also reflected in the second solvation time. This time, along with the fast time, is attributed to the dielectric relaxation of the solvent environment around the 4AP molecule. All of these middle times fall within the possible range of the dielectric relaxation times of the mixed solvents, listed in Table 4.8, and the fast times are comparable to the time of a rotation of a propanol molecule. For the most dilute solutions of 1-propanol, τ_2 is no longer needed to obtain a good fit; although the data can be fit with a time comparable to these numbers. At this low concentration, the dielectric relaxation time of the 1-propanol around the 4AP molecule may become faster since it no longer has a large network of hydrogen-bonds to break before rotation. The decrease in the alpha values for these two times is matched by an increase in the contribution from the third solvation time, which is attributed to the diffusion of the propanol to the 4AP molecule.

Shown in Table 4.10 are the percent of τ_1 in the dielectric relaxation mechanism and the percent of τ_3 in the entire shift of the 4AP molecule. The increase in the ratio of $\tau_3/(\tau_1 + tau_2 + tau_3)$ is a better indication of the increase in contribution of the diffusional mechanism as the 1-propanol is diluted by toluene. The amount of the dielectric relaxation of the solvent due to τ_1 is once again fairly constant, around 40%. The addition of toluene

Table 4.9

Three Exponential Fits of Peak Position versus Time Data for 4AP in 1-Propanol:Toluene Mixtures

Volume % of Propanol	Dielectric Relaxation α_1	τ_1 (ps)†	Dielectric Relaxation α_2	τ_2 (ps)‡	Diffusional Relaxation α_3	τ_3 (ps)‡
100	1.56	15	2.06	90		
90	1.41	13	2.11	78	0.51	170
80	1.35	17	2.47	87	0.33	168
70	1.32	14	2.04	81	0.86	165
60	1.68	17	1.48	83	1.13	164
50	1.00	13	1.25	71	1.75	167
40	0.76	11	0.97	94	1.98	179
30	0.37	15	0.50	55	2.26	217
20	0.33	26	0.45	78	2.41	265
12	0.20	20			2.33	498
4.2	0.03	20			2.74	1080
1.0						2700

† Error on these values is ± 10 ps.

‡ Error on these values is ± 10%.

to 1-propanol is expected to break up the hydrogen-bonding network of the alcohol. This breakup may cause a higher number of monomeric propanol molecules than in a pure propanol solution. The result in Table 4.10 indicates that, at least immediately around the 4AP molecule, the 1-propanol seems to retain its hydrogen-bonding structure.

This three exponential fit of the peak position versus time data has thus shown two important mechanisms of the solvation dynamics of the excited-state dipole of the 4AP molecule: at high propanol concentrations, the dielectric relaxation time of the alcohol dominates, whereas at very low propanol concentrations, the rate of diffusion of the alcohol to the excited molecule is the only solvation time seen. At the propanol concentration of 0.1% by volume where no spectral shift was extractable, the plot in Figure 4.9 indicates that this diffusion time would be on the order of 8000 ps. As suspected earlier, this time is slow enough to be competing with the fluorescence lifetime of the 4AP molecule. This low concentration result helps explain the experiments of *Detoma* and *Brand*[48] on the fluorescence of 2-anilinonaphthalene mentioned in Chapter 3. Using nanosecond spectroscopy, they found a two exponential decay for the fluorescence lifetime of this solute at very low concentrations of ethanol in cyclohexane. They attributed the appearance of the second decay to a complex formation between the ethanol and the 2-anilinonaphthalene. One of these components could be the fluorescence lifetime of the solute while the other could be the diffusion of the ethanol to the excited molecule. At higher concentrations of ethanol, the diffusional rate would be too fast to see with nanosecond time resolution so a single exponential would be seen for the fluorescence lifetime.

This type of combined mechanism is also consistent with the theory of unit cells proposed by *Mazurenko*[50,51] and mentioned in the introduction of this chapter. While a diffusional mechanism changes the cells around the solute from nonpolar to polar, the unit cells around the solute which are already polar rearrange by a dielectric relaxation mechanism.

Table 4.10

Contributions of Exponentials to Spectral Shifts

Volume % of Propanol	$\frac{a_1 \times 100\%}{a_1+a_2}$	$\frac{a_3 \times 100\%}{a_1+a_2+a_3}$
100	43%	
90	40%	13%
80	36%	8%
70	39%	20%
60	53%	26%
50	45%	44%
40	43%	53%
30	43%	72%
20	42%	76%
12		92%

I. Conclusion

Although the data can be fit to three exponentials which correspond well with a combined dielectric relaxation and diffusion mechanism, separating the two mechanisms would eliminate the number of unknowns needed to fit the data. To eliminate the diffusion component, a pure solvent is needed and, as shown in Chapter 3, the time dependence of the fluorescence shift of 4AP in a pure solvent can be described by dielectric relaxation. To eliminate the dielectric relaxation component, a polar solvent with a fast relaxation time could be used. Such a solvent is formamide or N-methylformamide. In Chapter 3, these solvents were found to have as large an effect on the shift of 4AP fluorescence as the alcohols, plus their dielectric relaxation times were too fast to measure. These solvents would be useful only if their corrected dielectric relaxation times in a solvent mixture remained low. Currently no information is available on the dielectric behavior of formamides in mixed solvents.

The viscosity is another variable which would be useful to eliminate in the analysis. 1-Propanol and decalin have comparable viscosities;[31] however, there is no reason to expect mixtures of these two to have the same viscosity. Small amounts of the decalin in 1-propanol could break up the extensive hydrogen-bonding that is responsible for the viscosity of 1-propanol, and the viscosity of the solution could lower. However, the viscosities of these mixtures would not vary as widely as the viscosities of the 1-propanol:toluene mixtures. Also, dielectric relaxation data for 1-propanol:decalin mixtures are not readily available. Some of the above experiments could help better understand the processes occurring in these mixed solvents. The one mixture studied has already increased the knowledge of what processes are important to a solute in a mixed solvent environment.

Chapter 5

Conclusion

Picosecond fluorescence techniques were found to be valuable in studying solvation. The type of excited-state process described in Figure 1.2 provided a means to probe directly the solvent rearrangement around a solute molecule placed suddenly in an un-equilibrated solvent environment. The 4-aminophthalimide molecule was a valuable tool in this solvation study because of its interactions with polar solvents. Both the pure solvent and the mixed solvent work revealed important aspects of the solvation process.

The time of solvation of a solute by a pure solvent was shown to be dependent on the dielectric relaxation times of the solvent and independent of the solute molecule. The extensive hydrogen-bonding interactions in alcohols made them the only solvents with dielectric relaxation times slow enough to measure. In order to observe the solvation of 4AP in a solvent other than an alcohol, several experiments can be tried. For those solvents which rearranged just barely too fast for the time resolution of the instrumentation (formamide and N-methylformamide) lowering the temperature could increase the dielectric relaxation times to values slow enough to observe. For example, the corrected dielectric relaxation time of N-methylformamide increases from 3.6 ps at 20 °C to about 25 ps at 0 °C [35], a value which can just be measured with this instrumentation. To observe the solvation of 4AP in the non hydrogen-bonding solvents, a faster excitation pulse and detection device would have to be used. Since these solvents rearrange on a subpicosecond time scale, observed dynamics of fluorescence of the 4AP molecule would become more complicated. The time scale of rearrangement of these solvents may compete with the vibrational relaxation or the rotations of the amino group of the 4AP molecule. Both these processes were too fast to be seen with the picosecond resolution of the instrumentation described in Chapter 2.

The model of solvation of 4AP by the mixed solvent, 1-propanol:toluene required an additional element to explain the relaxation of the 4AP excited state. The steady-

state spectra, fluorescence lifetimes and rotation times of 4AP in the solvent mixtures indicated a higher 1-propanol concentration around the excited 4AP molecule than was present in the bulk solution. A larger number of the polar propanol solvent molecules can be around the higher dipole moment of the excited state of 4AP than the lower one of the ground state. These extra molecules had to diffuse toward the 4AP molecule from the bulk solution. The solvation of the 4AP molecule was controlled not only by the dielectric relaxation of the solvent already around the solute, but by the diffusion rate of the propanol molecules. The experiments described in the conclusion of Chapter 4 will help to better understand the environment around the 4AP molecule in these mixed solutions.

These results can be important in determining a solvent for a reaction where solvation of an intermediate is important. If a quickly forming intermediate has a different electronic configuration than its precursor, the solvent will have to react to this new species. Although the solvent may be able to solvate the intermediate, if the lifetime of the intermediate is less than the dielectric relaxation time of the solvent, the solvent will not have a chance to stabilize the intermediate. Solvent mixtures can give a large range of solvation times which can be used to selectively solvate an intermediate which may have a longer lifetime than another unfavorable intermediate.

The picosecond laser coupled with the ultrafast streak camera has proved to be a powerful tool for probing the microscopic environment of a solution. The studies described here have elucidated the processes that are important in the interactions between a solvent and solute and confirmed results obtained by theoreticians.

References

1. A.T. Amos and B.L. Burrows; *Advan. Quantum Chem.* **7** (1973) 289.
2. E.G. McRae; *J. Phys. Chem.* **61** (1957) 562.
3. T. Abe; *Bull. Chem. Soc. Japan* **38** (1965) 1314.
4. Y.T. Mazurenko and N.G. Bakhshiev; *Opt. Spectrosc.* **28** (1970) 490.
5. B. Bagchi, D.W. Oxtoby and G.R. Fleming; *Chemical Physics* **86** (1984) 257.
6. G. van der Zwan and J.T. Hynes; *J. Phys. Chem.* **89** (1985) 4181.
7. W.T. Brown; Ph.D. Thesis; University of California, Berkeley, 1986.
8. W.S. Struve and P.M. Rentzepis; *Chem. Phys. Lett.* **29** (1974) 23.
9. D. Huppert, S.D. Rand, P.M. Rentzepis, P.F. Barbara, W.S. Struve and Z.R. Grabowski; *J. Chem Phys.* **75** (1981) 5714.
10. S.L. Shapiro and K.R. Winn; *Chem. Phys. Lett.* **71** (1980) 440.
11. W.R. Ware, P. Chow and S.K. Lee; *Chem. Phys. Lett.* **2** (1968) 356.
12. W.R. Ware, S.K. Lee, G.J. Brant and P.P. Chow; *J. Chem. Phys.* **54** (1971) 4729.
13. L.A. Philips; Ph.D. Thesis, University of California, Berkeley, 1985.
14. H. Nathel; Ph.D. Thesis, University of California, Berkeley, 1986.
15. S.W. Yeh; Ph.D. Thesis, University of California, Berkeley, 1985.
16. S.W. Yeh, S.P. Webb and J.H. Clark; in preparation.
17. T.N. Demas; *Excited State Lifetime Measurements* (Academic Press Inc.,New York, 1983) 80.
18. Ibid., 89.
19. T.V. Veselova, L.A. Limareva, A.S. Cherkasov and V.I. Shirokov; *Opt. Spectrosc.* **19** (1965) 39.
20. N.G. Bakhshiev and I.V. Piterskaya; *Opt. Spectrosc.* **20** (1966) 437.
21. A.S. Cherkasov; *Opt. Spectrosc.* **12** (1962) 35.
22. I.V. Piterskaya; *Opt. Spectrosc.* **23** (1967) 9.
23. Y.T. Mazurenko; *Opt. Spectrosc.* **36** (1974) 283.
24. C. Reichardt; *Solvent Effects in Organic Chemistry* (Verlag-Chemie 1979) 237.
25. H. Langhals; *Angew. Chem. Int. Ed. Engl.* **21** (1982) 724.

26. K. Dimroth and C. Reichardt; *Z. Anal. Chem.* **215** (1966) 344.

27. T.R. Griffiths and D.C. Pugh; *J. of Solution Chemistry* **8** (1979) 247.

28. H. Dodiuk and E.M. Kosower; *J. Phys. Chem.* **81** (1977) 50.

29. D. Huppert, H. Kanety and E.M. Kosower; *Chem. Phys. Lett.* **84** (1981) 48.

30. These data and results were obtained from a private communication with Sheila W. Yeh.

31. Riddick and Bunger; *Techniques of Chemistry Vol. II, Organic Solvents, third edition* (Wiley-Interscience, New York, 1970).

32. C.P. Smyth; *Dielectric Behavior and Structure* (McGraw-Hill Book Company, Inc., New York, 1955).

33. A. Mozumder; *J. Chem Phys.* **50** (1969) 3153.

34. S.K. Garg and C.P. Smyth; *J. Phys. Chem.* **69** (1965) 1294.

35. M.W. Sagal; *J. Chem. Phys.* **36** (1962) 2437.

36. D. Bertolini, M. Cassettari and G. Salvetti; *J. Chem. Phys.* **78** (1983) 365.

37. R. Chahine and T.K. Bose; *J. Chem. Phys.* **65** (1976) 2211.

38. H.A. Rizk and I.M. Elanwar; *Zeit. für Phys. Chem.* **62** (1968) 225.

39. S.J. Bass, W.I. Nathan, R.M. Meighan and R.H. Cole; *J. Phys. Chem.* **68** (1964) 509.

40. M. Evans; *J. Mol. Liq.* **25** (1983) 149.

41. H. Behret, F. Schmithals and J. Barthel; *Zeit. für Phys. Chem.* **96** (1975) 73.

42. G.R. Fleming, J.M. Morris and G.W. Robinson; *Chemical Physics* **17** (1976) 91.

43. P. Debye; *Polar Molecules* (Dover Publications, New York, 1945).

44. L.A. Hallidy and M.R. Topp; *Chem. Phys. Lett.* **48** (1977) 40.

45. A. Declemy, C. Rulliere and P. Kottis; *Chem. Phys. Lett.* **101** (1983) 401.

46. H. Inoue, M. Hida, N. Nakashima and K. Yoshihara; *J. Phys. Chem.* **86** (1982) 3184.

47. S.R. Flom and P.F. Barbara; *J. Phys. Chem.* **89** (1985) 4489.

48. R.P. Detoma and L. Brand; *Chem. Phys. Lett* **47** (1977) 231.

49. T. Okamura, M. Sumitani and K. Yoshihara; *Chem. Phys. Lett.* **94** (1983) 339.

50. Y.T. Mazurenko and V.S. Udaltsov; *Opt. Spectrosc.* **44** (1978) 233.

51. Y.T. Mazurenko, I.V. Piterskaya, V.I. Studenov and N.G. Bakhshiev; *Opt. Spectrosc.* **44** (1978) 272.

52. T.V. Veselova, A.S. Cherkasov and V.I. Shirokov; *Opt. Spectrosc.* **39** (1975) 615.

53. N. Vlahovici and A. Vlahovici; *J. of Luminescence* **15** (1977) 421.

54. L.A. Hallidy and M.R. Topp; *J. Phys. Chem.* **82** (1978) 2415.

55. C. Campbell, J. Crossley and L. Glasser; *Advances in Molecular Relaxation Processes* **9** (1976) 63.

56. T. Koshii, E. Arie, M. Nakamura, H. Takahashi and K. Higasi; *Bull. Chem. Soc. Japan* **47** (1974) 618.

57. R. Minami, K. Itoh, H. Sato, H. Takahashi and K. Higasi; *Bull. Chem. Soc. Japan* **54** (1981) 1322.

58. W.P. Conner and C.P. Smyth; *J. Am. Chem. Soc.* **65** (1943) 382.

This report was done with support from the Department of Energy. Any conclusions or opinions expressed in this report represent solely those of the author(s) and not necessarily those of The Regents of the University of California, the Lawrence Berkeley Laboratory or the Department of Energy.

Reference to a company or product name does not imply approval or recommendation of the product by the University of California or the U.S. Department of Energy to the exclusion of others that may be suitable.

TECHNICAL INFORMATION DEPARTMENT
LAWRENCE BERKELEY LABORATORY
UNIVERSITY OF CALIFORNIA
BERKELEY, CALIFORNIA 94720